RADAR
Research Archive and Digital Asset Repository

OXFORD BROOKES UNIVERSITY

Smart Technology for Telerehabilitation: A Smart Device Inertial-sensing Method for Gait Analysis

Dax Steins (2016)

https://radar.brookes.ac.uk/radar/items/adbc3997-d0bf-46ce-b72f-e6e616d204ec/1/

Note if anything has been removed from thesis:

Copyright © and Moral Rights for this thesis are retained by the author and/or other copyright owners. A copy can be downloaded for personal non-commercial research or study, without prior permission or charge. This thesis cannot be reproduced or quoted extensively from without first obtaining permission in writing from the copyright holder(s). The content must not be changed in any way or sold commercially in any format or medium without the formal permission of the copyright holders.

When referring to this work, the full bibliographic details must be given as follows:

Steins, D (2016) *Smart Technology for Telerehabilitation: A Smart Device Inertial-sensing Method for Gait Analysis* PhD, Oxford Brookes University

WWW.BROOKES.AC.UK/GO/RADAR

Smart Technology for Telerehabilitation:
A Smart Device Inertial-sensing Method for Gait Analysis

Dax Steins

Thesis submitted in partial fulfillment of the requirements for the degree of Doctor of Philosophy

Department of Sport and Health Sciences
Oxford Brooks University

OXFORD BROOKES UNIVERSITY

This thesis is dedicated to my grandmother Willy Bus-Berger and the memory of my grandfather and grandmother,
Leonardus Jozef Steins & Tiny Steins-Rutjes

Abstract

The aim of this work was to develop and validate an iPod Touch (4th generation) as a potential ambulatory monitoring system for clinical and non-clinical gait analysis. This thesis comprises four interrelated studies, the first overviews the current available literature on wearable accelerometry-based technology (AT) able to assess mobility-related functional activities in subjects with neurological conditions in home and community settings. The second study focuses on the detection of time-accurate and robust gait features from a single inertial measurement unit (IMU) on the lower back, establishing a reference framework in the process. The third study presents a simple step length algorithm for straight-line walking and the fourth and final study addresses the accuracy of an iPod's inertial-sensing capabilities, more specifically, the validity of an inertial-sensing method (integrated in an iPod) to obtain time-accurate vertical lower trunk displacement measures.

The systematic review revealed that present research primarily focuses on the development of accurate methods able to identify and distinguish different functional activities. While these are important aims, much of the conducted work remains in laboratory environments, with relatively little research moving from the "bench to the bedside." This review only identified a few studies that explored AT's potential outside of laboratory settings, indicating that clinical and real-world research significantly lags behind its engineering counterpart. In addition, AT methods are largely based on machine-learning algorithms that rely on a feature selection process. However, extracted features depend on the signal output being measured, which is seldom described. It is, therefore, difficult to determine the accuracy of AT methods without characterizing gait signals first. Furthermore, much variability exists among approaches (including the numbers of body-fixed sensors and sensor locations) to obtain useful data to analyze human movement. From an end-user's perspective, reducing the amount of sensors to one instrument that is attached to a single location on the body would greatly simplify the design and use of the system.

With this in mind, the accuracy of formerly identified or gait events from a single IMU attached to the lower trunk was explored. The study's analysis of the trunk's vertical and anterior-posterior acceleration pattern (and of their integrands) demonstrates, that a combination of both signals may provide more nuanced information regarding a person's gait cycle, ultimately permitting more clinically relevant gait features to be extracted.

Going one step further, a modified step length algorithm based on a pendulum model of the swing leg was proposed. By incorporating the trunk's anterior-posterior displacement, more accurate predictions of mean step length can be made in healthy subjects at self-selected walking speeds. Experimental results indicate that the proposed algorithm estimates step length with errors less than 3% (mean error of 0.80 ± 2.01cm). The performance of this algorithm, however, still needs to be verified for those suffering from gait disturbances.

Having established a referential framework for the extraction of temporal gait parameters as well as an algorithm for step length estimations from one instrument attached to the lower trunk, the fourth and final study explored the inertial-sensing capabilities of an iPod Touch. With the help of Dr. Ian Sheret and Oxford Brookes' spin-off company 'Wildknowledge', a smart application for the iPod Touch was developed. The study results demonstrate that the proposed inertial-sensing method can reliably derive lower trunk vertical displacement (intraclass correlations ranging from .80 to .96) with similar agreement measurement levels to those gathered by a conventional inertial sensor (small systematic error of 2.2mm and a typical error of ≤3mm). By incorporating the aforementioned methods, an iPod Touch can potentially serve as a novel ambulatory monitor system capable of assessing gait in clinical and non-clinical environments.

Presentations and Publications Relevant to Thesis

Steins Dax, Ruben Zijlstra, Johnny Collett, Patrick Esser, Helen Dawes. "Assessment of Walking Features from Lower Trunk Inertial Sensing: A Reference Model." *Journal of Gait & Posture*. (Undergoing first-round review.)

Steins Dax, Johnny Collett, Patrick Esser, Helen Dawes. "A Modified Step-length Estimation Model for Gait Analysis." *Journal of Biomechanics*. (Undergoing first-round review.)

Steins Dax, Ian Sheret, Patrick Esser, Johnny Collett, Helen Dawes. "A Smart Device Inertial-sensing Method for Gait Analysis." *Journal of Biomechanics*. 47(15), 3780-85, July 2014.

Steins Dax, Helen Dawes, Patrick Esser, Johnny Collett. "Wearable Accelerometry-based Technology Capable of Assessing Functional Activities in Neurological Populations in Community Settings: A Systematic Review." *Journal of Neuroengineering and Rehabilitation* (JNER), 11(1), 36, March 2014.

Steins Dax, Helen Dawes, Patrick Esser, Johnny Collett. "Systematic Review on State-of-the-Art Technology Capable of Assessing Functional Activities in Neurological Populations in Community Settings." Conf. Proc. The Society of Research in Rehabilitation (SRR), Bath, 2013, 27:1048-54: SAGE.

Steins Dax, Patrick Esser, Johnny Collet, Helen Dawes. "One Step Closer to Stepping Right: A Modified Pendulum Model for Step Length Estimations." OBU Research Student Symposium 2014, January 15, Oxford Brookes University.

Acknowledgements

I would like to express my gratitude to my research supervisors, Helen Dawes, Johnny Collett, and Patrick Esser.

I would also like to acknowledge Daan Meesters, Francesca Liu, Marloes Franssen, and Tom O'Leary, among other colleagues, for their support all throughout.

Ian Sheret cannot be forgotten for his help with designing and implementing a Kalman filter. The same goes for Lesley Smith, who helped to design the search strategy for my systematic review (adapted into Chapter Three).

My thanks extend to all the study participants as well. Without their time and effort, this project would not have been possible.

Finally, I would like to thank my family members, especially my parents, Hans & Marleen Kam-Bus, for their sacrifices and understanding. And, then, to my best friend, Ery Shin: thank you for your faith in me from the beginning.

Tables of Contents

Glossary

2D	Two-dimensional
3D	Three-dimensional
4D	Four-dimensional
a	Acceleration
AT	Accelerometry-based Technology
ADC	Analog digital converter
ANOVA	Analysis of Variance
AP	Anterior-posterior
BW	Body Weight
CI	Confidence Interval
cm	Centimeters
COM	Center of Mass
COG	Center of Gravity
CP	Cerebral Palsy
DOF	Degrees of Freedom
ϵ	Error
F	Force
F_c	Coriolis Force
FFC	Final Foot Contact
FIR	Finite Impulse Response
FP	Force Plate
GC	Gait Cycle
GE	Gait Event
GRF	Ground Reaction Forces
h	Vertical excursion
HD	Huntington disease
HST	Heel-strike Transient
Hz	Hertz
i,j,k	Complex numbers
IFC	Initial Foot Contact
ICC	Intraclass Correlation Coefficient
ICF	International Classification of Functioning, Disability, and Health
IIR	Infinite Impulse Response

IMU	Inertial Measurement Unit
IP	Inverted Pendulum
k	Constant
K	Kalman Gain
kg	Kilogram
l	Pendulum length
m	Mass
MEMS	Micro-Electro-Mechanical Systems
MesH	Medical Subject Heading
ML	Medio-lateral
ms^{-1}	Metres per second
ms^{-2}	Acceleration
MS	Multiple Sclerosis
MS	Mid-stance
NHS	National Health Service
NSF	National Service Framework
OMCS	Optical Motion Camera System
p	P-value
PD	Parkinson disease
PDA	Personal Digital Assistant
r	Correlation coefficient
RLA	Ranchos Los Amigos
SEM	Standard Error of Measurement
SL	Step Length
SSWS	Self-selected walking speed
STS	Sit-to-Stand
WHO	World Health Organization
vi	Visual Instrument
VT	Vertical
UK	United Kingdom

List of Figures

List of Tables

Chapter 1

Introduction

1.1 Objectives

This thesis works toward developing an ambulatory monitoring system to support research and healthcare delivery to those with neurological conditions and musculoskeletal (or anyone, for that matter) in short-term, supervised and unsupervised monitoring situations. To do so, it organizes itself around two main goals:

- to develop and propose alternative gait feature extraction methods for clinical gait assessments (or step feature selection to identify and classify movements performed by subjects) from a single device attached near the center of mass of the body.

- to establish and validate an unobtrusive ambulatory monitoring system (based on one inertial measurement unit attached near the center of mass of the body) against a gold standard for gait assessments.

The ideal ambulatory monitoring system in this context can assist in the assessment of functional ability, support physicians in their clinical decision-making process, and improve rehabilitation efforts undertaken in both clinical and non-clinical settings by:

- producing evidence-based practice according to NICE guidelines
- supporting clinical research and testing to promote independent living
- promoting partnership between local and national health and social services

In accordance with the above aims, a smart device inertial-sensing method for gait assessments has been developed, one equipped to determine spatiotemporal gait parameters from the lower trunk. Relevant temporal gait parameters and step features, including mean step length estimations, can now be derived within ten minutes in clinical settings and free-living environments. The assessment will normally, although not necessarily, be performed in the presence of a health professional.

1.2 Motivation

One of the common causes behind serious disability, neurological conditions exert a major, but often popularly unrecognized, impact on health and social services (The Neurological Alliance 2003). Each year, approximately 600,000 people (1% of the UK population) are diagnosed with neurological conditions, such as stroke, multiple sclerosis, and Parkinson's

disease. In 2003, it was estimated that approximately 10 million UK citizens bear a neurological condition (excluding migraines), of which 350,000 individuals require daily care (The Neurological Alliance 2003). The latter figure is expected to rise sharply over the next two decades as survival rates, healthcare, and diagnostic techniques all improve.

In response to this growing pressure, the Department of Health evolved, in 2005, the National Service Framework (NSF) to better address the long-term needs of those with neurological conditions. Building on both the National Health Service (NHS) Improvement Plan "Putting People at the Heart of Public Services" (Department of Health 2004) and ongoing research initiatives, the NSF aims to ensure that high-quality healthcare services are uniformly available across England. Its core provides a set of evidenced-based requirements designed to prioritize individual needs and service patients effectively from their diagnosis onward (National Audit Office 2011).

Since the NSF's introduction, there has been a marked spending increase on neurological services. Between 2006 and 2010, such health expenditures (excluding those reserved for neurological pain) increased by 38%, from £2.1 to £2.9 billion. Spending on social services for adults with neurological conditions, however, has remained roughly the same since 2005. While the NSF is expected to be fully implemented by 2015, a recent study conducted by the National Audit Office regarding health and social care services delivery has concluded that current progress on locally enforcing the NSF's quality requirements has been severely hampered (National Audit Office 2011). Moreover, no major improvements in neurological condition-oriented service provision have been made, with ongoing care being poorly coordinated.

Against this national infrastructural backdrop (and as if to compensate for its limitations), translational research into gait-related health implications posed by neurological conditions has gained momentum. Specifically, for the purposes of this work, given that gait is an important skill for independent living, neurological disorders often incur gait problems that significantly affect an individual's quality of life (Schrag, Jahanshahi et al. 2000; Mitchell, Benito-Leon et al. 2005), how up-and-coming telerehabilitation (Brennan, Mawson et al. 2009)[1] can expand key clinical deliverables—say, the measurement of daily functioning, assessment of medication effects on physical ability, evaluation of exercise compliance, and access to adequate feedback and up-to-date therapy instructions (Dobkin and Dorsch 2011)—has garnered fresh interest and technological leads in the field of movement science. Much contemporary work has been reported on the use of wearables for monitoring patients over extensive period of time in different fields (Bonato 2003). An obvious example is the use of ambulatory systems for mobility (Scanaill, Carew et al. 2006), physical activity (Giansanti, Macellari et al. 2008), and fall risk monitoring (Weiss, Sharifi et al. 2011; Weiss, Brozgol et al. 2013; Weiss, Herman et al. 2014). Weiss et al., for instance, demonstrated that a body-fixed sensor worn for 3 days can be used to evaluate fall risk in patients with Parkinson's (Weiss, Herman et al. 2014). By using such tools, research knowledge and technology

[1] Telerehabilitation refers to the use of Information and Communication Technologies to provide rehabilitation services to people remotely in their homes or other environments.

development can be translated to practice providing access to care outside the clinic, where wearing off and intrinsic and extrinsic environments impact performance, thus helping to properly assess functional status and expanding continuity of care to persons with disabling conditions (Brennan, Mawson et al. 2009).

Neurological disorders frequently cause motor impairments and physical deconditioning, leading to postural instability, gait disturbances, increased fall risks, mobility loss, increased fatigability, and reduced independence (De Groot, Phillips et al. 2003; Stolze, Klebe et al. 2004; Alexander and Goldberg 2005)—factors which, when taken altogether, pose serious obstacles to community participation. Here, ambulatory monitoring devices designed to measure functional status as part of a rehabilitation program to reduce or remove gait impairments (in their early as well as late stages) may help subjects to re-engage with their social surroundings. Investigating the effectiveness of these interventions is, therefore, a matter of due course (Barbeau and Fung 2001), not only for patients, but also for their caregivers, treatment providers, and policy makers (WHO 2006).

So far, any investigations of this sort have proved difficult to carry out as, to borrow Paolo Bonato's words, "[I]t is often questioned whether assessments performed in the clinical setting are truly representative of how a given clinical intervention affects the real life of patients" (Kiani, Snijders et al. 1997; Bonato 2005). Two high-profile cohort studies, for instance, indicated that 70-85% of stroke survivors can walk independently in hospital settings (Kelly-Hayes, Beiser et al. 2003; Lord, McPherson et al. 2004), yet only two-thirds can actually do so in real-life, despite demonstrating sufficient mobility levels (Lord, McPherson et al. 2004). To counter the 'Hawthorne Effect' (also known as the observer effect, which influences aspects of people's behavior in response to their awareness of being observed (McCarney, Warner et al. 2007), what is needed is an alternative technology capable of gathering clinically accurate data in free-living environments. Supplementing clinical rehabilitation initiatives, it would track a range of important parameters of movement in order to identify changes in health or functional status and to monitor for emergency events, such as falls (Mathie, Coster et al. 2004). Ideally, such technology would not only refine telerehabilitation efforts, but also reduce hospital costs and demands (clinical assessments being cost-intensive) without compromising, of course, healthcare quality.

The recent development of advanced sensor and remote monitoring technologies have ushered in a new era of wearable sensors—particularly inertial sensors that contain accelerometers, gyroscopes, and occasionally magnetometers—that can easily attach to various body parts and measure targeted physical quantities. Low-powered, compact, and light-weight, such sensors (usually accelerometers and gyroscopes) have been deployed to provide objective measurements of physical activity and motor functioning in chronically ill (Allet, Knols et al. 2010) and elderly populations (Zijlstra and Aminian 2007; de Bruin, Hartmann et al. 2008). When accelerometers (Troiano, Berrigan et al. 2008) and gyroscopes (Najafi, Aminian et al. 2003) are combined (resulting in what is called an inertial measurement unit [IMU]), in fact, the study of human motion becomes more accurate (Cuesta-Vargas, Galán-Mercant et al. 2010).

Numerous systematic and non-systematic reviews on the use of accelerometry for telerehabilitation (Bussmann and Stam 1998; Mathie, Coster et al. 2004; Kairy, Lehoux et al. 2009; Gregory, Alexander et al. 2011; Johansson and Wild 2011; Patel, Park et al. 2012), physical activity monitoring (Steele, Belza et al. 2003; Culhane, O'Connor et al. 2005; Zheng, Black et al. 2005; de Bruin, Hartmann et al. 2008; Preece, Goulermas et al. 2009; Allet, Knols et al. 2010; Gebruers, Vanroy et al. 2010; Cheung, Gray et al. 2011), and human motion analysis (Zheng, Black et al. 2005; Berlin, Storti et al. 2006; Cuesta-Vargas, Galán-Mercant et al. 2010; Yang and Hsu 2010; Cheung, Gray et al. 2011) exist today. Some provide in-depth overviews of automated classifications (Mathie, Coster et al. 2004; Preece, Goulermas et al. 2009) and applications for gait and balance evaluation, fall risk assessment, and mobility monitoring in various populations and environments (de Bruin, Hartmann et al. 2008; Allet, Knols et al. 2010; Gebruers, Vanroy et al. 2010; Cheung, Gray et al. 2011), ultimately verifying the feasibility of adopting wearable motion-sensing technology. Yet no review has surveyed valid motion-sensing technology capable of assessing functional activities in home and community settings for neurological populations. A clearer understanding of translational research on existing motion-sensing technology validated for the community would provide a better grasp of what has been, and needs to be, done to close the gap between basic science and practice (Wandersman, Duffy et al. 2008). Thus, the question that needs to be answered, to achieve the latter, is to what extent have accelerometry-based technology been implemented as telerehabilitation tools. This type of approach constitutes the conceptual basis of the present study.

1.3 Internal Structure

The thesis is sub-divided into eight chapters:

- Chapter One elaborates on the need for an ambulatory monitoring system capable of gathering clinically accurate data in supervised and unsupervised environments, thereby supplementing clinical rehabilitation for, among other patient types, neurologically affected subjects. Such technology would affordably expand current telerehabilitative initiatives, allowing healthcare professionals to monitor human movement in order to assess functional status in free-living environments.

- Chapter Two overviews the current available literature on wearable accelerometry-based technology intended for telerehabilitation purposes that can assess, in home and community settings, mobility-related functional activities in subjects with neurological conditions. In doing so, it will extend and revise the insight set forward by others.

- Chapter Three describes the accelerometer and gyroscope mechanics behind an IMU, establishing the methodological basis of this thesis in the process. How sensor fusion can provide time-accurate measurements of linear acceleration and angular velocity, why quaternions should be used over Euler angles to obtain global frame measurements, and which parts of signal processing are relevant in this context—such issues will drive forward the discussion here.

- Chapter Four surveys the general field of human locomotion, contextualizing the scholarly background from which this study takes shape. The first section details the gait cycle itself, including how gait events, phases, and patterns can be evaluated from a point near the body's center of mass. The second section explores the clinical role of gait analysis and its constraints under present-day laboratory conditions.

- Chapter Five presents an alternative method for more accurate gait event detection, based on the acceleration signal of a single IMU attached to the lower trunk.

- Chapter Six provides a modified step length model based on the acceleration signal of a single IMU attached to the lower trunk. This algorithm is able to estimate mean step length without the need for individual correction factor.

- Chapter Seven describes and validates the IMU-dependent sensor fusion algorithm within a smart device for ambulatory monitoring purposes.

- Chapter Eight discusses the applications and limitations of the proposed gait methods and system. Recommendations for further validating and improving this project's novel ambulatory monitoring system are included.

Chapter 2

Literature Review[2]

2.1 Summary of Contents

This chapter explores the present utility of accelerometry-based technology (AT) for assessing mobility-related functional activities in non-clinical setting. As mentioned earlier, recent development of advanced sensor and remote monitoring technologies have fostered much interest in wearable inertial sensors. Because inertial sensors are light-weight, portable, energy-efficient, and user-friendly, they can easily evaluate a subject's gait, balance, fall risks, and general mobility outside laboratories. In this manner, AT has the potential to not only more thoroughly verify the effectiveness of rehabilitative treatments, but also gather more accurate, well-rounded data to draw up such treatments in the first place.

2.2 Introduction

The World Health Organization's Framework of International Classification of Functioning, Disability, and Health (ICF) relies on a biopsychosocial model to describe human functioning through the capture of body function and through the individual's activity and participation within his or her social and physical environment. It is important to note that in the activity and participation construct, there is a distinction made between a person's ability to perform a skill in a clinic and his or her ability to perform that same skill in a natural environment. Ideally, an individual's performance should be consistent across place and time; often enough, however, for the reasons mentioned in Chapter One, performance varies and may not accurately reflect a patient's functional ability in their normal environment (Kiani, Snijders et al. 1997). There is a need for systems that are able to provide low-cost, objective measurement of functional ability of free-living subjects in the home environment (Mathie, Coster et al. 2004).

Nowadays, enhancements in microelectromechanical system (MEMS) technology—particularly inertial sensors—have made it possible to assess the type, intensity, duration, frequency, and quality of various mobility-related functional activities (Dobkin and Dorsch 2011). These sensing systems can be used to provide telerehabilitation, that is, the delivery of rehabilitative services to remote sites, thereby introducing new possibilities for continuous, unsupervised, objective monitoring of mobility and functional activities in clinical (Berlin, Storti et al. 2006) and non-clinical settings (Bussmann and Stam 1998). Because MEMS-based accelerometers form the basis for many motion-sensing applications, this review only

[2] In slightly adapted form, this chapter originally appeared in the Journal of Neuroengineering and Rehabilitation. See D. Steins, H. Dawes, J. Collett, and P. Esser, "Wearable accelerometry-based technology capable of assessing functional activities in neurological populations in community settings: a systematic review," J. Neuro. Eng. Reh. Vol. 11, 36, 2014.

considers wearable technology that contains accelerometers—at times, in conjunction with other MEMS applications. Accelerometers, in short, form a necessary, but by no means sufficient, criteria condition.

In this Chapter we explore the potential for using AT in this context. We begin by reviewing the work done using AT to measure various aspects of mobility-related functional activities (e.g. the type, quantity, and quality) in neurological populations in home and community settings. It will do so by addressing the following questions: Which sorts of accelerometry-based methods can accurately assess functional activities? Which types of outcome measures are suitable for obtaining quality measures of functional activities? Have these methods been implemented in home and community settings for rehabilitative purposes?

2.3 Methods

2.3.1 Study Characteristics

Neurological disorders are categorized as major chronic diseases (Giampaoli, Oyen et al. 2008). Because of their immense variety, this review only focuses on the most frequently occurring chronic conditions that induce motor fluctuations and movement disorders: Parkinson's disease (PD), multiple sclerosis (MS), stroke, Cerebral Palsy (CP), and Huntington's disease (HD).

While it defines mobility as the process of changing (d410-d429) and maintaining body positions (d450-d469) (WHO 2001), the ICF does not provide a unified definition of functional activities. Neither does general literature. Given such general omissions, in this review, "functional activities" denote basic functional abilities considered vital for independent living, such as walking, sitting, standing, and activity transitions.

2.3.2 Literature Search

A literature search was conducted on the following electronic bibliographic databases from January 2012 to January 2013: Cochrane (1940-2013), EMBASE (1974-2013), PubMed (1950-2013), Web of Knowledge (1980-2013), and IEEE Xplore (1946-2013). References from retrieved articles were checked using the Web of Science database. Generic search and MeSH terms for each database were used to identify relevant studies (see Appendix A). The search strategy was anchored on the following three categories: telemetry and rehabilitation, wireless technology, and human locomotion. Language restrictions were set. Only English studies were included.

2.3.3 Study Selection

Figure 2.1 illustrates the selection procedure used to screen studies. For each database search, titles and abstracts were screened by three independent reviewers. Literature eligibility was initially determined by whether or not the title and abstract involved AT for assessing mobility-related functional activities in neurological populations. The following exclusion criteria were used to further identify potentially relevant studies: 1) telephone counseling

interventions; 2) network interventions; 3) miscellaneous outcome measures (e.g. energy expenditure, activity behavior); 4) miscellaneous technology used for assessing functional activities (e.g. robotics, pedometers, force-sensing resistors, virtual reality, cueing devices); 5) reviews; 6) book reports; and 7) off-topic articles. Studies that provided insufficient information for the adequate interpretation of outcome measures and results were also excluded.

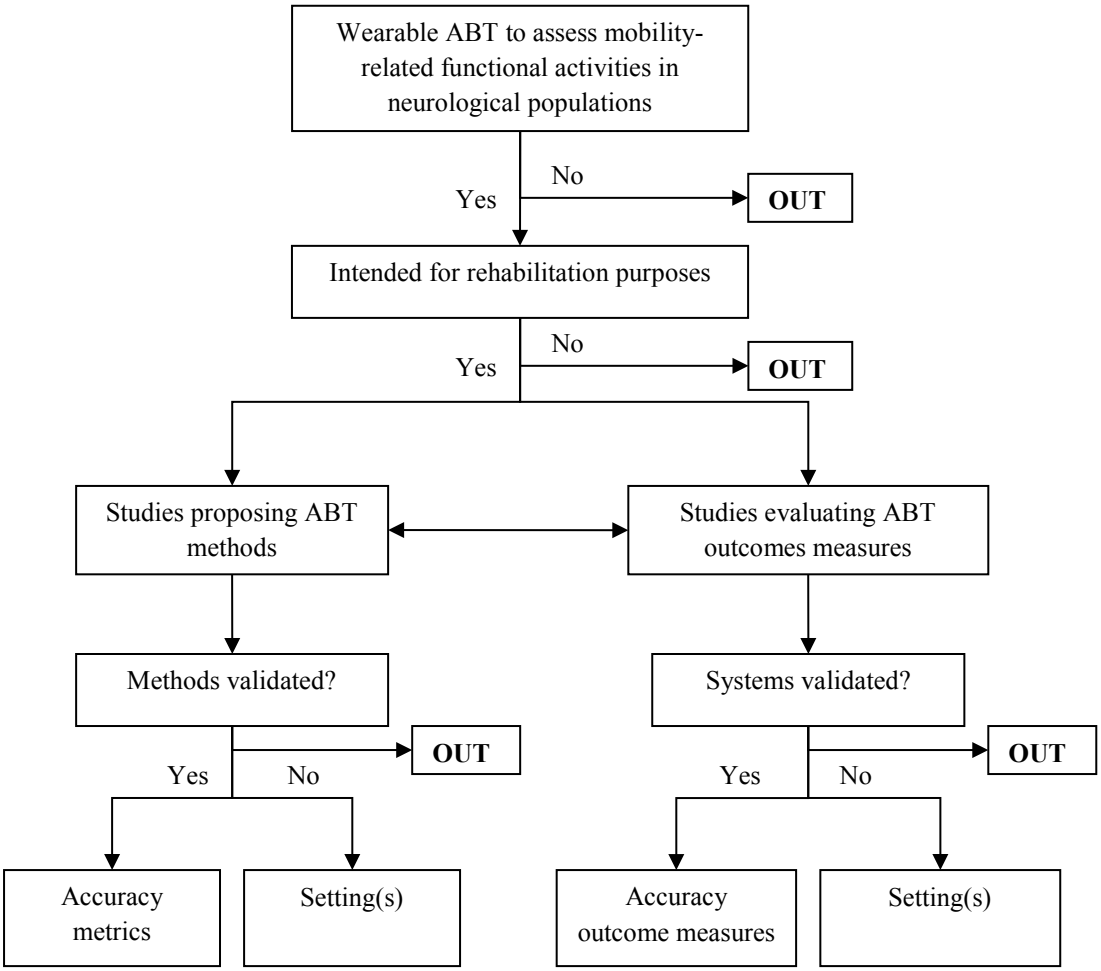

Figure 2.1 Procedure for the study selection and organization.

Full-text articles were then retrieved and evaluated by four independent reviewers. Studies were included if they: 1) concerned neurological conditions, 2) employed wearable AT, 3) evaluated mobility characteristics of the lower extremity through functional activities, and 4) were intended for rehabilitation purposes in home and community settings. Motor symptoms due to neurological disorders affecting mobility (e.g. spasticity, tremor) were additionally included in this review only if they were integrated as an aspect of mobility through functional activity testing. In order to ensure that results across studies were comparable, this

review distinguished studies using AT to evaluate the aforementioned outcome measures (mobility characteristics of functional activities) from studies proposing AT approaches. The validation of AT-systems served as the final screening measure for inclusion.

2.3.4 Assessment of Methodological Quality

Three authors independently evaluated the selected studies using two customized versions of methodological criteria adapted from the PEDro scale (Health 2012) and CONSORT (Group 2010) and Trend statements (Des Jarlais, Lyles et al. 2004). One version was founded on AT that evaluates outcome parameters of functional activities, while the other drew upon AT-methods.

Both customized versions were piloted to assess the reliability of the quality assessment process. All authors were blinded to paper authors, affiliations, publication dates, journals, funding sources, and references. Disagreements were resolved through consensus meetings.

The next step of the quality assessment process involved extracting information regarding the content, construction (e.g. measurement protocols), population (e.g. population size, reports of baseline characteristics), and measurement properties of each system. Extracted measurement properties were: content and criterion validity. The quality of measurement properties was determined by internal validity components (e.g. sample size) as well as external validity components (e.g. generalization). Study results needed to be founded on statistical methods, including accuracy metrics.

Accelerometry-based outcome measures were deemed valid if the methods were cross-validated with a gold standard criterion, such as an optical motion camera system. Going further, studies that introduced AT-methods based on activity classifiers or other approaches were also considered valid if their output successfully compared with that of suitable population-specific questionnaires (e.g. UPDRS) or cross-validated with appropriate statistical analysis (e.g. *K*-fold cross-validation, bootstrap method, leave-one-out method).

2.4 Results

The initial literature search resulted in the retrieval of 1738 studies (see Appendix B; flowchart of literature search results). After screening for relevant titles and abstracts, then winnowing out duplicates and off-topic studies, 522 studies remained. Most studies were excluded on the basis that they did not involve neurological conditions (see Appendix C; pie chart of screening results from literature search). In other cases, when authors published several studies on the same research initiative, only their most recent studies that satisfied the inclusion criteria were kept. After such selective factors were applied, fourteen studies remained. A reference search on the Web of Science retrieved two more relevant studies. The now sixteen studies (Higashi, Sekimoto et al. 2001; Sabelman, Fiene et al. 2004; Motoi, Higashi et al. 2005; Moore, MacDougall et al. 2007; Salarian, Russmann et al. 2007; Lau, Tong et al. 2009; Mizuike, Ohgi et al. 2009; Cancela, Pansera et al. 2010; Mitoma, Yoneyama et al. 2010; Zwartjes, Heida et al. 2010; Barth, Klucken et al. 2011; Dobkin, Xu et

al. 2011; Prajapati, Gage et al. 2011; Yang, Hsu et al. 2011; Zampieri, Salarian et al. 2011; Mera, Heldman et al. 2012) were categorized according to whether they proposed AT-methods (*N*=11), evaluated AT-outcome measures (*N*=6) able to assess mobility characteristics of functional activities, or performed a combination of both. A total of twelve studies passed the validation screening and were finalized for this review: nine method studies (Motoi, Higashi et al. 2005; Moore, MacDougall et al. 2007; Salarian, Russmann et al. 2007; Lau, Tong et al. 2009; Cancela, Pansera et al. 2010; Zwartjes, Heida et al. 2010; Barth, Klucken et al. 2011; Dobkin, Xu et al. 2011; Yang, Hsu et al. 2011) and four outcome studies (Mizuike, Ohgi et al. 2009; Dobkin, Xu et al. 2011; Prajapati, Gage et al. 2011; Zampieri, Salarian et al. 2011), with one study (Dobkin, Xu et al. 2011) straddling both categories.

2.4.1 Study Quality

The methodological quality scores for those studies evaluating outcome measures for mobility-related functional activities were consistently high. Scores ranged from 10 to 12 (max 12), whereas quality scores for studies proposing AT-methods were generally lower, ranging from 4 to 9 (max 13; see Appendix D and E).

Studies evaluating outcome measures of mobility-related functional activities largely involved stroke (*n*=3) (Mizuike, Ohgi et al. 2009; Dobkin, Xu et al. 2011; Prajapati, Gage et al. 2011) and PD (*n*=1) (Zampieri, Salarian et al. 2011). Stroke studies showed great diversity in study design, population demographics (e.g. population size, disease onset), and methodology. They consisted of pilot studies (*n*=2) (Dobkin, Xu et al. 2011; Zampieri, Salarian et al. 2011), one cross-sectional study (Mizuike, Ohgi et al. 2009), and one experimental study (Prajapati, Gage et al. 2011). Across all stroke studies, the age range was fairly comparable. Population demographics, conversely, were not comparable between studies, because of insufficient information. Most studies used a control group (*n*=3) (Mizuike, Ohgi et al. 2009; Dobkin, Xu et al. 2011; Zampieri, Salarian et al. 2011), of which only one adopted an age-matched control group (Zampieri, Salarian et al. 2011). System measurement properties were determined through internal validity components, which were stopwatch measures (Dobkin, Xu et al. 2011), optical motion-sensing systems (Mizuike, Ohgi et al. 2009; Zampieri, Salarian et al. 2011), or footswitches (Prajapati, Gage et al. 2011). Outcome measures were reasonably similar, mainly focusing on correlation and accuracy levels.

Studies evaluating AT-methods were mainly PD studies (*n*=6) (Moore, MacDougall et al. 2007; Salarian, Russmann et al. 2007; Cancela, Pansera et al. 2010; Zwartjes, Heida et al. 2010; Barth, Klucken et al. 2011; Yang, Hsu et al. 2011) and, to a lesser extent, stroke studies (*n*=3) (Motoi, Higashi et al. 2005; Lau, Tong et al. 2009; Dobkin, Xu et al. 2011). None involved other neurological conditions. The PD and stroke studies were all based on experimental study designs with small population groups ($n \leq 10$), minus two PD studies (Cancela, Pansera et al. 2010; Barth, Klucken et al. 2011), which recruited testing groups of 20 subjects or more. Between stroke studies, the population age ranged widely (45-68 years). Some studies were conducted without a control group altogether (Motoi, Higashi et al. 2005;

Lau, Tong et al. 2009). None featured an age-matched control group (Dobkin, Xu et al. 2011). The report of baseline characteristics and eligibility criteria revealed much diversity in medication treatment, disease onset, and disease severity (e.g. UPDRS scores), whether or not patients were sensitive to deep brain stimulation and experienced motor fluctuations. The measurement properties used to determine validity were primarily based on external validity components cross-validated with video recordings (Moore, MacDougall et al. 2007; Yang, Hsu et al. 2011) and statistical methods, such as *K*-fold cross-validation (Lau, Tong et al. 2009; Barth, Klucken et al. 2011). Three studies employed a combination of internal and external validation procedures (Salarian, Russmann et al. 2007; Cancela, Pansera et al. 2010; Zwartjes, Heida et al. 2010).

All studies demonstrated notable variation in terms of methodology, study design, population demographics, and outcome measures, making it difficult to evaluate study results. This rendered a meta-analysis unfeasible. For reading ease, the results are chronologically described below, according to this review's stated aims.

2.4.2 Accelerometry-based Methods able to Accurately assess Functional Activities

The term "accuracy" was applied in three ways. Firstly, it was used to describe if AT-methods were able to distinguish healthy from non-healthy subjects (i.e. quantity tick box). Secondly, it was used to assess disease severity levels (i.e. quality tick box). Thirdly, the term was used to signify the precision of reported metrics.

As previously mentioned, nine studies (Motoi, Higashi et al. 2005; Moore, MacDougall et al. 2007; Salarian, Russmann et al. 2007; Lau, Tong et al. 2009; Cancela, Pansera et al. 2010; Zwartjes, Heida et al. 2010; Barth, Klucken et al. 2011; Dobkin, Xu et al. 2011; Yang, Hsu et al. 2011), consisting of six PD studies (Moore, MacDougall et al. 2007; Salarian, Russmann et al. 2007; Cancela, Pansera et al. 2010; Zwartjes, Heida et al. 2010; Barth, Klucken et al. 2011; Yang, Hsu et al. 2011) and three stroke studies (Motoi, Higashi et al. 2005; Lau, Tong et al. 2009; Dobkin, Xu et al. 2011), proposed valid accelerometry-based methods able to identify mobility-related functional activities. These methods were founded on various machine-learning classifiers (Salarian, Russmann et al. 2007; Lau, Tong et al. 2009; Cancela, Pansera et al. 2010; Zwartjes, Heida et al. 2010; Barth, Klucken et al. 2011; Dobkin, Xu et al. 2011), algorithms (Moore, MacDougall et al. 2007; Yang, Hsu et al. 2011), and gait cycle parameters (Motoi, Higashi et al. 2005). Table 2.1 provides an overview of the different classification techniques used to determine the types of functional activities and their capabilities whirrs Table 2.2 provides a more detailed overview on the type of sensors, sensor placement, and the study results.

Table 2.1 Overview of AT methods.

Authors	Population	Method	Validity	Quality	Quantity	Activity
Lau et al (2009)	Stroke	SVM, MLP, RBF	Leave-one-subject-out method	-	-	Walking
Barth et al (2010)	PD	Boosting with Decision Stump as weak learner, LDA, and SVM with linear and RBF kernel	Leave-one-subject-out method	x	x	Walking, foot circling, and heel-toe tapping
Cancela et al (2010)	PD	*k*NN, Parzen, Parzen density, binary decision tree, Bpxnc Train NN by back-propagation, and SVM	Cross-validation	x	-	Daily activities (i.e. walking, lying, sitting, drinking a glass of water, opening and closing a door)
Salarian et al (2007)	PD	Logic Regression model with Mamdani fuzzy rule-based classifier	Cross-validation	-	x	sit-to-stand and stand-to-sit
Zwartjes et al (2010)	PD	Decision tree	Leave-one-subject-out method	x	-	lying, sitting, standing, and walking
Yang et al (2011)	PD	Autocorrelation method	Video recordings	-	x	Walking
Motoi et al (2005)	Stroke	Sagittal angle changes		-	-	Walking and sit-to-stand
Moore et al (2007)	PD	Mathematical step-length algorithm	Pen techniques and video recordings	x	x	Walking
Dobkin et al (2011)	Stroke	NB classifier in combination with Gaussian discretization followed by a maximum likelihood estimation	Stopwatch	-	x	Walking

Abbreviations: LDA, Linear Discriminant Analysis; SVM, Support Vector Machines; RBF, radial basis function neural network; K-NN, K-nearest neighbour; NN, Neural Network; MLP, multi-layer perception; Quality, methods assessing severity levels, Quantity, methods able to distinguish healthy from non-healthy subjects.

2.4.2.1 Parkinson's Disease

Classifiers. Four out of the six PD studies (Salarian, Russmann et al. 2007; Cancela, Pansera et al. 2010; Zwartjes, Heida et al. 2010; Barth, Klucken et al. 2011) employed machine-learning classifiers. Three of these four used their classifier to identify ambulatory activities (Cancela, Pansera et al. 2010; Zwartjes, Heida et al. 2010; Barth, Klucken et al. 2011) and other functional activities (e.g. sitting, standing (Cancela, Pansera et al. 2010; Zwartjes, Heida et al. 2010)). The remaining study used its activity classifier to detect sit-to-stand (STS) transitions from non-transitions (Salarian, Russmann et al. 2007). From these four studies, Barth et al. (Barth, Klucken et al. 2011) and Cancela et al. (Cancela, Pansera et al. 2010) evaluated various activity classifiers. Barth et al. (Barth, Klucken et al. 2011) evaluated

the following activity classifiers to detect gait patterns able to distinguish healthy controls from PD patients and mild gait impairments from severe ones: Boosting with decision stump (i.e. one-level decision tree), Linear Discriminant Analysis (LDA), and SVM with linear and Radial Basis Function (RBF) kernel. The accuracy of their sensor system was based on three activities from the UPDRS (Part III), namely 10m walking, heel-toe tapping, and foot circling. The LDA classifier achieved the best overall accuracy, classifying patients and controls with a sensitivity of 88% and specificity of 86%. When optimized for the most accurate features, it reached a 100% sensitivity and specificity. The most optimal features were derived from step features (step duration), signal sequence (entropy (Shannon 1948), variance), and frequency analysis (energy ratio and 0.5-3Hz energy band). Cancela et al. (Cancela, Pansera et al. 2010), on the other hand, used six different activity classifiers—*k*-nearest neighbour [*k*NN], Parzen, Parzen density, Binary decision tree, feed-forward neural network [Bpxnc], and SVM—to detect the severity of walking-derived bradykinesia according to UPDRS scores. Using two statistical features (root mean square values and range) over a 5s interval, with a 50% overlap, the SVM classifier related the best to clinical UPDRS output scores, with an accuracy ranging between 70% and 86%.

Besides evaluating activity classifiers, Cancela et al. (Cancela, Pansera et al. 2010), like Zwartjes et al. (Zwartjes, Heida et al. 2010), also assessed symptom severity levels in PD as part of their detection process. Zwartjes et al. (Zwartjes, Heida et al. 2010) employed a decision tree for a complete motor assessment by simultaneously analyzing various functional activities and symptom severity (i.e. tremor, bradykinesia, hypokinesia) at different levels of deep brain stimulation, with an overall accuracy of 99.3%. Their motor assessment was mainly founded on UPDRS-items (Part III), including foot-tapping and several daily activities. Their PD monitor correlated well with the UPDRS and could detect significant changes in rest and kinetic tremor, with an accuracy ranging from 78.7% to 94.1%, depending on the activity performed.

The remaining study by Salarian et al. (Salarian, Russmann et al. 2007) used an activity classifier to categorize STS transitions. Able to separate transitions from non-transitions and to differentiate between sit-to-stand and stand-to-sit with a sensitivity of 83.8% for PD and 94.4% for healthy controls, their method used a mamdani fuzzy rule-based classifier in tandem with two statistical classifiers based on a generalized logistic regression model. Acceleration and tilt measures of the trunk, previously described by Najafa et al. (Najafi, Aminian et al. 2002; Najafi, Aminian et al. 2003), were used to detect transitions. Salarian et al.'s method (Salarian, Russmann et al. 2007) has been integrated into the iTUG (Instrumented Timed-Up and Go Test) (Salarian, Horak et al. 2010; Zampieri, Salarian et al. 2011), which also contains a 180 degrees turn analyzing algorithm (Salarian, Zampieri et al. 2009).

The two other PD studies (Moore, MacDougall et al. 2007; Yang, Hsu et al. 2011) based their method on algorithms. For ambulatory rehabilitation and gait assessments, Yang et al. (Yang, Hsu et al. 2011) validated the vertical acceleration's autocorrelation function for the real-time analysis of disabling PD gaits. Moore et al. (Moore, MacDougall et al. 2007), conversely, developed a validated stride length algorithm able to accurately estimate the stride length of

healthy and PD subjects in their natural environment. The ensuing stride length measures exhibited a linear relationship to actual stride lengths (r=.98), obtaining a higher accuracy (mean error ± 0.05m) than that of previous techniques (Miyazaki 1997; Aminian, Najafi et al. 2002). In a follow-up study, the stride length monitor's capabilities were extended with the detection of freezing events in PD (Moore, MacDougall et al. 2008).

2.4.2.2 Stroke

Classifiers. Two out of the three stroke studies (Lau, Tong et al. 2009; Dobkin, Xu et al. 2011) employed machine-learning classifiers for the detection of ambulatory activities, whereas the remaining stroke study assessed functional activities through angle measurements (Motoi, Higashi et al. 2005).

In presenting a possible tool for pathological gait analysis, pattern recognition, and activity monitoring, Lau et al. (Lau, Tong et al. 2009) explored the performance of various classifiers (i.e. SVM, artificial neural network [ANN], RBF, Bayesian belief network [BBN]) in different walking conditions (e.g. level ground, stair ascent, stair descent, upslope, downslope) for stroke subjects with dropped foot. The SVM proved superior to other classifiers, achieving an overall accuracy of 92.9% to 96.8% for both groups and individuals. In addition, it distinguished stair ascent and descent from other conditions with 100% accuracy and classified all five conditions with 84% accuracy.

Dobkin et al. (Dobkin, Xu et al. 2011) successfully implemented a naive Bayes method to estimate the walking speed of stroke patients in home and community settings. This method only needed 10 repetitions of a purposeful movement or 2 walks of 10 m at >1 speed to fulfill the requirements. Feature extraction was based on time domain data (e.g. dominant frequencies, amplitudes, waveforms of acceleration, signal derivatives) that was converted into vector form. The estimation of outdoor walking speeds highly correlated with stopwatch-measured speeds (r=.98; p=.001), including repeated measures (p=.01).

Unlike the two studies above, Motoi et al. (Motoi, Higashi et al. 2005) presented a gait and STS analyzing method based on angle and acceleration patterns to determine the level of long-term care. Noticeable angle changes and fluctuations of the trunk, thigh, and knee were detected between different severity and care levels.

Table 2.2 Studies proposing AT-methods to assess mobility-related functional activities in neurological populations

Year	Author	Population/study design	Sensor system	Methodology	Validation procedure	Results	Correlation with clinical measure
2010	Barth et al.	- Experimental study - Parkinson's disease (*N*=27); Group 1 – mild PD, UPDRS Scores <15 (*N*=14); Group 2 – intermediate PD, UPDRS >20 (*N*=13) - Healthy controls (*N*=16)	2 inertial sensors (attached on each lateral heel of a shoe) Sample frequency: 100Hz	Distinguish mild and severe gait impairment Feature extraction based on frequency, step, and sequence features from single steps and complete gait cycle Tested 3 different classification techniques: - Boosting with Decision Stump as a weak learner - Linear Discriminant Analysis - Support Vector Machine with linear and Radial Basis Function kernel	Classifier accuracy assessed with *leave-one-subject-out* method	The best overall accuracy was reached in each case using the LDA classifier. Classification: Control vs. Group 1: sensitivity 88%, specificity 86% (10m walk test). Distinction of both Control vs. Group 2 and Group 1 vs. Group 2 reached a sensitivity and specificity of 100%	—
2010	Cancela et al.	- Experimental study - Parkinson's disease (*N*=20); stable dopaminergic treatment, experiencing motor fluctuations - Healthy controls (*N*=16)	6 tri-axial accelerometers (attached on the limbs, trunk, and belt) Sample frequency: *unknown*	Determine severity of bradykinesia - using the resultant vector (Euclidean vector method) - Statistical features: Root Mean Square, entropy, range of values and cross correlation in 12 different combinations 6 classifiers used to classify the epochs: - *K*-Nearest Neighbor - Parzen - Parzen density - Binary decision tree - Bpxnc Train Neural Network - Support Vector Machine Method output according to the UPDRS, score between 0 and 4	Clinician *UPDRS* scores Classifier - Cross-correlation method (training and test set)	Symptom severity accuracies lay within the range of 70% - 86%	Related output scores to the UPDRS, but no correlation measures

Abbreviations: UPDRS, Unified Parkinson Disease Rating Scale; f/s, Frames per Second.

Table 2.2 (Continued)

Year	Author	Population/study design	Sensor system	Methodology	Validation procedure	Results	Correlation with clinical measure
2011	Dobkin et al.	- Pilot study - Stroke (*N*=12) - Healthy controls (*N*=6)	2 tri-axial accelerometers (attached above the ankle) Sample frequency: 320Hz	Detection and activity classification based on a Naive Bayes classifier Features: frequencies, amplitudes, and waveforms of accelerations, and time averages and derivatives Gaussian discretization of features into model-free clusters, followed by maximum likelihood estimation for real classification	Stopwatch measures, observer step counts, and activity logs	Concurrent validity comparison between stopwatch timed and algorithm-derived outdoor walking speeds, as well as their relationship to the indoor walking speeds *Walking speed* Stroke: *Pearson's r* outdoor walking speed *r*=.98 (*p*=.001); test-retest reliability for repeated walks was high (*p*=.01) Healthy: *r*=.98 (*p*=.001)	—
2007	Moore et al.	- Experimental study - Parkinson's disease (*N*=7) - Healthy controls (*N*=10)	1 inertial sensor (attached on the shank) Sample frequency: *unknown*	Estimation of stride length by proposing a novel step-length algorithm based on the vertical acceleration and pitch angular velocity - Least-square error fit	Pen technique Comparison to video recordings	Accuracy stride monitor estimation, mean error 0.05m	—
2005	Motoi et al.	- Experimental study - Stroke (*N*=14) - Healthy controls (*N*=11)	2 dual-axial accelerometers and 1 inertial sensor (dual-axis acc. + single axis gyro (attached on the sternum, thigh and calf) Sample frequency: 25Hz	Detection of dynamic and static posture changes Motion characteristics: - Angle changes in sagittal plane - Walking speed	Comparison to video recordings 30f/s	Comparison wearable system accuracy against video recordings - Walking speed; *r*=.992 - Angle change; *r*=.997 Comparison rehabilitation program before and after (no data presented) - Before: more fluctuations maximum values angle changes - After: higher repeatability in detecting maximum values	—

Table 2.2 (Continued)

Year	Author	Population/study design	Sensor system	Methodology	Validation procedure	Results	Correlation with clinical measure
2009	Lau et al	- Experimental study, observational classifier - Stroke (*N*=7) - No Control group	2 inertial sensors (one attached to the shank and one to the foot) Sample frequency: 240 Hz	Test 3 different classifiers: Support Vector Machine Neural Network using Multi-layer Perceptron Radial Basis Function Network Feature extraction, dataset variables: - Sh(AV_{ps}) – pre-swing phase - Sh(Acc_{ps}) – pre-swing phase - Ft(Acc_{ps}) – pre-swing phase - Sh(Acc_{is}) – initial swing phase - Ft (Acc_{is}) – initial swing phase Dataset 1: Shank variables Dataset 2: Foot variables Dataset 3: Shank and foot variables	Dataset: 50% training set and 50% testing set	The SVM technique always performed better than MLP and RBF The overall accuracy increased from 92.9% to 96.8% in 3-class classification for a group and for an individual	—
2007	Salarian et al	- Experimental study - Parkinson's disease (*N*=10) - Healthy controls (*N*=10)	3 inertial sensors (one attached to the trunk, two to the shanks) Sampling frequency: 200Hz	Detection and classification of transition Features used: - TD (s) - Min ($\theta_{g\text{-}lp}$) - Range($\theta_{g\text{-}lp}$) - Range($a_{trunk\text{-}lp}$), Max($a_{trunk\text{-}lp}$), Min($a_{trunk\text{-}lp}$), t0, t[Max($a_{trunk\text{-}lp}$)] Separate transitions from non-transitions - two statistical classifiers based on logistic regression model Classification of the activities - implemented a fuzzy classification method (6 fuzzy variables used)	Video comparison, event detection Face to face validity with the *UPDRS* Trained method (transition/non-transition): 70% data set (randomly) and 30% used for evaluation of outcomes	Detection of posture transitions, compared to video recording as a reference - Sensitivity 94.4% (Controls) and 83.8 (PD) - Specificity 96.9% (Controls) and 87.0% (PD) Classification of basic activities (i.e. walking, standing, sitting, and lying - Sensitivity controls - walking (99.1%), standing (96.1%), sitting (99.5%), and lying (100%) - Sensitivity PD- walking (98.5%), standing (83.6%), sitting (86.3%), and lying (91.8%)	Significant correlation (p<.05) with the *UPDRS*: - TD, r= .64 - Max($a_{trunk\text{-}lp}$), r=-.55 - Min($a_{trunk\text{-}lp}$), r=.69 - Range($a_{trunk\text{-}lp}$), r=-.65

Abbreviations: UPDRS, Unified Parkinson Disease Rating Scale; TD, Transition Duration, defined as the time interval between two peaks; Min ($\theta_{g\text{-}lp}$), the amplitude negative peak trunk flexion/extension; Range($\theta_{g\text{-}lp}$), the range of anterior-posterior tilt of the trunk; Range($a_{trunk\text{-}lp}$), Max($a_{trunk\text{-}lp}$), Min($a_{trunk\text{-}lp}$), t[Min($a_{trunk\text{-}lp}$)], t[Max($a_{trunk\text{-}lp}$)], the norm of the acceleration vector of the trunk sensor; SVM, Support Vector Machine; MLP, Neural Network using Multi-layer Perceptron; RBF, Radial Basis Function Network; Sh(AV_{ps}), Shank Angular Velocity, Sh(Acc_{ps}), amplitude values of the anterior-posterior acceleration.

Table 2.2 (Continued)

Year	Author	Population/study design	Sensor system	Methodology	Validation procedure	Results	Correlation with clinical measure
2011	Yang et al	- Experimental study - Parkinson's disease (*N*=5); H&Y stage II and III - Healthy controls (*N*=5)	1 tri-axial accelerometer (attached to the trunk) Sample frequency: 50Hz	Autocorrelation procedure Gait cycle features obtained: - Step regularity - Stride regularity - Step symmetry - Cadence	Cadence validation through video recordings	Cadence validation: Mean absolute percentage error 4.89% Comparison multiple slide windows (Mean CV, Mean error): Cadence: 1.21%, 0.67%; Step/Stride regularity: 8.53%, 2.44%; 9.34%, 4.47%; Step symmetry: 7.78%, 2.04%	—
2010	Zwartjes et al	- Clinical trial with control group - Parkinson's disease (*N*=6); sensitive to DBS treatment (<5min), no major motor fluctuations due to medication - Healthy controls (*N*=7)	4 inertial sensors (attached on the trunk, wrist, thigh and foot of the MAS) Sample frequency: 50Hz	Classify motor activity to differentiate between lying, sitting, standing, standing up, and walking using 7 Binary decision nodes Feature extraction for particular nodes are based on the integrals of the absolute value of the accelerometer output: Motor Symptom Monitor - Classify motor symptom severity (i.e. rest/ kinetic tremor, bradykinesia, and hypokinesia) Tremor: feature extraction - Frequency analysis - Algorithm TS = $i\sqrt{d}$ Bradykinesia: feature extraction - average value of acceleration (during periods of AAM) - step length, step velocity - duration standing-up Hypokinesia - % arm movement during the entire sitting and standing time - Arm swing and thigh swing correlation	Compared to video recordings (25 f/s) – test-retest reliability not assessed	Activity detection - PD – Overall accuracy of 98.9% - Controls - Overall accuracy of 99.3% MSM - Quantify tremors - PD - accuracy of rest tremor; sitting (84.5%) and standing (94.1%) in the arm; sitting (79.1%) and standing (90.1%) in the thigh - Kinetic tremor in the arm detection; accuracy sitting (78.7%) and standing (81.7%) Proposed method/monitor can discriminate between different settings of the DPS stimulator; Arm, thigh, and trunk rest tremor (p<.05, p=.01, and p<.01)	Quantification tremor with *UPDRS* 20 scores - Best correlation - rest tremor in arm, r=.84 (p<.01) - Kinetic tremor, r=.67 (p<.01) up to *UPDRS* item 21

Abbreviations: H&Y, Hoehn & Yahr; AC, Activity Classifier; DBS, Deep Brain Stimulation; MSM, Motor Symptom Monitor; AAM, Active Arm Movement; TS, Tremor Severity; MAS, Most Affected Side; CV, Coefficient of Variance.

2.4.3 Outcome Measures suitable for obtaining Quality Measures of Functional Activities

Research on the effectiveness of neurorehabilitation is of upmost importance and necessitates the determination of appropriate outcome measures beforehand. Four out of six studies (Mizuike, Ohgi et al. 2009; Dobkin, Xu et al. 2011; Prajapati, Gage et al. 2011; Zampieri, Salarian et al. 2011) (three stroke studies (Mizuike, Ohgi et al. 2009; Dobkin, Xu et al. 2011; Prajapati, Gage et al. 2011), one PD study (Zampieri, Salarian et al. 2011)) passed the eligibility criteria (Section 2.3) and were categorized as valid (see Table 2.3) whirrs Table 2.4 provides a more detailed overview on the type of sensors, sensor placement, clinical outcome, parameters measures, and the overall studies results

Table 2.3 Overview of accelerometry-based outcome measures.

Authors	Population	Outcome parameters	Validity	Quality	Quantity	Activity
Dobkin et al. 2011	Stroke	Walking speed, bouts of walking, gait symmetry	LOOCV	-	x	Walking
Zampieri et al. 2011	PD	Stride length, stride velocity, cadence, peak arm swing velocity on the MAS, and turning velocity	LOOCV	-	x	Sitting, Standing, Walking, Turning
Mizuike et al. 2009	Stroke	Accelerometers derivatives Raw RMS Normalized RMS Autocorrelation function	Cross-validation	x	x	Walking
Prajapati et al. 2011	Stroke	Walking bouts Total walking time Gait speed Number of steps Gait symmetry Swing symmetry Cadence	Cross-validation	x	-	Walking

Abbreviations: MAS, most affected side; LOOCV, Leave-one-subject-out method; Quality, studies assessing severity levels; Quantity, studies able to distinguish healthy from non-healthy subjects.

Stroke. Walking speed is generally considered to be a significant, sensitive, and reliable marker of deficit severity and walking ability (Patterson, Forrester et al. 2007) and a predictor of falls (Guimaraes and Isaacs 1980, Luukinen et al. 1995). With this understanding in mind, Dobkin et al. (Dobkin, Xu et al. 2011) and Prajapati et al. (Prajapati, Gage et al. 2011) both affirmed walking speed as a sensitive outcome measure able to evaluate the effect of rehabilitation on movement quality and stroke severity indices. Dobkin et al. (Dobkin, Xu et al. 2011) found walking speed could be related to stroke severity and recovery. Patients who walked faster than $0.8ms^{-1}$ could reach higher speeds under different walking conditions than

those who walked below 0.8ms^{-1}. Prajapati et al. (Prajapati, Gage et al. 2011) more or less confirmed this observation by finding a correlation between walking speed; balance impairment, as measured by the Berg Balance Scale (Berg, Wood-Dauphinee et al. 1995) (r=.60; p<.013); and walking period (r=.51; p=.045) (see Appendix H).

Mizuike et al. (Mizuike, Ohgi et al. 2009) proposed a different outcome measure, an acceleration-derived one, normalizing the root mean square (nRMS) values of acceleration to forge a new measure by which to evaluate gait characteristics and form an index of treatment outcomes for rehabilitation. The values of the nRMS may serve as an indicator for the dynamics of walking patterns, reflecting motor recovery and gait abilities. nRMS values were also able to discriminate between groups (p<.01) and several Brunnstrom Stages (III-V, IV-V, p<.05).

Parkinson's disease. Previous studies on the performance of the iTUG by Zampieri et al. (Zampieri, Salarian et al. 2010) and Salarian et al. (Salarian, Horak et al. 2010) determined sensitive outcome measures that formed the basis for the home feasibility study conducted by Zampieri et al. (Zampieri, Salarian et al. 2011). Peak arm swing velocity on the most affected side, average turning velocity, cadence, and peak trunk rotation were significantly slower in PD than in control subjects. These factors may potentially be used to detect disease progression and patient response to symptomatic and disease-modifying treatments. The iTUG's STS components (e.g. duration, range of motion, angular velocity) were the least reliable, while walking and turning components (e.g. stride length and velocity, cadence, peak arm swing velocity, turning velocity) were the most reliable. Zampieri et al. (Zampieri, Salarian et al. 2011) demonstrated that from the aforementioned outcome measures, stride velocity (p=.02) and length (p=.002) affected PD subjects significantly when assessed at home, resulting in slower and shorter steps.

Table 2.4 Studies evaluating AT-outcome measures to assess mobility-related functional activities in neurological populations

Year	Author	Population/study design	Sensor system/ validation procedure	Clinical outcome measure(s)	Gait parameters	Results	Correlation with clinical measure
2011	Dobkin et al	- Pilot study - Stroke (*N*=12) - Healthy controls (*N*=6)	2 tri-axial accelerometers (*unknown*; 320Hz) attached above the ankle Stopwatch calculations	50-ft clinic walks at slow, casual, and fast speeds 300-ft clinic-outdoor walks	Gait speed Bouts of walking Cadence Swing time	Pearson correlation between stopwatch measured indoor walking speed and algorithm-calculated speed, r=.98, p=.001 and for repeated measures (p=.01)	—
2009	Mizuike et al	- Cross-sectional study - Stroke (*N*=63); Brunnstrom stage III(10), IV(22), V(15), VI(16) - Control group (*N*=21); elderly	1 tri-axial accelerometer (200Hz) on the waist Recorded observations	10m walk test	Accelerometers derivatives (x, y, z axis): Raw RMS Normalized RMS Autocorrelation function	Raw RMS and AC values significantly lower and normalized RMS values were significantly higher at all axes in stroke patients compared to controls. These parameters were also significantly different between control groups and each group in the different Brunnstrom motor recovery stages.	Brunnstrom Stages
2011	Prajapati et al	- Experimental study - Subacute Stroke (*N*=16); BBS 41.8±9.9 - No control group	2 tri-axial accelerometers on the ankle (50Hz) Footswitch system – comparing FO and FC events	Compared laboratory gait assessment with GAITRite system	Walking bouts Total walking time Gait speed Number of steps Gait symmetry Swing symmetry Cadence	Significant association between the number of walking bouts to the total walking time (r=.76; p< .006) and laboratory gait speed (r=.51; p<.45) Laboratory gait speed and BBS (r=.60; p<.013) Significant gait symmetry increase between day-long measurement compared with standard laboratory assessment (p=.006), 12 out of 16 were more asymmetrical during the day-long measurement	Lower laboratory gait speed and lower BBS score
2011	Zampieri et al	- Pilot study - Parkinson's disease (*N*=6); early-to-mid stages, UPDRS 28.6±15 and H&Y 1.9±0.7 - Healthy controls (*N*=8)	5 inertial sensors. 2 rate gyros on the wrist and shank and one sensor on the sternum, 200Hz Reported in Simoes et al. (Simoes 2011) – compared to a Vicon system	iTUG test – 7m walkway (three trails conducted at home and laboratory setting)	Stride length Stride velocity Cadence Peak arm swing velocity Turning velocity	- Distances walked at home were slower and with shorter steps in the PD group than the laboratory, but similar between groups: PD = 5.9±0.5m, Control = 5.9±0.6m in laboratory - Significant group effect for stride velocity (p=.03), cadence (p=.001), peak arm swing velocity MAS (p=.002), and turning velocity (p=.02) - Significant interaction effect for stride velocity (p=.02), and stride length (p=.002) - Significant location effect for turning velocity (p=.002) in control group	—

Abbreviations: UPDRS, Unified Parkinson Disease Rating Scale; H&Y, Hoehn & Yahr Score; iTUG, Instrumented Timed Up and Go Test; MAS, Most Affected Side; 5WMT, 5-min Walking Test; BBS, Berg and Balance Scale ;FO, Foot Off; FC, Foot Contact.

2.4.4 Accelerometry-based Technology implemented in Non-Clinical Settings

From this review's twelve featured studies, only three (Moore, MacDougall et al. 2007; Dobkin, Xu et al. 2011; Zampieri, Salarian et al. 2011) actually took measurements in both clinical and non-clinical environments. Two out of these three studies, both incidentally dealing with stroke, proposed ambulatory activity pattern estimations, one for stride length (Moore, MacDougall et al. 2007) and the other for walking speed (Dobkin, Xu et al. 2011). The remaining study by Zampieri et al. (Zampieri, Salarian et al. 2011), a PD one, investigated the possibility of implementing the iTUG in home environments. It was the only study in this review to broach this subject (see Appendix F).

Results for the remaining neurological studies were only garnered through clinical assessments carried out at hospitals or laboratory environments. Although all studies were intended for telerehabilitation purposes, only Salarian et al.'s (Salarian, Russmann et al. 2007) and Motoi et al.'s (Motoi, Higashi et al. 2005) methodological studies helped pave the way for later studies that examined the implementation of MEMS-based accelerometers in non-clinical settings.

2.5 Discussion

Search results indicate that a vast amount of literature exists (*N*=522), especially in the engineering field, on wearable motion-sensing applications that assess functional activities. Only 22.2% of the studies mentioned, however, use AT in neurological populations. Only 9.7% of these targeted studies, in turn, are intended for rehabilitative purposes in non-clinical settings. Of this last group, the majority of studies focus on the classification and quantification of ambulatory activities in Parkinson or stroke survivors, excluding subjects coping with other neurological diseases. The quantification of mobility-related functional activities—walking, in particular—generates much information on a patient's physical capabilities, recovery, and activity behavior. But it is ill-equipped to address the qualitative measures of exercise performance, inevitably omitting those details clinicians require to tailor therapies and medications to an individual's needs.

Although this review has identified a few studies that evaluate outcome measures able to address rehabilitation's impact on movement quality, the primary challenge still remains: How can more appropriate outcome measures be established—those more useful to determining the movement quality of each severity stage? While the main focus of this review lies in the accurate classification of various functional activities, future research should analyze such activities beyond the scope of step counts and duration.

2.5.1 Accuracy of AT-methods

The number of studies (*N*=12) that covers the measurement properties of the reliability, validity, and responsiveness of accelerometry-based systems in neurological populations remains relatively low. Those methodological studies included that cover measurement properties may, in

some cases, be compromised in terms of sample size. For those studies proposing methods based on activity classifiers (Salarian, Russmann et al. 2007; Lau, Tong et al. 2009; Cancela, Pansera et al. 2010; Barth, Klucken et al. 2011; Dobkin, Xu et al. 2011), sample sizes range from 5 to 27 subjects. Such numbers are usually too small to generalize accuracy levels. Two out of such activity classifier-based studies, moreover, lacked a control group (Lau, Tong et al. 2009; Cancela, Pansera et al. 2010). It is therefore important to evaluate activity classifier performance according to larger, homogeneous population sets that include an equal number of healthy and non-healthy participants (Domingos 2012).

How effective or well-performing a classifier is not only depends on its overarching study design, but also on the study's selected features and AT accuracy. In general, difficulties evaluating a particular classifier's success stem from the relative silence regarding the feature extraction process, which depends on the analysis of movement patterns (Theodoridis and Koutroumbas 2008). How AT plays into classifier performance remains less obscure because it is well-canvassed in comparison to feature extraction. While generally considered to be an easy-to-use and inexpensive type of technology, AT is prone to offset fluctuations, sensor noise, and estimation errors, which lead to integration drift (Zhou and Hu 2008). Placing multiple accelerometers in combination with gyroscopes across the body increases the accuracy to achieve classification of multiple activities and postures. A range of classifications can, however, also be achieved using a single instrument (Murakami and Makikawa 1997; Mathie, Coster et al. 2003). Another possible solution is the integration of a Kalman filter with received signal strength indicator (RSSI) measurements can drastically reduce this drift, increasing overall accuracy (Zhou, Hu et al. 2010; Blumrosen and Luttwak 2013). Blumrosen et al. (Blumrosen and Luttwak 2013) have recently assessed the feasibility of employing RSSI in coordination with AT for body tracking and feature extraction purposes, establishing various criteria and analytical methods to facilitate this end.

Most studies wielding AT in neurological populations for remote rehabilitation employ various machine-learning classifiers that cover different aspects of neurorehabilitation, ranging from activity classification and symptom severity level assessment to long-term activity monitoring. While the question of which classifier is ideal for remote monitoring naturally follows, it currently cannot be addressed due to scant research in the field of telerehabilitation. This review did, however, identify studies that cross-examine the performance of different activity classifiers and their feature selections (Lau, Tong et al. 2009; Cancela, Pansera et al. 2010; Barth, Klucken et al. 2011). The SVM, LDA, and decision tree seem to perform better than their counterparts. The SVM, it must be added, was presented in the top ten most influential machine-learning algorithms (Domingos 2012).

2.5.2 Potential of AT in non-clinical settings

In the process of gathering studies that deploy AT intended for rehabilitation purposes in non-clinical settings, this review identified several promising studies (Zwartjes, Heida et al. 2010;

Dobkin, Xu et al. 2011; Zampieri, Salarian et al. 2011). Dobkin et al. (Dobkin, Xu et al. 2011) present a pilot study that grounds its feature extraction on a naive Bayes method in a Medical Daily Activity Wireless Network (Dobkin and Dorsch 2011; Xu, Batalin et al. 2011). Its machine-learning algorithm can not only identify, quantify, and qualify different activities, but also assess activity behavior during the day. Naive Bayes (or simply "Bayes") is easy to construct and can be readily applied to large data sets, as the method does not need any complicated iterative parameter estimation schemes.

In terms of assessing mobility deficits in patients with early to mid-PD, Zampieri et al. (Zampieri, Salarian et al. 2011) successfully test the feasibility of assessing the iTUG in home environments. Several papers (Salarian, Zampieri et al. 2009; Salarian, Horak et al. 2010; Zampieri, Salarian et al. 2010) have contributed to this approach, including Salarian et al.'s feature extraction paper on STS transitions (Salarian, Russmann et al. 2007). Salarian et al.'s method can not only distinguish between PD and healthy subjects, but also between "on" and "off" conditions in PD subjects. In terms of feature selection, their feature sets correlate reasonably well with the UPDRS, indicating that severity levels can potentially be judged and monitored.

Exploring this potential, Zwartjes et al. (Zwartjes, Heida et al. 2010) actually classify PD symptoms in various functional activities and their severity, correlating their AT method with UPDRS scores (e.g. tremor r=.87, p<.01) as other studies do (Hoff, van den Plas et al. 2001; Salarian, Russmann et al. 2007). Strikingly enough, their PD monitor detects changes between different conditions of brain stimulation, whereas the UPDRS does not. The UPDRS is the most widely used instrument for measuring PD symptom severity, having excellent test-retest reliability for motor scores (ICC 0.90) and moderate-to-good reliability for symptom-based scales (ICCs ranging from 0.69-0.88) (Siderowf, McDermott et al. 2002). That an AT-based PD monitor not only nicely correlates with the UPDRS, but also allows for more sensitive readings of PD symptoms renders it an attractive measurement tool to assist the UPDRS.

So far, MEMS-based accelerometers, embedded with machine-learning algorithms, are deemed able to accurately assess various mobility-related functional activities and disease symptom severity levels. The performance of these activity classifiers, however, heavily rely on the purpose of the study and their approach. At present, much variability exists among approaches (including the numbers of body-fixed sensors and sensor locations) to obtain useful data to analyze human movement. From an end-user's perspective, reducing the amount of sensors to one instrument that is attached to a single location on the body would greatly simplify the design and use of the system. Mizuike et al., was the only identified study in this review that used a single sensor near the center of mass of the subject (Mizuike, Ohgi et al. 2009). A location considered suitable to derive simple parameters, such as step and cycle time and stride symmetry (Evans, Duncan et al. 1991; Auvinet, Berrut et al. 2002). In addition to the former, their results (based on solely a 10m walk) demonstrate that, using a rectified version of the acceleration signal (normalized by velocity and mean step length), healthy subjects can be distinguished from

non-healthy subjects (i.e. stroke survivors) as well as their disease severity levels. From a clinician's perspective, one can ask themselves why measure over extended periods if short measurement periods can provide sufficient information to support the clinical decision-making process.

Although the AT's utility to accurately assess various functional activities and disease severity levels is promising, research on the effectiveness of AT in home-based rehabilitation regimens has a long way to go. Zampieri et al. (Zampieri, Salarian et al. 2011) most relevantly address such questions, drawing out significant links between, for instance, testing locations and stride length and velocity. Whether the iTUG can easily be administered in non-clinical settings without supervision, in particular, remains a pressing issue, as the device requires five inertial sensors for testing.

2.6 Limitations

The original database search included MesH terms of specific neurological diseases, which prevented a significant number of engineering articles from being considered due to their indexing method. That the IEEE Xplore database only permitted limited search term bindings posed an additional hurdle to widening the review's scope. A broader search strategy was implemented at this stage, one eliminating neurological terms while still including only those studies on the use of wearable AT for rehabilitation purposes. More relevant studies were consequently extracted. Many articles, especially engineering ones, did not provide clear or complete titles, abstracts, or research contexts with which to discern their relevance at first glance. Full texts often fared no better, giving rise to interpretative problems on multiple levels (e.g. methodology, intervention). Such hermeneutic struggles rendered the search to find eligible articles more difficult.

Because of the broad search strategy, strict eligibility criteria were implemented, weeding out seemingly relevant studies (Macko, Haeuber et al. 2002; Salarian, Russmann et al. 2007; Moore, MacDougall et al. 2008; Weiss, Sharifi et al. 2011) from review. The only validated studies that qualified for review related to PD and stroke, all analyzing the movement patterns of different functional activities, with an emphasis on quantitative and qualitative outcomes. No validated studies around other neurological diseases were identified.

2.7 Conclusion

This systematic review focuses and clarifies the degree to which AT have been successfully implemented in the field of telerehabilitation. Extending and revising the insights set forward by Bonato et al. (Bonato 2005) and Patel et al. (Patel, Park et al. 2012), among other studies, this review both surveys today's AT appliance in neurological populations and draws out its limitations within telerehabilitative contexts heretofore unaddressed. By thoroughly and

meticulously sifting through 1738 articles and identifying the few that actually utilize AT-methods capable of remotely assessing functional activities in neurological populations, it assists researchers in making informed, time-sensitive decisions regarding which current methods to use in target populations and why. In this case, only twelve studies were determined to reliably assess functional activities in neurological populations, of which only three implemented AT in home environments. As small as this number appears, it is a hard-won indication of the need for more versatile research that adopts or improves current AT-methods in various populations. Dobkin et al. (Dobkin and Dorsch 2011) point out how extensive research has been undertaken within engineering—initiatives that, bolstered by current advances in MEMS technology, are slowly fulfilling demands in telerehabilitation and telemedicine. As this review emphasizes, however, clinical and real-world research significantly lag behind their engineering counterpart.

The main challenges facing the deployment of AT rest in: 1) the difficulty in homogenizing a range of distinct research methods and features to realize the same aims, 2) the lack of appropriate outcome measures for movement quality assessment, and 3) the lack of awareness surrounding AT's clinical usefulness. In order to address such challenges, research should keep the following three initiatives in mind. Firstly, research should set analytical standards in different target populations, allowing researchers to better justify any potential deviations from existing methods. Secondly, research should aim to employ more appropriate outcome measures to obtain qualitative movement features. Researchers can distinguish healthy from non-healthy subjects and classify functional activities and symptom severity levels relatively accurately, but hardly explore the qualitative dimensions of motor performance. It is well known that the performance of activity recognition algorithms heavily rely on robust and time-accurate features for test and training data. At present, the detection of time-accurate and robust gait features remains a continuous challenge.

From this chapter it can be concluded that feature extraction plays an important role as this drives the recognition rates of the activity classifiers. The ability to assess patient movement in clinical and non-clinical settings with greater nuance (insight into an aspect of quality of gait) would permit researchers, clinicians, and caretakers within the areas of prevention, diagnostics, disease progression, telerehabilitation, and telemedicine to improve individual health and well-being.

In the next chapters this thesis sets out to establish and validate an unobtrusive ambulatory monitoring system for clinical and non-clinical gait assessments. In addition, this work sets out to explore accuracy of current gait feature extraction methods and finding alternative ways to more precisely capture gait features from a single device attached near the center of mass of the body.

Chapter 3

Mechanics

3.1 Summary of Contents

This chapter investigates a suitable pre- and post-processing approach for lower trunk gait accelerometry signals. Why certain approaches were chosen over others for this thesis will be clarified in the process. The first section contextualizes the mechanics behind MEMS accelerometers and gyroscopes, including their sensor error properties. The second section introduces sensor fusion, which permits orientation measurement and the application of a previous developed tilt correction technique about the vertical plane. The third section briefly discusses how various pre-processing operations can reduce error and noise. The last section examines the effects of such pre- and post-processing operations (tilt correction and denoising) on gait accelerometry signals.

3.2 Introduction

Over the course of the last 20 years, several approaches have been employed to assess gait, in particular body-worn accelerometers (Mayagoitia, Nene et al. 2002; Luinge and Veltink 2005; Hartmann, Murer et al. 2009; Godfrey, Del Din et al. 2015). Accelerometry-based gait assessments have become a widely adopted approach, due to its reliability and high precision (Hartmann, Luzi et al. 2009). It also enables computing a wide range of outcome measures to evaluate gait. In order to evaluate gait properly and extract accurate gait features, it is crucial for gait-accelerometry signals to be pre-processed accordingly in order to remove noise and/or minimize the effect of the gravity component over the measured accelerations (Moe-Nilssen 1998; Kavanagh and Menz 2008).

A number of lower trunk tilt correction techniques (static and dynamic) have been developed for gait analysis which uses accelerometers on their own (Moe-Nilssen 1998; Kavanagh and Menz 2008; Millecamps, Lowry et al. 2015). These techniques measure the inclination of the trunk in the sagittal and frontal planes with respect to a common reference axis (the gravity vector). The application of these techniques, however, is limited in that gravity effects cannot be fully compensated for during walking (Kavanagh and Menz 2008) and therefore may affect evaluation of gait by certain gait models.

On the contrary, IMUs, when combining the output from 3D accelerometers, gyroscopes, and magnetometers—a process known as sensor fusion, may correct for the effects of a dynamically tilting accelerometer during walking. Data from these complementary sensors cannot only

correct for gravity effects, but also remove integration drift by continuously correcting estimated orientations via rate gyro data (Roetenberg, Luinge et al. 2009). The main purpose of this Chapter, however, was not to establish an alternative tilt correction technique, but merely examine the effects of previously adopted approach (Esser, Dawes et al. 2009) in obtaining linear accelerations in the local vertical plane[3]. We first extracted features (i.e. peak, amplitude, RMS) from the raw acceleration signal. Then, we examined the gravity correction effects on the extracted features, followed the post-processing effects on the double integrated signal (i.e. position). At this stage, it is important to point out that this Chapter only focuses on the post- and pre-processing schemes for gait accelerometry signals, and it is beyond the scope of the current thesis to comprehensively analyze the sensor's error characteristics.

3.2.1 Accelerometers

An accelerometer is an electromechanical device that measures specific force or proper acceleration (i.e. relative to free-fall). The term accelerometer refers to a transducer, which converts dynamical changes of mechanical variables (acceleration, vibration, and mechanical shock) into electrical outputs. An accelerometer's underlying mechanism is often described as a simple mass-spring system that operates through the principles of Hooke's Law ($F = -kx$) and Newton's Second Law of Motion ($F = ma$). The mass-spring system is based on a mechanical sensing element that contains a proof mass (seismic mass) attached to a mechanical suspension system (spring or cantilever beam). When a mass-spring system is submitted to compression or stretching due to movement, the displacement of the mass with respect to the case is directly proportional to the acceleration of the case.

$$F = ma = -kx$$

$$a = \frac{-kx}{m} \tag{3.1}$$

In this way, the problem of measuring acceleration is turned into one of measuring the displacement of a proof mass connected to a spring. To keep the springs from causing the mass to overshoot and oscillate about the reference position, some form of damping is normally required. This is usually obtained by filling the case with oil. In order to measure 3D acceleration, this system needs to be replicated along all three axes, *x*, *y*, and *z* axis.

Nowadays, accelerometers are used to study joint kinematics as well as kinetics of the lower limbs and trunk providing another dimension to gait analysis that alternative techniques cannot

[3] Previous work done within Oxford Brookes' Movement Science Group 'established' a sensor fusion method reliant on quaternions. This piece of work was already intended to be used as a foundation for the development of a novel ambulatory activity monitor.

(Williamson and Andrews 2001; Kavanagh and Menz 2008; Seel, Raisch et al. 2014). At present, accelerometers attached to the foot, limb, or trunk can measure clinically important gait characteristics, such as cadence and step duration, for balance and mobility assessment. Furthermore, they can also measure the shockwave propagation of transient vibrations upon foot contact (Smeathers 1989; Mercer, Devita et al. 2003), which has been associated with different joint degenerative pathologies (Whittle 1999).

Accelerometers measure acceleration with respect to an inertial reference frame. This includes gravitational and rotational acceleration as well as linear acceleration (Tzafestas 2012). The gravity component is useful to calibrating the sensitivity, but can also be used to measure the degree of inclination through basic trigonometry. This feature provides the possibility to examine postural control (postural sway) during standing (Hansson, Asterland et al. 2001; Moe-Nilssen and Helbostad 2002) as well as discriminating postures and orientations of body segments (Veltink, Bussmann et al. 1996; Moe-Nilssen and Helbostad 2002; Luinge and Veltink 2005; Lyons, Culhane et al. 2005). Under dynamic conditions, however, gravitational accelerations are considered artifacts that contaminate true linear accelerations (Elble 2005). Removing the gravitational artifact, as many gait analysis methods require (Auvinet, Berrut et al. 2002; Menz, Lord et al. 2003; Zijlstra and Hof 2003), becomes more difficult with accelerometers alone (Kavanagh and Menz 2008). Although average tilt correction suffice (Millecamps, Lowry et al. 2015), rate gyroscopes can provide additional detail on the orientation of the sensor, and thus enhance the possibility of correcting for the gravity effects (Kavanagh and Menz 2008).

3.2.2 Gyroscopes

Mostly used for inertial navigation systems, a gyroscope is an angular velocity or rotation sensor, used for measuring or maintaining orientation. Gyroscopes are broadly divided into two categories: mechanical and vibratory gyroscopes.

A mechanical (or conventional) gyroscope consists of a spinning wheel supported on an axis that is free to move on its own. The spinning wheel (rotor) is mounted on a pivoting support that allows rotation around a single axis (gimbal). These gyroscopes operate according to the principle of conservation of angular momentum ($N \cdot m \cdot s$ or $kg \cdot m^2/s$) by sensing the change in the rotation amount, taking into account its mass, shape, and speed. Angular momentum (L) is a vector quantity that is often described as the rotational analog of linear momentum. For a rigid body, this is the product of the body's moment of inertia (I) and angular velocity (ω).

$$L = I\omega \tag{3.2}$$

Unlike mechanical gyroscopes, vibrating gyroscopes are rate-gyros, working to measure the Coriolis force in order to measure angular rate. The Coriolis force is an apparent force proportional to the angular rate of rotation within a rotating reference frame (see Figure 3.1).

$$F_c = -2m(\omega \cdot v) \tag{3.3}$$

ω is the angular velocity of the frame of reference, m is the proof mass, and v is the velocity of the moving mass. By detecting the Coriolis force and performing an integration of the gyroscopic signal, angular rate can be obtained.

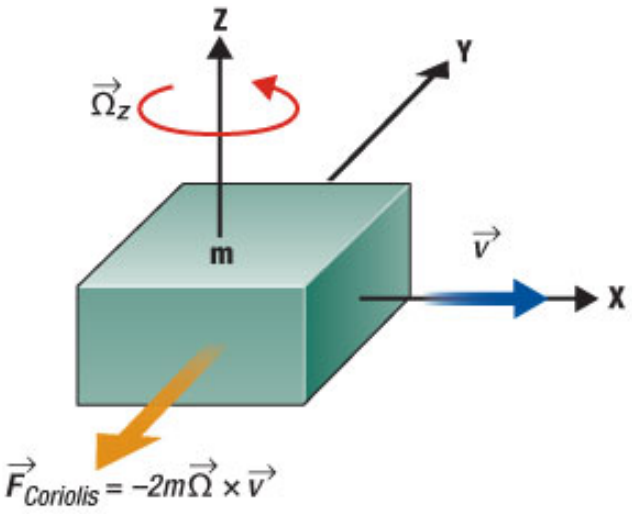

Figure 3.1 Coriolis Effect (source: www.findmems.com).

Unlike accelerometers, gyroscopes measure, in theory, only the rotational rate—nothing else. In practice, however, gyroscopes are sensitive to linear acceleration and vibrations, a trait that drastically affects their accuracy. The main error sources for MEMS gyroscopes are similar to those for MEMS accelerometers. For MEMS devices, angle random walk (white noise), zero-bias, scale factors, and misalignment are typically the error sources that limit the device's performance, which normally need to be determined beforehand by means of static calibration (Woodman 2007; Tee, Awad et al. 2011). However, the relative importance of each error source depends on the specific device being used.[4] This being said, it was beyond the scope of this thesis to work out these error sources.

3.2.3 Sensor Fusion

Figure 3.2 illustrates the process of how an inertial sensor can track 3D orientation and position. During this process, integrated angular velocities of the rate-gyroscope can provide the absolute orientation of the sensor if the initial orientation is known. The acceleration signal is, then

[4] For more information regarding error propagation by inertial sensors, the author recommends Oliver J. Woodman's technical report. An introduction to inertial navigation.

projected on to the global frame, corrected for gravity, and integrated twice to obtain the position signal.

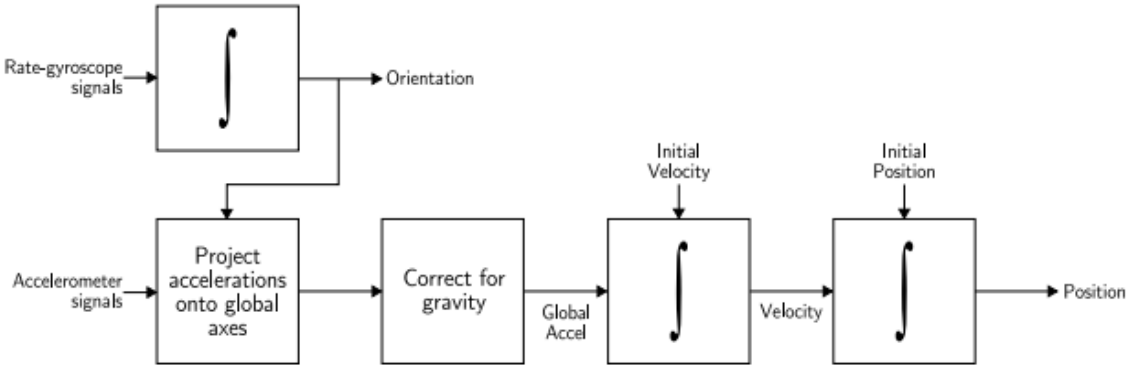

Figure 3.2 The process of tracking orientation and position though MEMS inertial sensors (Woodman 2007).

This process sounds straightforward and easy, yet uncorrected error sources can cause huge drift problems over time, in particular a small offset error in the gyroscope signal, and therefore fail to provide accurate 6-DOF information (Luinge and Veltink 2005). In this context, sensor fusion algorithms that combine sensory data from gyroscopes, accelerometers, and magnetometers can be used to reduce drift, calculate 3D orientation, and ascertain the position of individual body segments (Luinge, Veltink et al. 1999; Luinge and Veltink 2005).

The most commonly employed sensor fusion algorithm is the Kalman filter, which, belying its name, is no filter but an estimator that relates to least-squares or maximum likelihood statistics (Lacey ; Roger 1967). The Kalman filter was developed as a recursive solution to the discrete-data linear filtering problem (Welch and Bishop 1995). It relies on the assumption that the current state linearly dependent on the previous state. The state is a description of all the parameters required to describe the current system and perform the prediction.

3.2.3.1 Kalman Filter

This section provides a practical introduction to the discrete Kalman filter[5]. This introduction includes a brief description and discussion on the basic Kalman filter without any results. The Kalman filter consists of a set of mathematical equations that implements a predictor-corrector type estimator, which minimizes the estimated error covariance when the condition of a linear-Gaussian is met (Welch and Bishop 1995). It addresses the general problem of trying to estimate the state of a discrete-time controlled process through the following linear stochastic equations:

[5] For a basic understanding of the Kalman filter, the author recommends Roger, M. (1967). du Plessis. Poor Man's Explanation of Kalman Filtering or how I stopped worrying and learned to love Matrix Inversion.

$$x_k = Ax_{k-1} + Bu_{k-1} + w_{k-1} \tag{3.4}$$

$$z_k = Hx_k + v_k \tag{3.5}$$

Each x_k (state estimate) is a linear combination of its previous value plus u_k (control signal), and w_k (noise process). The second part (3.5) assumes that any measurement value is a linear combination of the signal and the noise, both considered to have a normal probability distribution. The process and measurement noise, w_k and v_k, are statistically independent and characterizes the uncertainties in the states and correlations within it. The entities A, B, and H are generally m x n matrices, known as the transition, control, and observation matrix, but can also denote numerical values, depending on the amount of dimensions. For more details on the mathematical derivation, see (Welch and Bishop 1995).

The next step is determining the necessary noise parameters. For this iteration process, the Kalman filter uses two stages to solve numerical problems through feedback control. One stage governs the time update (prediction), while the other, the measurement update (correction) that computes the Kalman Gain. During the first stage, the filter produces a prediction based on the last estimate (time update), one that is later corrected in the measurement update stage. Specific equations for time and measurement updates are presented below (Figure 3.3).

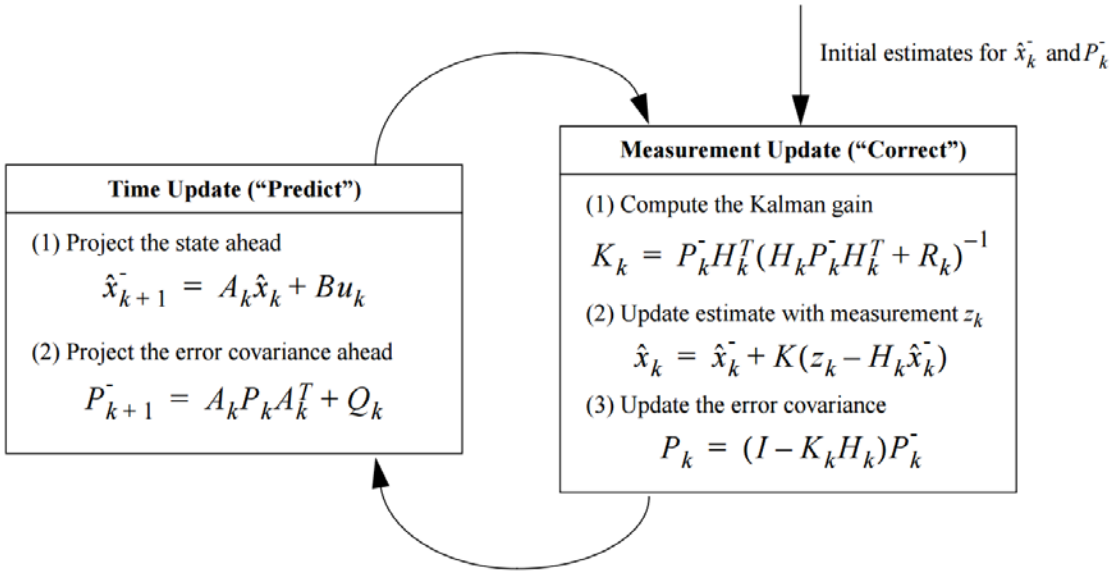

Figure 3.3 A flow diagram of the Kalman filter operation. A, B, and H are from equation 3.4 and 3.5, while Q and R are the process and measurement noise covariance, and K_k is the Kalman Gain.

The Kalman Gain (K_k in the measurement update equation) is derived from minimizing the error covariance. If the measurement covariance R approaches zero, the actual measurement z_k is trusted more and more, while the predicted measurement is trusted less and less. On the other hand, when the covariance P approaches zero the outcome is vice versa.

To efficiently blend the data gathered by an IMU, a complementary Extended Kalman filter was designed by Dr. Ian Sheret. A more detailed description behind the filter's design is given in Chapter Seven. However, no problems and solutions regarding the performance of this filter can be discussed as this was beyond the scope of this thesis to fully review. Solutions to existing problems can be found in various references (Kalman 1960; Kalman and Bucy 1961; Mau 2005).

3.2.4 Sensor Output

Again, sensor fusion permits the calculation of orientation by rate-gyroscopes. Orientation is commonly expressed in either Euler angles or quaternions here. Both outputs are briefly explained in the next few sections.

3.2.4.1 Euler Angles

Euler angles represent an object's 3D orientation through a combination of three consecutive principle rotations about different axes in the local frame. There are twelve ways to select a sequence of three rotations, divided in two groups:

- *Classic Euler* angles (z-x-z, x-y-x, y-z-y, z-y-z, x-z-x, y-x-y)
- *Tait-Bryan* angles (x-y-z, y-z-x, z-x-y, x-z-y, z-y-x, y-x-z)

The convention type depends on how the three principal rotations are perceived. Principal rotations may either be rotations about the original axes (earth or space-fixed) or successively rotated axes (body-fixed). Tait-Bryan angles are reserved for intrinsic angles in the body frame, whereas classic Euler angles are rotations in relation to the earth-frame. Using Tait-Bryan angles (*z*-*y*-*x*) (see Figure 3.4), principal rotations are formulated in terms of roll (*x*), pitch (*y*), and yaw (*z*):

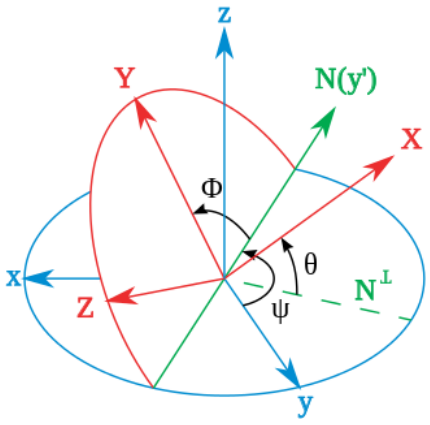

Figure 3.4 Tait–Bryan angles using the *z*-*y*-*x* convention.[6]

[6] If θ is zero, there is no rotation about *y*. As a consequence, *Z* coincides with *z*, ψ and Φ represent rotations about the same axis (*z*), and the final orientation can be derived through a single rotation about *z*, at an angle equal to $\psi+\Phi$.

1. A rotation by angle ψ about the z-axis,
2. A rotation by angle θ about the y-axis,
3. A rotation by angle Φ about the x-axis.

The various names given to these symbols include:

ψ yaw, heading, azimuth,

θ pitch or elevation,

Φ roll, bank, tilt.

Rotation matrices can be used at this point to represent a sequence of intrinsic rotations in 3D space. For instance,

$$R = R_z(\psi), R_y(\theta), R_x(\Phi) \tag{3.6}$$

This rotation is equal to the product of the following rotation matrices (z-y-x):

$$R_\psi = \begin{bmatrix} cos\ \psi & sin\ \psi & 0 \\ -sin\ \psi & cos\ \psi & 0 \\ 0 & 0 & 1 \end{bmatrix}, R_\theta = \begin{bmatrix} \cos\theta & 0 & -sin\ \theta \\ 0 & 1 & 0 \\ sin\ \theta & 0 & cos\ \theta \end{bmatrix}, R_\Phi = \begin{bmatrix} 1 & 0 & 0 \\ 0 & cos\ \Phi & sin\ \Phi \\ 0 & -sin\ \Phi & cos\ \Phi \end{bmatrix} \tag{3.7}$$

$$R = \begin{bmatrix} cos\ \psi & sin\ \psi & 0 \\ -sin\ \psi & cos\ \psi & 0 \\ 0 & 0 & 1 \end{bmatrix} \begin{bmatrix} \cos\theta & 0 & -sin\ \theta \\ 0 & 1 & 0 \\ sin\ \theta & 0 & cos\ \theta \end{bmatrix} \begin{bmatrix} 1 & 0 & 0 \\ 0 & cos\ \Phi & sin\ \Phi \\ 0 & -sin\ \Phi & cos\ \Phi \end{bmatrix}$$

The rate-gyro data, however, are reported in the body frame and requires conversion to the inertial frame. The resulting transformation matrix for converting body-frame angular rates to Euler angular rates is:

$$D(\Phi, \theta, \psi) = \begin{bmatrix} 1 & \cos\Phi sin\ \theta & sin\ \Phi\ tan\ \theta \\ 0 & cos\ \Phi & -sin\ \theta \\ 0 & \sin\Phi/cos\ \theta & \cos\Phi\ /sin\ \theta \end{bmatrix} \tag{3.8}$$

Let p represent the body-frame x-axis gyro output, q represent the body-frame y-axis output, and r represent the body-frame z-axis output. Then the Euler angle rate data is computed as:

$$\begin{pmatrix} \dot{\Phi} \\ \dot{\theta} \\ \dot{\psi} \end{pmatrix} = D(\Phi, \theta, \psi) \cdot \begin{pmatrix} p \\ q \\ r \end{pmatrix} \tag{3.9}$$

Performing a rotation on a vector through Euler angles may result in gimbal lock singularities. Gimbal lock occurs in situations where the sensor's $\boldsymbol{y}$-axis operates near 90 degree angles. When converting gyro data to their proper coordinate frames, the division by $\cos(\frac{\pi}{2})$ in matrix D cause axes z and x to align, thereby losing one degree of freedom. In the case of Tait-Bryan angles, z-y-x convention, roll-rotation cannot be distinguished from yaw-rotation. Depending on the rotation sequence order, gimbal lock will occur in different positions and consequently prove to be an unavoidable problem when using Euler angles for rotation. To avoid the occurrence of such singularities, quaternions can be used as an alternative.

3.2.4.2 Quaternions

Quaternions provide a method for representing orientation by extending the set of complex numbers that are written as $a + ib$, where $i^2 = -1$ with two further imaginary numbers, j and k. They do not suffer from gimbal lock singularities and are computationally easier to calculate. But such advantage comes at the expense of intuitive ease. Discovered by Sir William Rowan Hamilton in 1843, the fundamental formula for quaternion multiplication is:

$$i^2 = j^2 = k^2 = ijk = -1 \tag{3.10}$$

A quaternion ($\boldsymbol{q}$) is denoted as $\boldsymbol{q} = w + xi + yi + zi$. The first term w is called the real or scalar part of $\boldsymbol{q}$, and $xi + yi + zi$ is called the imaginary part of $\boldsymbol{q}$.[7] The quaternion in terms of axis-angle is:

$$\boldsymbol{q} = cos\left(\frac{\theta}{2}\right) + i\left(x \cdot \sin\left(\frac{\theta}{2}\right)\right) + j\left(y \cdot \sin\left(\frac{\theta}{2}\right)\right) + j\left(z \cdot \sin\left(\frac{\theta}{2}\right)\right) \tag{3.11}$$

[7] Several other conventions exist to denote a quaternion. The Xsens MTx represent $\boldsymbol{q} = [w + xi + yi + zi]$ as $[q_0 + q_1 + q_2 + q_3] = (q_0, \boldsymbol{q_{1:3}})$

where θ is the rotation angle and x, y, and z are the vectors representing the rotation axis. The expression may also be assumed in the form:

$$\boldsymbol{q} = (\cos\left(\frac{\theta}{2}\right), \sin\left(\frac{\theta}{2}\right)\vec{\boldsymbol{r}}) \tag{3.12}$$

where $\vec{\boldsymbol{r}}$ is (x, y, z).

Quaternions have four dimensions, one real dimension and three imaginary dimensions (i, j, k). Each of these imaginary dimensions has a unit value of $\sqrt{-1}$, but all are mutually perpendicular to one other (see Figure 3.5).

From this knowledge, we can determine all the possible products of i, j, and k (Hamilton's Rules):

$$ij = k, ji = -k \tag{3.13}$$

$$jk = i, kj = -i$$

$$ki = j, ik = -j$$

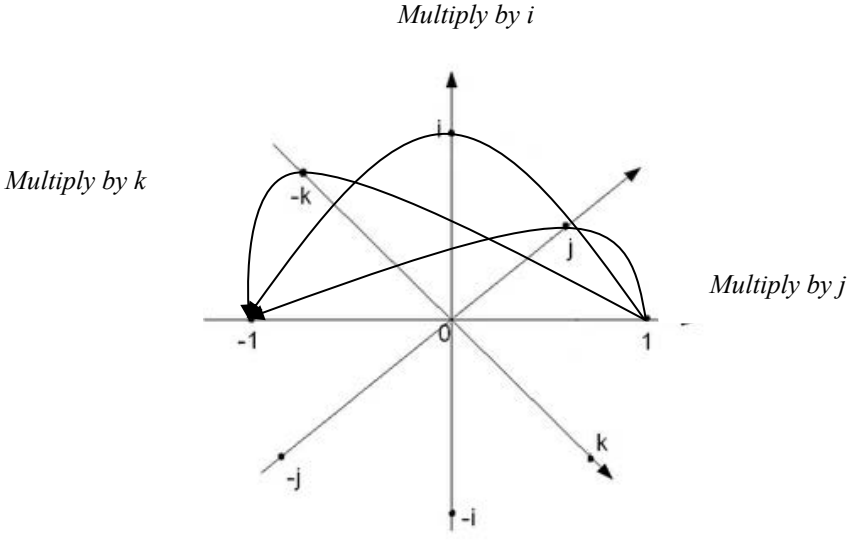

Figure 3.5 Graphical representation of the imaginary dimensions.

The conjugate of a quaternion represents the opposite rotation and is defined as:

$$\boldsymbol{q}^* = q_0 - iq_1 - jq_2 - kq_3 \tag{3.14}$$

The product of a quaternion with its conjugate is considered "pure-real" and is called the norm of **q**:

$$\boldsymbol{q}\boldsymbol{q}^* = \boldsymbol{q}^*\boldsymbol{q} = q_0^2 + q_1^2 + q_2^2 + q_3^2 \tag{3.15}$$

The modulus of a quaternion is defined as the square root of the norm:

$$\|q\| = \sqrt{\boldsymbol{q}\boldsymbol{q}^*} = \sqrt{q_0^2 + q_1^2 + q_2^2 + q_3^2} \tag{3.16}$$

A quaternion is a unit quaternion if $\|\boldsymbol{q}\| = 1$. In that case, $\boldsymbol{q}\boldsymbol{q}^* = \boldsymbol{q}^*\boldsymbol{q} = 1$, which implies that, a unit quaternion's conjugate is its multiplicative inverse $\boldsymbol{q}^{-1} = \boldsymbol{q}^*$

Unlike complex numbers in 2D, quaternions in 4D are not commutative. Quaternion multiplication between **q** and **p** is defined by:

$$\begin{aligned}\boldsymbol{p}\boldsymbol{q} &= (p_0 + ip_1 + jp_2 + kp_3)(q_0 + iq_1 + jq_2 + kq_3) \\ &= (p_0q_0 - p_1q_1 - p_2q_2 - p_3q_3) \\ &+(p_1q_0 + p_0q_1 + p_2q_3 - p_3q_2)i \\ &+(p_2q_0 + p_0q_2 + p_3q_1 - p_1q_3)j \\ &+(p_3q_0 + p_0q_3 + p_1q_2 - p_2q_1)k\end{aligned} \tag{3.17}$$

3.2.4.3 Transformations using Quaternions

A rotation in 3D Euclidean space by quaternions goes as follows:

$$\boldsymbol{p}(0,\boldsymbol{r})\boldsymbol{p}^{-1} = \boldsymbol{p}(0,\boldsymbol{r})\boldsymbol{p}^* \tag{3.18}$$

Let $\boldsymbol{r} = (r_1, r_2, r_3)$, which represent the point in 3D space by *i*, *j*, and *k* parts of the quaternion, 0 is the real part. The multiplication by the conjugate deems counterintuitive as the vector, $\boldsymbol{r}$, is first rotated and then rotated back. Since quaternions have 4 dimensions, the first multiplication

by $\boldsymbol{p}$ would rotate the point in 4D space. However, the rotation of interest is in 3D. For this the point is multiplied by the conjugate, see Figure 3.6.

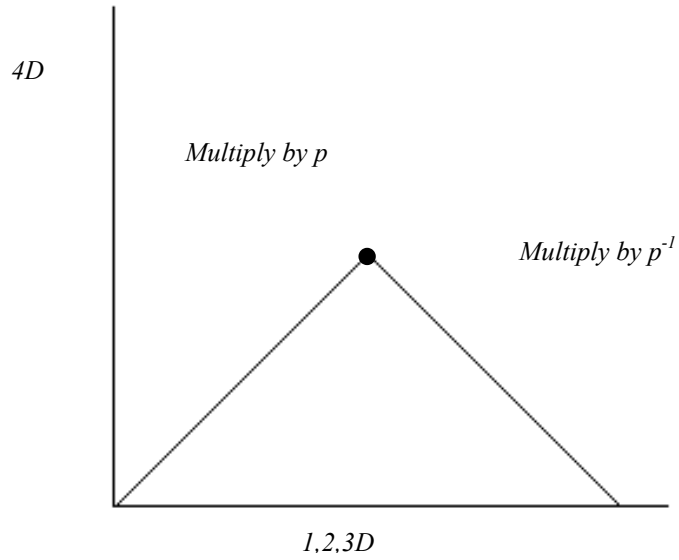

Figure 3.6 Transformation using quaternion multiplication. Rotation of the vector *r* is first rotated by p and then rotated back by its conjugate.

The quaternion representation of the composition of two rotations by $\boldsymbol{p}$ and $\boldsymbol{q}$ on $\boldsymbol{r}$ is obtained by first rotating with the rotation operation induced by $\boldsymbol{p}$ and then by $\boldsymbol{q}$. This composite rotation is the same as the single rotation induced by quaternion product $\boldsymbol{pq}$, also known as the sandwich product.

$$\boldsymbol{q}\{\boldsymbol{p}(0,\boldsymbol{r})\boldsymbol{p}^*\}\boldsymbol{q}^* = \{\boldsymbol{qp}\}(0,\boldsymbol{r})\{\boldsymbol{qp}\}^* \tag{3.19}$$

To rotate a point or vector in 3D Euclidean space by a unit quaternion $|\boldsymbol{q}| = 1$, its product with a 3x3 matrix represent the rotation of a point about the origin. The corresponding quaternion rotation matrix is[8]

$$R_q = \begin{bmatrix} (q_0^2 + q_1^2 - q_2^2 - q_3^2) & (2q_1q_2 - 2q_0q_3) & (2q_1q_3 + 2q_0q_2) \\ (2q_1q_2 + 2q_0q_3) & (q_0^2 - q_1^2 + q_2^2 - q_3^2) & (2q_2q_3 + 2q_0q_1) \\ (2q_1q_3 - 2q_0q_2) & (2q_2q_3 + 2q_0q_1) & (q_0^2 - q_1^2 - q_2^2 + q_3^2) \end{bmatrix} \tag{3.20}$$

[8] A detailed explanation of this generally accepted and used rotation matrix can be found on Richard Baker's website: http://www.euclideanspace.com/maths/geometry/rotations/conversions/quaternionToMatrix/ as well as many other sources.

, which can be optimized in the following equivalent form

$$R_q = \begin{bmatrix} 1-2(q_2^2+q_3^2) & 2(q_1q_2-q_0q_3) & 2(q_1q_3+q_0q_2) \\ 2(q_1q_2+q_0q_3) & 1-2(q_1^2+q_3^2) & 2(q_2q_3-q_0q_1) \\ 2(q_1q_3-q_0q_2) & 2(q_2q_3+q_0q_1) & 1-2(q_1^2+q_2^2) \end{bmatrix} \tag{3.21}$$

Unlike Euler angles, quaternions are robust and exhibit no singularities. Consequently, this quaternion matrix multiplication approach has been used to obtain translatory acceleration in the sensor's local frame:

$$a(\ddot{x},\ddot{y},\ddot{z}) = a\begin{bmatrix} x \\ y \\ z \end{bmatrix} \cdot R_q(q_0, \boldsymbol{q_{1:3}}) \tag{3.22}$$

3.3 Acceleration, Velocity, and Position

Vibration is a mechanical oscillation of an object (with mass) around a reference point of equilibrium, such as a pendulum's motion or the pickoff displacement of an accelerometer's proof mass. Vibrations can be measured in terms of acceleration, velocity, and displacement over time. These time variables are closely related to each other. If the measured time variable is acceleration, the other two variables can be found through single and double integration. The conversion process can be implemented in either hardware via analog integration or software via digital integration.

Nowadays, almost all measurement signals are discrete (digitalized), so integration must be carried out numerically with various integration methods, for instance, the rectangular rule, the trapezoidal rule, and Simpson's rule. All of these methods combine integrand evaluations to derive an approximation for the definite integral. The integrand is evaluated at a finite set of integration points. A weighted sum of these values is subsequently used to approximate the integral.

Depending on the signal type, Simpson's rule usually provides more accurate approximations of the area under curve, as it uses parabolas or other higher order polynomials instead of straight line segments. Similar to other integration methods, this method will only provide an adequate description of the exact integral if the integration interval is small enough, which depends on the sampling rate. The higher the sampling rate, the more accurate the integration process becomes as the number of subintervals increases proportionally. The general rule of thumb remains that sampling frequency should be at least double the highest frequency contained in the signal in order to avoid aliasing (Olshausen 2000). Aliasing happens when a signal is discretely sampled at a rate that is insufficient to capture changes in that signal, resulting in a loss of information.

More complex signals, such as gait, necessitate a much higher sample frequency than the Nyquist rate in order to get an accurate representation of the signal. In a repetitive movement such as walking, the majority of gait-related movements are dominated by relatively low frequencies that present themselves in multiples (harmonics) of the fundamental frequency (i.e. step frequency). Using the Fast Fourier Transform revealed that the frequency content of gait by means of an IMU presents frequencies up to 25Hz, which would necessitate a sampling rate of at least 50Hz. Yet, a closer examination of the gait accelerometry signal uncovers subtle important inconsistencies in time and amplitude quantization of the signal when it is digitized at 50 and 100Hz. For that reason, a sampling rate of 100Hz was deemed more appropriate. In conjunction with the sample frequency, both the trapezoidal rule and Simpson's rule showed to perform equally well. But because of gait's complex signal, Simpson's rule of integration was chosen for this study's numerical analysis.

3.3.1 Gravity-offset Effects

Most accelerometer-based motion-sensing applications use DC-coupled accelerometers that can measure dynamic as well as static acceleration due to gravity. Unlike AC-coupled accelerometers, DC-coupled accelerometers contain a gravity-offset component in the acceleration signal. The offset refers to the accelerometer output signal's bias from the true value (in ms^{-2}). To obtain dynamic acceleration from motion, this gravity component must be subtracted. This section will briefly discuss the effects of offset and low unwanted frequencies on the integrated acceleration signal.

Even when acceleration data has been properly sampled, integrating acceleration to calculate velocity or displacement in the time domain often leads to distorted results. The issue is not caused by the loss of information during the digitization process. Neither is it due to the effects of amplitude or time quantization. The problem is, in fact, rooted in the very nature of integrated trigonometric functions, specifically how their amplitudes increase with decreasing frequency. Evidently, low frequency components dominate the integrated acceleration output, which can ultimately present misleading results (Moe-Nilssen and Helbostad 2002). In the same way that low frequencies can dominate the shape of an integrated signal, the presence of even a small DC offset can completely alter the structure and magnitude of an integrated signal as shown in Figure 3.7. As a result, velocity errors grow linearly, and displacement over time errors grow quadratically $s(t) = \epsilon \cdot \frac{t^2}{2}$ (Woodman 2007).

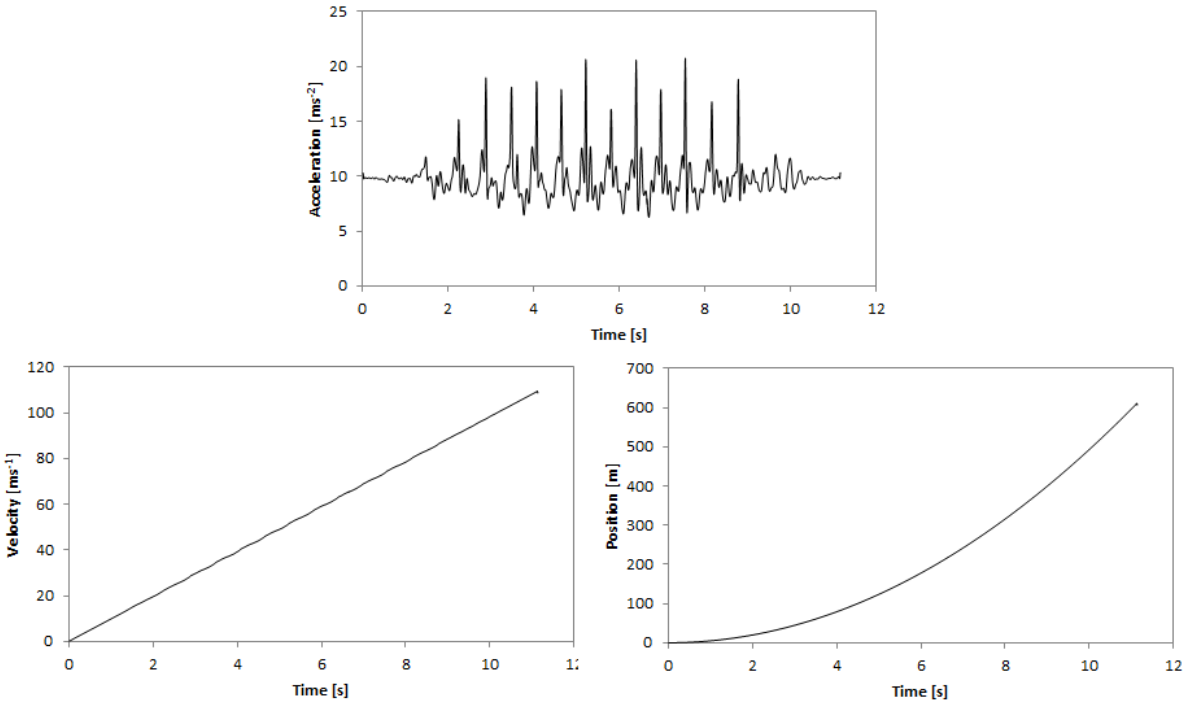

Figure 3.7 The DC offset in the acceleration signal causes a linear drift in velocity that grows quadratically in position.

Correcting for the DC offset alone is not enough. For unwanted low frequencies can likewise alter the integrated acceleration signal, as shown in Figure 3.8.

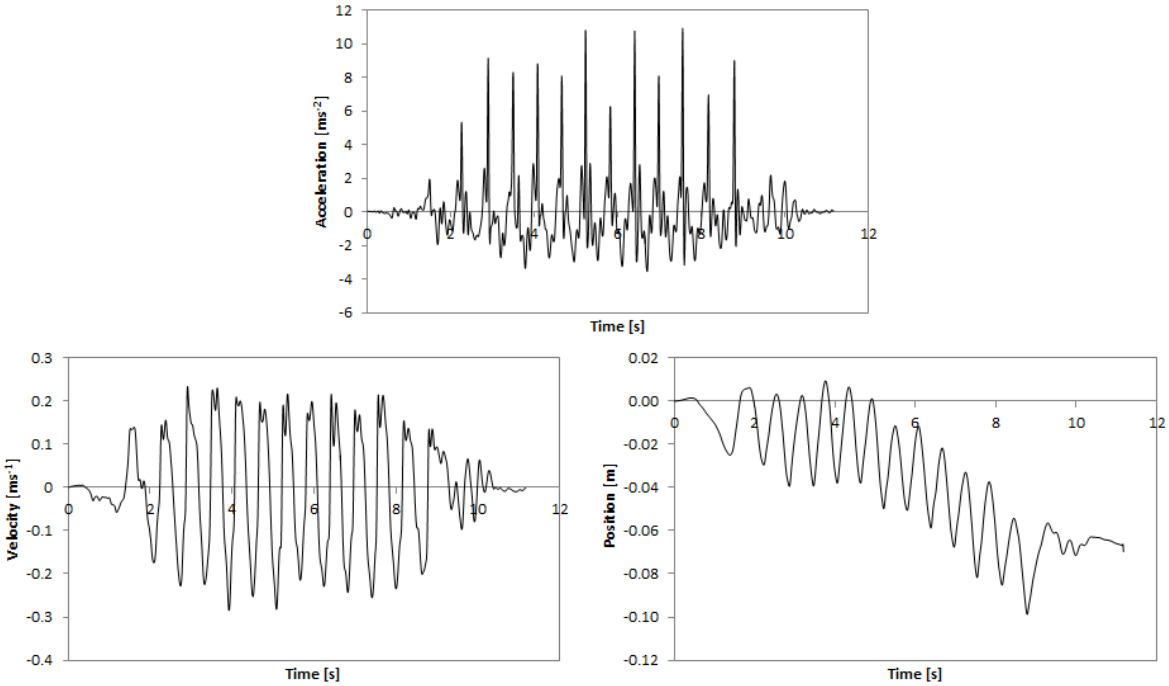

Figure 3.8 Low frequency components have significant effect on the integrated signal, especially in position.

To eliminate both problems associated with drift and unwanted low frequencies, digital filtering is required. Digital filters are primarily used to attenuate noise frequencies from a discrete signal.

3.3.2 Digital Filters

In signal pre-processing, a digital filter can separate or restore certain aspects of a sampled signal. The purpose of filtering is to allow some frequencies to pass unaltered, while attenuating other frequencies (Smith 2013). The pass-band refers to those frequencies that pass, while the stop-band, those frequencies that are blocked. An ideal filter would have amplitude response with a constant gain in the pass-band and zero in the stop-band. The gain, moreover, should increase from the stop-band's zero to the pass-band's higher gain at a single frequency—a process also known as the transition band. The frequency response of an ideal low-pass, high-pass, band-pass, and band-stop filter are shown in Figure 3.9 (a), (b), (c), and (d).

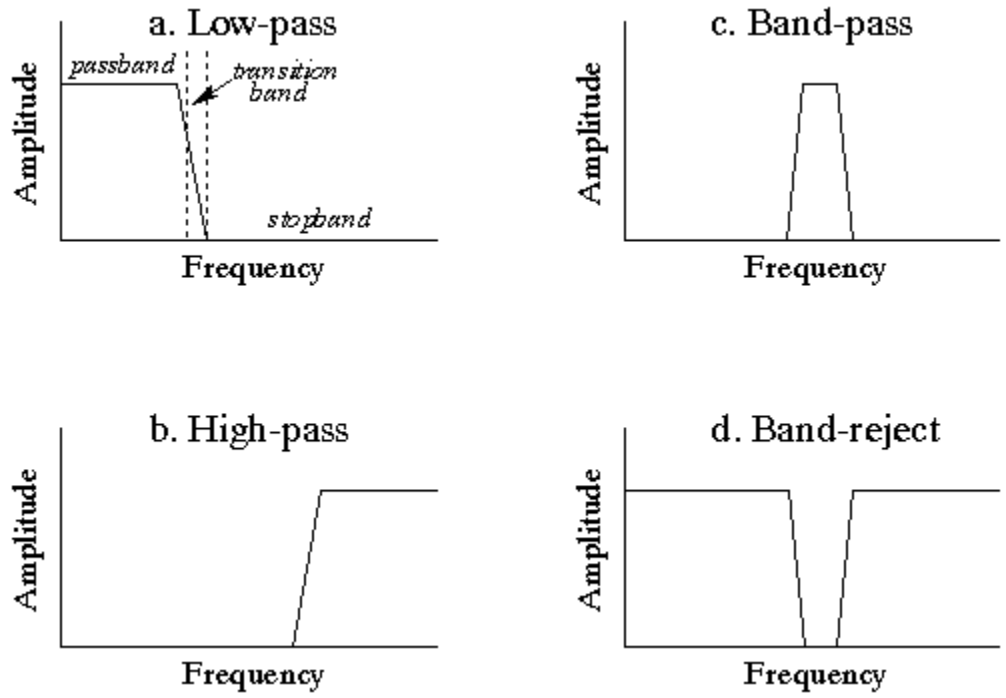

Figure 3.9 Four common frequency responses. Frequency domain filters are generally used to pass certain frequencies (pass-band), while blocking others (stop-band) (Smith 1997).

The terminology used to define the filter's performance in the frequency domain is: cut-off frequency, ripple, and roll-off.

- Cut-off frequency is the frequency beyond which the filter will not pass signals.
- Ripple is the variation of the filter's insertion loss in the passband.
- Roll-off is the rate at which attenuation increases beyond the cut-off frequency.

3.3.2.1 FIR and IIR Filters

Digital filters can broadly be divided into two types: finite impulse response (FIR) and infinite impulse response (IIR) filters.[9] The output of FIR filters is solely a function of its input, whereas for IIR filters, depend on previous input and output samples, hence called a recursive filter. Non-recursive FIR filters are implemented by convolution, where each sample in the output is calculated by weighting and adding together the samples in the input. The most elementary form of an FIR filter is the moving average, which applies coefficients of equal weight. Recursive filters are an extension of a moving average, using previously calculated values from the output and points from the input.

[9] In signal processing, a dynamic system's impulse response denotes when the system's output is presented with a brief input signal. More generally speaking, an impulse response refers to any dynamic system's response to external change.

The general expression for an FIR filter is:

$$T(z) = a_0 + a_1 z^{-1} + a_2 z^{-2} + a_3 z^{-3} \dots a_n z^{-n} \tag{3.24}$$

The general expression for an IIR filter is:

$$T(z) = \frac{a_0 + a_1 z^{-1} + a_2 z^{-2} + a_3 z^{-3} \dots a_n z^{-n}}{1 - b_1 z^{-1} - b_2 z^{-2} - b_3 z^{-3} \dots b_n z^{-n}} \tag{3.25}$$

These input samples are passed through a series of buffer registers (z^{-1}), and then multiplied by a set of forward (a_0) and reverse (b_0) filter coefficients.

IIR filters can achieve the same level of attenuation as FIR filters do, but with far fewer coefficients. This makes IIR filters significantly faster and more efficient than FIR filters. Thus digital IIR filters can be based on well-known solutions for analog filters such as the Butterworth which have maximally flat passbands in the filters of the same order, the Chebyshev type I which are equiripple in the passband, the Chebyshev type II which are equiripple in the stopband, and the Elliptic filters which are equiripple in both the passband and the stopband.

LabView provides a digital version of each of them. The filter setup below (Figure 3.10) has been used through the whole of this thesis. The first visual instrument (vi) automatically generates a set of Butterworth filter coefficients to implement an IIR filter. Direct form implementation of a Butterworth filter may cause instability because of coefficient quantization. A solution for this is to use a cascade structure. The second vi converts the filter coefficients from the cascade form to the direct form. In the direct form, these coefficients (forward and reverse) are funneled to a zero-phase filter, before performing a discrete integration of the sampled data using the Simpson's rule (see third and fourth vi). To avoid phase distortion, a zero-phase filter is applied prior to each integration step for signal comparisons between systems.

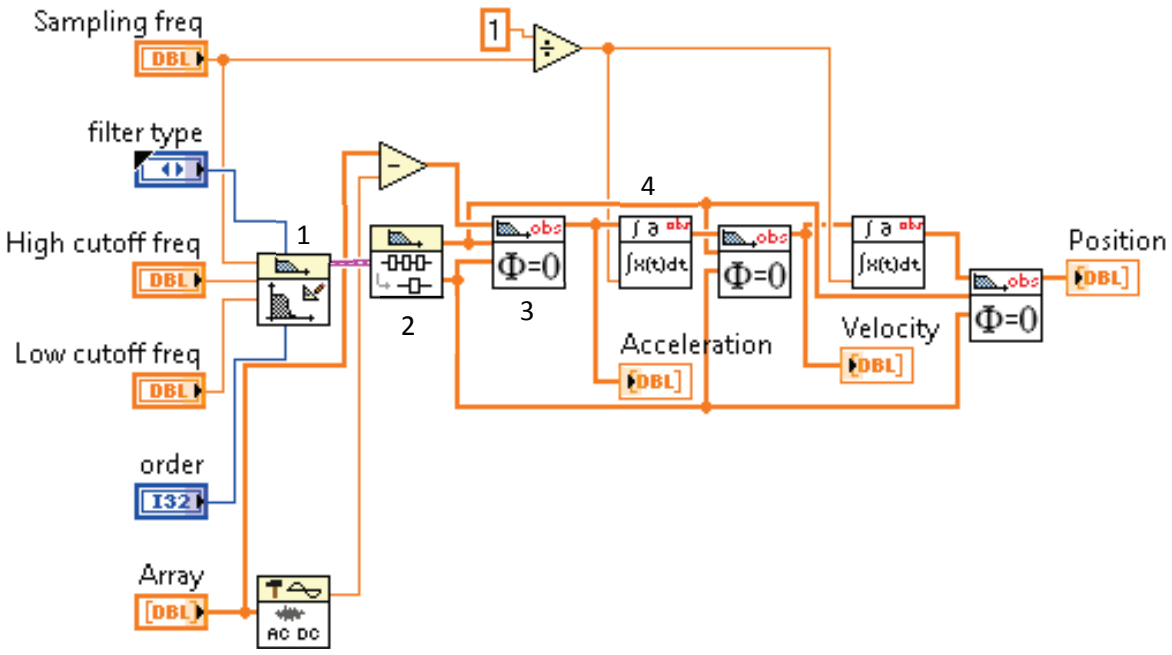

Figure 3.10 Filter design created in LabView.

3.4 Application to Research

To reiterate, MEMS accelerometers are capable of deriving many spatiotemporal gait features (e.g. step length) which are often based one estimated COM displacement data. Mean step length estimations are based on such displacement, however, are significantly undershot and normally require a correction factor (Zijlstra 2004). A potential reason behind such underestimation rests in sensor's misalignment. As mentioned before, accelerometers generally measure some degree of gravitational acceleration, an artifact of the transducer's mechanism of operation that usually obscures inertial acceleration, which is the actual measurement of interest. When there is no rotational motion, the gravity component can easily be subtracted by high-pass filtering (Elble, 2005). This, however, cannot be performed during gait, when gravitational accelerations will be present at any frequency of rotational motion due to the accelerometer's axis rotating in space.

IMUs, on the other hand, can measure uncontaminated accelerations in the earth or global frame through complicated sensor fusion algorithms. Since sensor misalignment has already been suggested as an error source for various applications, this pilot study examines the difference between transposed and un-transposed gait accelerometry data about the sensor's origin, in terms of specific extracted features (i.e. peak, amplitude, and root mean square [RMS]).

3.4.1 Methods

In order to examine the magnitude of this error source in the COM data, ten healthy participants walked four times, barefoot, over a 10m straight walkway. Acceleration was measured by an IMU (MTx, Xsens, Enschede) attached to the lower trunk. The main sensor readings provided by

the Xsens IMU (i.e. acceleration and quaternions) were used to transpose vertical acceleration in the global frame using the aforementioned quaternion multiplication matrix approach. To examine the magnitude of the gravitational artifact, similar post-processing steps were employed on both transposed and un-transposed data. An IIR band-pass filter, supplied with forward and backward second order Butterworth coefficients (cut-off frequency, 0.5-25Hz), was applied to remove drift and integration errors. Amplitude changes in the vertical axis were doubly integrated, according to the Simpson Rule to obtain vertical displacement data.

3.4.2 Results

The results of the post-processing approach are shown in Figure 3.11. Vertical acceleration (un-transposed and transposed), peak displacement measures over time, amplitudes, and root mean square values (RMS) are reported in Table 3.1 and 3.2. The tables also show whether the parameters were significant within each participant.

A one-way ANOVA between vertical transposed and un-transposed linear acceleration initially showed no significant differences between peak ($F[1,78]= 0.000$, $r=.99$), amplitude ($F[1,78]= 0.008$, $r=.93$), and RMS ($F[1,78]=0.000$, $r=1.00$) vertical acceleration. But when examining each individual separately on their four walking trials, Paired sample *t*-tests revealed significant differences in 6 out of 10 subjects for peaks, amplitude, and RMS. Overall, peak accelerations were about $0.005ms^{-2}$ lower (CV= 5.6%; $LOA_{95\%}= .39ms^{-2}$), whereas amplitudes were slightly increased by approximately $0.39ms^{-2}$ (CV= 5.6%; $LOA_{95\%}= .55ms^{-2}$) in comparison to un-transposed measures. Nonetheless, amplitude differences in acceleration showed no real effect on linear COM displacement (Mean difference= 0.1mm, $LOA_{95\%}$= 2.1mm) in healthy participants.

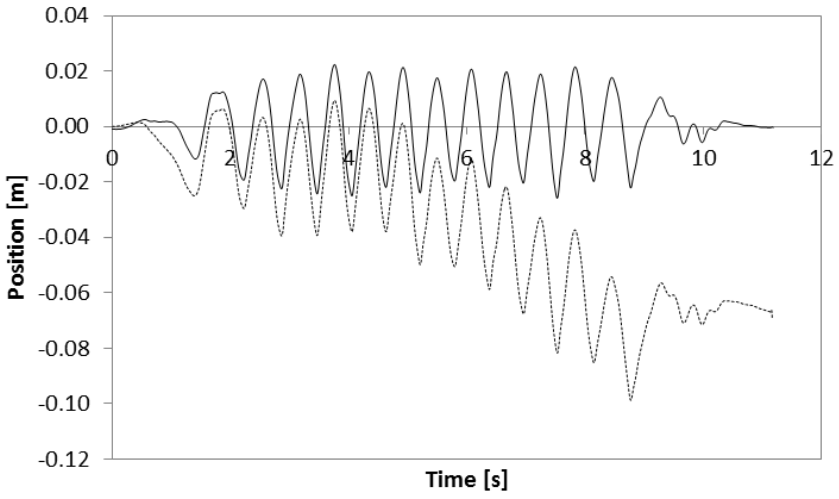

Figure 3.11 A band-pass filter with a cut-off frequency of 0.5-25Hz successfully removes drift errors associated with unwanted low frequencies.

3.4.3 Discussion

Results indicate that the gravitational artifact significantly affects the vertical acceleration signal, but not necessary in the derived displacement values. Tilt errors introduced by misalignment or orientation errors in each walking trial are relatively minor in healthy individuals, and as a result would hardly affect the COM displacement measures. However, sensor misalignments should still be taken into account when assessing individuals with gait disorders, as they may feature significant postural deficits, thereby affecting displacement data (Kavanagh and Menz 2008).

Other errors sources (e.g. bias error, scale-factor error, noise, and bias stability) which have not been investigated normally have an impact on the inertial sensor performance, thereby affecting the quaternion output given by the Xsens system. In absence of any static error analysis (calibration), it is highly likely that there is still a degree of error.

Table 3.1 Un-transposed versus transposed vertical acceleration

		Peak (Mean ± S.D.)			Amplitude (Mean ± S.D.)			RMS (Mean ± S.D.)		
Subject	Sex	Raw	Transposed	*P*	Raw	Transposed	*p*	Raw	Transposed	*P*
P1	M	**8.04 ± 0.80**	**7.98 ± 0.80**	.01**	**10.61 ± 1.02**	**10.54 ± 1.03**	.01**	2.12 ± 0.16	2.11 ± 0.16	.06
P2	F	**5.09 ± 0.25**	**4.72 ± 0.23**	.01**	**7.35 ± 0.52**	**6.98 ± 0.48**	.01**	1.82 ± 0.08	1.79 ± 0.08	.21
P3	M	**6.73 ± 0.27**	**6.60 ± 0.28**	.02*	**8.81 ± 0.53**	**8.66 ± 0.59**	.03*	**1.79 ± 0.14**	**1.77 ± 0.14**	.01*
P4	M	7.28 ± 0.65	7.34 ± 0.50	.55	9.51 ± 0.82	9.59 ± 0.64	.53	2.13 ± 0.12	2.12 ± 0.11	.18
P5	M	9.79 ± 1.26	10.07 ± 1.14	.14	13.35 ± 1.84	13.71 ± 1.65	.16	**2.85 ± 0.36**	**2.89 ± 0.37**	.01**
P6	F	6.63 ± 0.41	6.66 ± 0.45	.60	9.76 ± 0.65	10.07 ± 0.71	.25	2.56 ± 0.14	2.61 ± 0.13	.50
P7	F	**5.06 ± 0.75**	**5.18 ± 0.77**	.02*	**8.42 ± 1.06**	**8.60 ± 1.07**	.01**	**2.21 ± 0.17**	**2.21 ± 0.17**	.02*
P8	F	8.77 ± 1.12	8.80 ± 1.15	.17	11.69 ± 1.72	11.75 ± 1.76	.13	2.34 ± 0.35	2.34 ± 0.36	.64
P9	M	**6.01 ± 0.36**	**5.88 ± 0.34**	.01**	8.57 ± 0.40	8.41 ± 0.40	.01**	**2.05 ± 0.07**	**2.02 ± 0.07**	.01**
P10	F	**7.02 ± 0.19**	**7.14 ± 0.24**	.03*	**10.27 ± 0.63**	**10.44 ± 0.65**	.02*	**2.73 ± 0.19**	**2.70 ± 0.19**	.01**

* Significance at $p<.05$

** Significance at $p<.01$

Table 3.2 Un-transposed versus transposed vertical displacement

		Peak (Mean ± S.D.)			Amplitude (Mean ± S.D.)		
Subject	Sex	Raw	Transposed	*P*	Raw	Transposed	*P*
P1	M	0.0177 ± 0.0004	0.0171 ± 0.0008	.12	0.039 ± 0.002	0.038 ± 0.002	.18
P2	F	0.0116 ± 0.0009	0.0115 ± 0.0011	.51	0.026 ± 0.002	0.026 ± 0.002	.18
P3	M	0.0142 ± 0.0014	0.0142 ± 0.0013	.39	0.032 ± 0.002	0.032 ± 0.002	1.00
P4	M	0.0151 ± 0.0003	0.0149 ± 0.0007	.34	0.033 ± 0.002	0.033 ± 0.001	.39
P5	M	0.0239 ± 0.0030	0.0238 ± 0.0033	.93	0.052 ± 0.006	0.052 ± 0.006	.39
P6	F	0.0200 ± 0.0014	0.0209 ± 0.0017	.44	0.044 ± 0.002	0.045 ± 0.002	.42
P7	F	0.0185 ± 0.0022	0.0183 ± 0.0013	.68	0.039 ± 0.003	0.038 ± 0.003	.39
P8	F	0.0169 ± 0.0023	0.0169 ± 0.0021	.64	0.036 ± 0.004	0.036 ± 0.004	.18
P9	M	0.0186 ± 0.0010	0.0186 ± 0.0010	.83	0.039 ± 0.003	0.040 ± 0.003	.50
P10	F	0.0188 ± 0.0008	0.0190 ± 0.0009	.56	0.040 ± 0.001	0.040 ± 0.001	1.00

Chapter 4

Gait Analysis

4.1 Summary of Contents

This chapter contextualizes the current state of clinical gait assessments and alternative techniques that may improve patient outcomes. Divided into two sections, it briefly discusses the limitations surrounding clinical gait analysis undertaken in laboratory settings, advancing smart technology as a potential solution. The second section examines the basic principles underlying gait analysis, including popular gait models and their limitations.

4.2 Introduction

A person's gait can be greatly affected by injury or disease. While some gait abnormalities can be observed with a subjective visual examination, more subtle deficiencies require quantitative gait analysis assessments. Instrumented gait analysis offers a quantitative evaluation of the complexities defining an individual's gait pattern, allowing therapists to determine any weaknesses and adjust gait rehabilitation programs in response. For example, instrumented gait analysis has played a significant role in the understanding of pathological gait in individuals bearing spasticity-related central nervous disorders, especially children with CP (Gage 1994; DeLuca, Davis et al. 1997; Arnold, Anderson et al. 2005). Gait analysis has not only been clinically relevant to surgical decision-making, but has also reduced the number of extraneous surgical procedures performed, avoiding unnecessary psychological and financial costs (DeLuca, Davis et al. 1997; Simon 2004).

Whether in neurology (Benedetti, Piperno et al. 1999), rheumatology (Turcot, Aissaoui et al. 2008), orthopedics (Catani, Benedetti et al. 1999), sports, or beyond, clinical gait research has introduced many ways of obtaining valuable clinical information through gait laboratories. With regard to sports training, clinical gait analysis can help identify certain inefficiencies or faults in an athlete's movement for, say, golf, swimming, and running. More urgently, for those with neurological-based motor impairments, monitoring their gait variations, in particular stride-to-stride interval variations, has been linked to fall risks, disease severity, and underlying neuromuscular control mechanisms (Hausdorff 2005; Hausdorff 2007). By the same token, monitoring an individual's motor impairments helps healthcare professionals to evaluate the effectiveness of medications, interventions, and rehabilitation efforts. For instance, the success of levodopa therapy for Parkinson's patients has been tracked by recording their changes in stride length (Moore, MacDougall et al. 2007).

A typical motion laboratory uses image-based methods in conjunction with force plates to collect kinematic and kinetic data. The data generated can, then, be used to quantify the magnitude of gait deviations from the norm and help provide, with the aid of physical examination and visual assessments, qualitative explanations for them. Image-based methods (e.g. photogrammetric, optoelectronic, and video systems) have proven especially useful in assessing intervention or surgical treatment, posture and gait analysis, and functional abilities.

All this being said, clinical gait analysis is not without its limitations. While Wren et al.'s systematic review (Wren, Gorton et al. 2011) most recently affirmed the value of clinical gait analysis, providing strong evidence for its diagnostic accuracy and treatment efficacy, some questions still linger. Whether its existing image-based technologies can address clinical problems, whether such technologies can cope with a wide variety of medical disorders, whether its high-maintenance costs (e.g. set up and post-processing time (Hsiao and Keyserling 1990), laboratory personnel) can be afforded (Tomie 2000), whether results gleaned from gait laboratory settings accurately capture a subject's functioning abilities in non-idealized environments (Kiani, Snijders et al. 1997; Bonato 2005; Baker 2006; Narayanan 2007)—such issues complicate how useful clinical gait analysis can be for routine decision-making processes prior to surgery as well as patient care optimization.

Another source of contention lies in how clinical gait analysis' effect on individual patient outcomes and social integration remains undetermined. In its current state, clinical gait analysis generally do not mimic the dynamic environment experienced during real-life walking. Much of it, moreover, is undertaken for clinical research purposes only, automatically barring subject-specific initiatives. For unlike clinical testing that aims to arrive at clinical decisions for individual patients, clinical research endeavors to illuminate conditions or intervention effects that influence patient groups as a whole. Clinical testing stresses the particular; research, the general.

Here is where non-clinical gait analysis comes in, and conducted through body-worn accelerometers. To compensate for clinical gait analysis' inherent constraints—better yet, to complement its clinical correlate—non-clinical gait analysis brings movement science closer to grasping an individual's real-life activity pattern in its entirety. To the extent that it broaches life outside controlled conditions, body-worn accelerometers in the context of telerehabilitation retain a holistic premise. Beyond physical parameters and concepts, the study of human movement inevitably extends into the sociological, environmental, and psychological sphere (Spirduso 1995; Trew and T.H. 2001; Godfrey, Conway et al. 2008). It hence requires a holistic guiding philosophy from the outset. Pointing to such complex interrelations, Wanneen Spirduso delineates a web of causes (see Figure 4.1) that can lead to impaired or reduced movement (Spirduso 1995).

Body-worn accelerometers may extend this holistic ethos (Brooke and H. 1973; Godfrey, Conway et al. 2008). Complementing a conventional gait laboratory's

mechanical capacities, it can reform healthcare by providing primary and secondary care at remote sites (Patel, Park et al. 2012) as well as by solving clinically relevant application problems arising at gait laboratories (Simon 2004). In so doing, accelerometers can more sensitively examine the impact of clinical interventions on an individual's quality of life. Furthermore, they are small and inexpensive and currently equipped in many smart phones. By turning smart phones into smart health devices or applications, one can collect information more frequent and from more people, across larger and more diverse regions. In addition, they can provide feedback on the patient's progress, or send reminders about exercise and medication. Such systems hold great premise for more versatile research. Nevertheless, before such system can be used for any gait assessment, robust methods from which to deduce clinically relevant gait characteristics are needed. Consequently, this chapter reviews the basics of gait analysis and the current ways researchers have captured gait features from a single accelerometer attached near the body's center of mass.

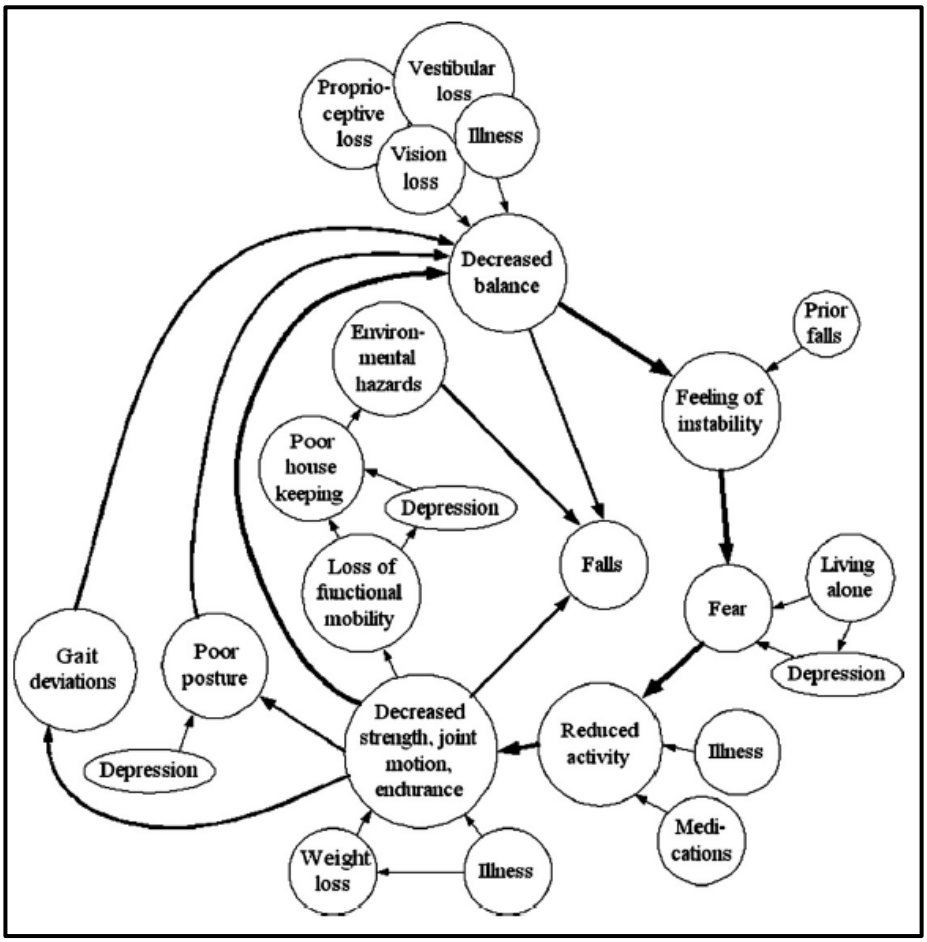

Figure 4.1 The web of causes (Spirduso 1995).

4.3 The Basics of Gait Analysis

Gait analysis signifies the systematic study of human locomotion, one augmented by instruments able to analyze movement and force patterns that constitute walking. Gait analysis roughly divides into three interrelated analysis components that not only allow distinctions to be drawn between pathological and normal gait, but also determine the parameters defining "normal" gait in the first place: kinematics and kinetics.[10] Kinematics describes motion in terms of the body's angles, positions, velocities, and accelerations, while kinetics is concerned with the relationship between the motion of body segments and its causes, for instance, ground reaction forces (GRFs) or forces generated by muscle contractions. This section elaborates on the gait cycle itself by detailing how gait events, phases, and patterns become detected.

4.3.1 The Gait Cycle

Generally speaking, gait entails a repetitive movement of body segments. For healthy individuals, gait is cyclic and symmetrical, meaning that it involves a relatively consistent and repeating pattern of individual gait cycles. Figure 4.2 illustrates the gait cycle, which covers a set of movement phases and events for each limb occurring between two successive initial contacts made by the same foot (Perry 1992).[11] So when a subject takes a right and left step, a complete stride or gait cycle has been completed. The gait cycle's duration is divided into two general phases: the stance phase, where the foot is in contact with the ground; and the swing phase, where the foot is in the air for limb advancement. The stance phase usually constitutes 60%, and the swing phase 40%, of each gait cycle's duration, which, in turn, varies with walking speed. The swing phase proportionally lengthens, and the stance phase shortens, as walking speed increases (Murray 1967; Whittle 2007). The gait cycle's fundamental functional tasks are, moreover, weight acceptance, single limb support, and swing limb. Weight acceptance and single-limb support become addressed during stance, while limb advancement primarily comes into play during swing.

Depending on the classification model being used (the traditional Ranchos classification (Perry 1992) or the alternatives posited by Sutherland, Fish & Nielsen, and Neptune (Sutherland, Olshen et al. 1980; Fish and Nielsen 1993; Neptune, Kautz et al. 2001)), five to eight movement phases can be identified. According to Rancho Los Amigos (RLA) terminology, gait consists of seven major events: initial contact, opposite toe-off, heel rise, opposite initial contact, toe-off, feet adjacent, and tibia vertical (Kirtley 2006). These seven events divide the gait cycle into eight sub-phases, five of which occur in stance, three during swing. In order, moving from stance to

[10] Instrumented gait analysis systems typically include the measurement of muscle activity and energy expenditure. However, in this thesis, only kinematic and kinetic measures are considered.
[11] Normally, the heel contacts the ground first. In patients bearing pathological gait patterns, the entire foot or the toes may contact the ground initially. For this reason, initial contact is the preferred term.

swing, they are: initial contact, loading phase, mid-stance, terminal stance, pre-swing, initial swing, mid-swing, and terminal swing (Perry 1992; Whittle 2007).

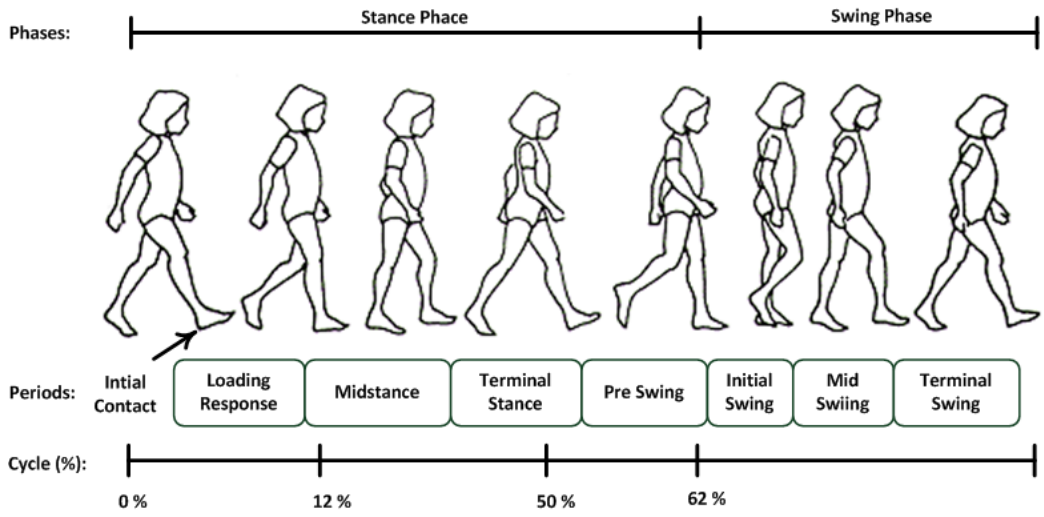

Figure 4.2 The gait cycle (Kirtley 2006).

Another RLA-derived gait concept is the foot rocker model, introduced in Jaqueline Perry's *Gait Analysis* (1992) (Perry 1992). The foot rocker model describes the behavior of the ankle-foot complex during the entire stance phase, and can be divided into three distinct phases: heel rocker, ankle rocker, and fore-foot rocker.

Evidenced in Figure 4.2, the timing of initial contact (0% GC) marks the beginning of the stance phase. (Initial contact also constitutes the inverted pendulum model's starting point, a topic to be detailed later on in this chapter.) Once the foot contacts the ground, the leading limb enters into its stance phase, an initial period of double-limb support (0-12% GC) where both feet are in contact with the ground. During the double-limb support period, the weight of the body becomes transferred from the opposite to the leading foot (loading response). By rocking the heel (heel rocker), the knee can flex for shock absorption and weight acceptance, while maintaining its forward progression (Kerrigan 1998).

The mid-stance period follows (12-30% GC) the single-limb support interval's first half. Here, the limb advances over the stationary foot through ankle dorsiflexion (ankle rocker), while the knee and hip extend. Mid-stance begins when the other foot lifts, continuing on until the subject's body weight aligns over the forefoot. Terminal stance period (30-48% GC) completes single-limb support and unfolds with the heel rising until the opposite foot strikes the ground (forefoot rocker). The final stage of stance, pre-swing (48-60% GC), takes off with the opposite foot initially contacting the ground and ends with ipsilateral toe-off. After pre-swing comes initial swing (60-73% GC). A forward and upward acceleration occurs as the foot lifts from the floor and the swing leg simultaneously accelerates forward, powered by hip and knee flexion and ankle dorsiflexion working together. Mid-swing (73-87% GC) takes place

when the accelerating limb is aligned with the stance limb. Terminal swing (87-100% GC) happens, finally, as the decelerating limb prepares for foot-ground contact. The swing phase is terminated by its next initial foot contact, completing the gait cycle.

4.3.2 Ground Reaction Forces of Gait

The gait cycle pattern is commonly studied through force plates. Force plates measure ground reaction force: an external force that acts upon the body when it contacts the ground. GRF is often used as an important descriptor of normal and pathological gait (Winter 1991; Perry 1992; Winiarski and Rutkowska-Kucharska 2009).

During quiet standing, the ground generates a reaction force equal and opposite to the body's weight. During gait, though, the resulting GRF vector—what David Winter articulates as the "reflection of the total mass times acceleration product of all body segments and therefore represent[ing] the total of all net muscle and gravitational forces acting at each instant of time over the stance period" (Winter 1984)—differs from the gravity line, as the former no longer remains completely vertical, now containing shear forces (horizontal forces). At this point, GRF divides into three components: vertical, anterior-posterior, and medial-lateral. See Figure 4.3 for a typical pattern of GRFs during a gait cycle, where the reaction force is expressed in the percentage of body weight (GRF/BW%).

The vertical force vector is the largest GRF component and accounts for the acceleration of the center of gravity (COG) in the vertical direction during walking. The vertical force pattern has a characteristic double hump, also known as an *M*-wave, which results from a combination of upward COG acceleration during early stance, decreased downward force as the body flies over the leg during mid-stance, and a second peak due to deceleration during late stance. The anterior-posterior force vector represents the foot's braking and propulsion forces, whereas the medial-lateral force vector characterizes its roll-off forces.

The GRF pattern starts with initial foot contact, followed by an abrupt transfer of body weight to the supporting structure of the heel as a result of the foot striking the ground (Gard and Childress 2001). This transfer of momentum from the moving leg to the ground is defined as the heel-strike transient (HST) (Whittle 2007); in Figure 4.3, it is represented by a short spike of force that occurs 10-50ms after initial contact (Whittle 1999; Henriksen, Christensen et al. 2008). The HST is an important marker within the gait cycle, as it might be associated with certain degenerative joint diseases, such as knee osteoarthritis (Radin and Paul 1971; Whittle 1999).

Succeeding HST, our body weight is entirely transferred over to the leading limb, a process known as loading response (LR). During this phase, the foot remains in full contact with the surface, and vertical GRF increases to the first maximum F_1 (approximately 120% BW). The LR phase occupies about 10% of the gait cycle and constitutes the period of double-limb support. During single-limb support, GRF

descends below that of normal standing force to its lowest point (mid-stance phase): between 60-80% BW.

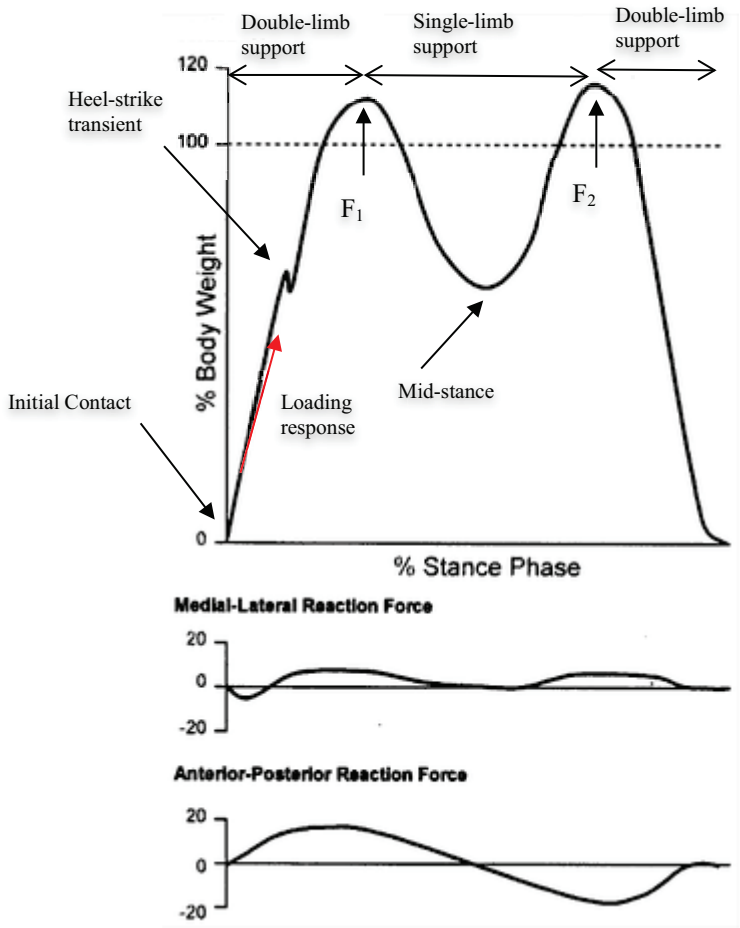

Figure 4.3 A typical GRF pattern observed during the stance phase (Ziaei, Nabavi et al. 2012).

Now, at mid-stance, the stance leg is relatively straight, while the opposite leg is in mid-swing. As the heel lifts away from the supporting surface (heel-off), GRF starts to increase again. The ascending second peak (F_2) in the vertical GRF pattern refers to terminal stance. This period opens with the heel rise and continues until the opposite foot strikes the ground. By the end of the toe-off phase, the vertical GRF pattern has dropped to zero. What follows terminal stance is another period of double-limb support. The cycle repeats itself here.

4.3.3 Center of Mass

Why the body's center of mass (COM) functions as a key reference point in gait analysis has to do with Newton's second law of motion. Since the net external force acting upon the body equals the latter's mass multiplied by its acceleration, the COM operates as the point through which all gravitational forces for all bodily orientations pass (Dempster 1955). As such, COM pattern displacement has become a common way to measure how the body translates from one point to another during walking, allowing researchers to estimate mechanical energy changes (Cavagna 1975), gauge efficiency (Saunders, Inman et al. 1953), external work (Cavagna, Saibene et al. 1963), and gait quality (i.e. phases, events).

The COM lies in the pelvis (before the second sacral vertebrae) during quiet standing. While walking, the COM follows a rhythmic upward-downward movement in the plane of progression. This pattern normally displays a smooth sinusoidal curve that moves through a complete cycle with each step (Inman 1966). The lowest displacement point occurs during the double-limb support stage. In mid-stance, the COM subsequently rises to its highest point, as the supporting limb goes vertical. The vertical COM displacement's peak-to-peak amplitude (i.e. vertical excursion) depends on the individual's walking speed (Whittle 1997), ranging from 3cm at slow paces ($0.8ms^{-1}$) to 4-5cm for self-selected speeds (Saunders, Inman et al. 1953; Murray, Drought et al. 1964), then 8cm for the fastest speeds ($2.2ms^{-1}$) (Gard and Childress 2001).

Vertical COM displacement can be calculated either through kinematic or kinetic data. Calculations based on kinematic data are derived from one reflective marker on the pelvis or trunk (the sacral marker method), or from a cluster of markers (the segmental analysis method, which is considered the gold standard in COM measurements (Eng and Winter 1993)). Calculations based on kinetic data, conversely, are gathered through two force plates. They are normally executed by double-integrating GRF data, expressed in the following mathematical equation:

$$a_z = \frac{F - F_z}{m} \tag{4.1}$$

$$s_z = \iint_0^t a_z \cdot dt^2 \tag{4.2}$$

Above, a_z signifies the COM's vertical acceleration component, F_z the GRF's vertical component in Newtons, F the vertical force measured by the force plate, and m the mass in kilograms. The vertical acceleration (a_z) is obtained by subtracting F_z from the force wave form. Vertical COM displacement, then, becomes calculated by double-integrating acceleration. Figure 4.4 demonstrates the relationship between force, acceleration, and displacement (Cross 1998).

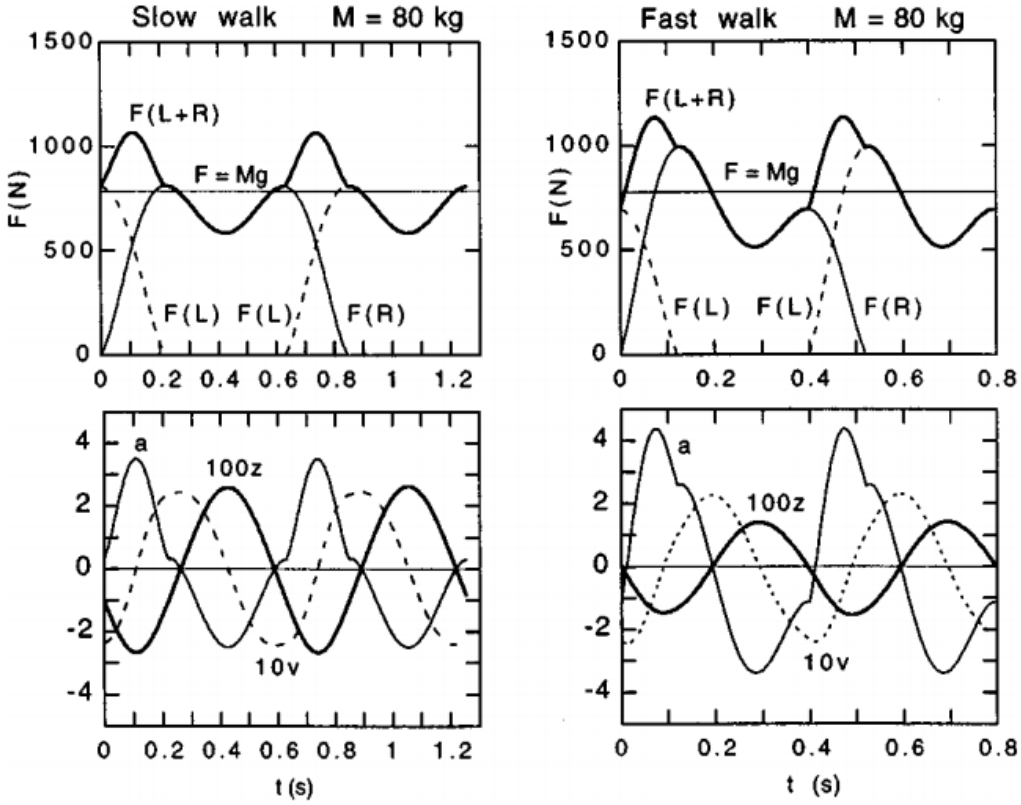

Figure 4.4 The vertical GRF pattern obtained by adding the force due to the left foot (L) and right foot (R). These results were used to calculate the vertical acceleration, velocity and displacement (Cross 1998). The thick line in the top two figures represents the sum of both feet's ground reaction component F(L+R). Derived from such ground reaction forces, the two lower figures depict vertical acceleration (ms^{-2}) (thin line), velocity (ms^{-1}) (dotted line), and displacement (m) (thick line).

In theory, the vertical COM displacement calculated from kinematic and kinetic data should be one and the same. But previous research reveals an imperfect match (Whittle 1997). Gard, Miff, and Kuo (Gard, Miff et al. 2004), among others (Thirunarayan, Kerrigan et al. 1996; Saini, Kerrigan et al. 1998), have examined this dilemma by comparing the sacral marker and segmental analysis method with their force plate counterpart at different walking speeds, ranging from 0.8-2.0ms^{-1}. They hypothesized that the sacral marker method would overestimate COM calculations, because it fails to represent actual body COM, only yielding lower trunk COM (see

Figure 4.5).[12] Their results indicated that all three techniques were fundamentally similar, in which the vertical COM displacement increased with increasing walking speeds, except at fast walking speeds (>1.4ms^{-1}). At faster speeds, the sacral marker method in comparison to other methods appeared to significantly overestimate COM displacement. Despite its inaccuracy, the sacral marker method provides a reasonable estimate of COM excursion for slow and self-selected walking speeds in healthy subjects (0.8-1.4ms^{-1}).

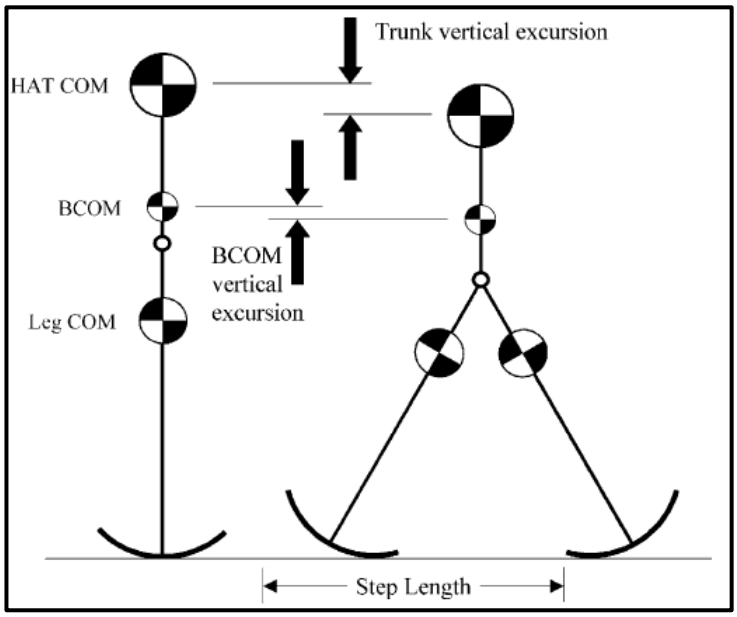

Figure 4.5 The differences between COM and trunk excursion. The reciprocal action exerted by the limbs during double-support raises the COM, causing its vertical excursion to be less than that of the lower trunk (Gard, Miff et al. 2004).

4.3.4 Models of Gait

Taken generally, walking can be conceptualized as the most energy-efficient translation of the COM through space. Based on this premise, several straightforward theoretical frameworks can be erected to clarify the mechanics underlying pathological gait. To first contextualize them, however, a review of two historically significant but opposed paradigms—the "six determinants of gait" theory and the inverted pendulum model—is given below.

4.3.4.1 Determinants of Gait

Many widely assimilated ideas regarding COM behavior originate from M. Saunders, V.T. Inman, and H.D. Eberhart's "six determinants of gait" theory. Released in 1953, their landmark article "The Major Determinants in Normal and Pathological Gait" proposed six determinants of gait—pelvic rotation, pelvic obliquity, stance-phase knee flexion, foot-ankle mechanics, ankle and knee interactions, and pelvic lateral

[12] The highest elevation of the COM's vertical position remains independent of step length, but its lowest elevation is substantially affected when longer steps are taken.

displacement—that smoothed or flattened COM trajectory to minimize the energy costs incurred by locomotion (Saunders, Inman et al. 1953; Inman 1966). The study was based on the premise that bipedal gait lacking these determinants would be characterized by excessive vertical COM displacement.

Till now, Saunders et al.'s determinants have largely been misconstrued (Kirtley 2006; Kuo and Donelan 2010), as many researchers have interpreted the group's argument to be: COM displacement should be minimized for optimal locomotion. Given how the voluntary reduction of COM displacement increases positive ankle and hip work and negative knee work, heightening metabolic energy costs (Ortega and Farley 2005; Gordon, Ferris et al. 2009), such a proposal would rightly provoke skepticism. However, as Saunders himself states, "[I]ndividual variations in locomotion are due to exaggerations in one or another of these several determinants. Owing to the interaction between the various factors, exaggerations in the range of one determinant are compensated for by reductions in another, so that the final pathway of the center of gravity remains essentially the same in that it is the most economical to maintain" (Saunders, Inman et al. 1953).(p553) Nowhere does he suggest that minimizing the COM optimizes gait. (And even if he were making that claim, it has been confirmed that three of his determinants—stance phase knee flexion (Gard and Childress 1999), vertical pelvic rotation, and fore-aft axes (Gard and Childress 1997)—hardly contribute toward reducing vertical COM displacement.) Instead, as Kuo et al. suggest (Kuo 2007), the six determinants should be judged more as kinematic gait features than anything else.

4.3.4.2 Inverted Pendulum Model

The inverted pendulum theory nicely complements the six determinants theory, as both point toward a more dynamic walking perspective (Kuo 2007). The inverted pendulum model works from a point mass that is equal to body mass and a rigid leg that connects body mass to the point of ground contact. During the stance phase, body mass vaults over the rigid leg, reaching its highest point at the middle of the stance phase (Cavagna, Thys et al. 1976; Margaria and Margaria 1976; Cavagna, Heglund et al. 1977). The inverted pendulum theory is more well-rounded than Saunders et al.'s six determinants theory in the sense that it can predict both the body's pattern of mechanical energy fluctuations (Cavagna, Thys et al. 1976; Margaria and Margaria 1976; Cavagna, Heglund et al. 1977) and the COM trajectory during walking (Zijlstra and Hof 1997). When walking at a moderate speed, according to the inverted pendulum model, the COM's kinetic and potential energy vacillate nearly 180 degrees out of phase (Cavagna, Thys et al. 1976).

Through the inverted pendulum model, a rough estimate of mean step length can be calculated from the COM's vertical excursion (Zijlstra and Hof 1997; Zijlstra and Hof 2003; Zijlstra 2004; Brandes, Zijlstra et al. 2006). Since changes in COM height depend on step length, the latter can be approximated when the former is known. In

the following formula, h equals vertical COM displacement changes, and l represents pendulum (leg) length:

$$\text{Step length} = 2\sqrt{2lh - h^2} \tag{4.3}$$

All this is not to imply that the inverted pendulum model is faultless. One of its disadvantages, for instance, is that it only addresses the gait cycle's single-limb support phase, ignoring the more energy-intensive double-limb support phase (Donelan, Kram et al. 2002; Kuo, Donelan et al. 2005) and seriously overestimating the COM trajectory's amplitude as a consequence (Gard, Miff et al. 2004; Sakka, Hayot et al. 2010). On the contrary, using this inverted pendulum model for mean step length estimations results in a significant underestimation (Zijlstra and Hof 2003). A generic correction factor of circa 1.25 on the IP model was consequently proposed but proved ineffectual, as its new estimates were somewhat inconsistent.

4.4 Spatiotemporal Gait Parameters

Gait analysis possesses a wide range of outcome measures. Under classical mechanics, kinematic and kinetic measures are considered the gold standard for any comprehensive gait assessment. But measuring such parameter types is relatively expensive and time-consuming, with clinically meaningful reductions in gait deviations being difficult to quantify.

Spatiotemporal outcome measures, on the other hand, have robust psychometric properties for all types of individuals, whether healthy (Murray, Drought et al. 1964; Boenig 1977) or neurologically affected (Rao, Quinn et al. 2005). They can more easily provide important information regarding a subject's walking ability or function (Collen, Wade et al. 1990; Stephens and Goldie 1999). The most commonly examined spatiotemporal gait parameters are cadence, walking speed, step length and width, step-time, stride-time, and swing and stance phase durations. Cadence refers to the number of steps taken in a given time, usually formulated in terms of steps per minute. Walking or gait speed, defined as the distance covered in a given time (measured in ms^{-1}), can be calculated by dividing stride length by stride time or by dividing step length by step time. Although many authors speak of velocity and speed interchangeably, they are not actually synonymous. Velocity is a vector, while speed is not. Step length refers to the anterior-posterior distance between consecutive opposite initial foot contacts, whereas step width denotes the medial-lateral distance between the aforementioned. Both step length and width can be measured in relation to stride.

In fact, most spatiotemporal parameters not only derive from, but also relate to, one another. Step frequency, for example, exhibits a roughly linear relationship to relativized walking speed (Grieve and Gear 1966). Some other parameter relationships are equally, if not more, straightforward. Since walking speed depends

on cadence and stride length, any changes in these two variables would alter the former. (In practice, people tend to change their walking speed by adjusting both their cadence and stride length.) Another way to express the relationship between speed, cadence, and stride length is through the "walk ratio": step length divided by step rate. All these outcome measures have been extensively used across a broad range of research topics and are considered reliable indicators of health, frailty (Maki 1997), and cognitive decline (Woo, Ho et al. 1995; Yogev-Seligmann, Hausdorff et al. 2008). While mean spatiotemporal gait parameters have been assessed for many years, gait-related research in last decade has shifted more towards the assessment of stride-to-stride fluctuations in the spatiotemporal gait parameters (Hausdorff 2009).

At present, the study of stride-to-stride fluctuations in walking offers a complementary way of quantifying locomotion and its changes with aging and disease as well as a means of monitoring the effects of therapeutic interventions and rehabilitation (Hausdorff 2005). Two complementary variables, gait variability and fractal dynamics, have been used to assess the variability and long-range correlations in stride interval patterns inherent in human gait. Gait variability simply refers to the overall level of consistency in the gait pattern. More specifically, it is typically the standard deviation of the mean for a given spatiotemporal parameter. For example, the deviation in stride time, rather than the mean value itself, is thought to be an important indicator of gait control (Chau, Young et al. 2005). On the other hand, fractal dynamics is based on measurement of the stride interval fluctuations of gait, rather than simply the overall level of consistency. This concept revolves around the theory that the apparent randomness of these fluctuations may actually not be random at all. When a large series of stride times (at least five minutes) are closely examined, long-range correlations are found to exist in the small fluctuations occurring between strides (Hausdorff, Peng et al. 1995). Fractal scaling of such time series tells us that each gait cycle is not an independent entity, but part of a complex pattern in which each gait cycle is dependent on a previous gait cycle. Similar to gait variability, fractal dynamics is thought to be an indicator of gait control, but appears to be more sensitive to the high level of coordination and self-organization in the peripheral and central inputs needed in the control of gait (Goldberger, Amaral et al. 2002). Given the significance of these stride-to-stride fluctuations in gait control, they have been used in the study of the effects of age on gait and fall risk (Callisaya, Blizzard et al. 2010). Mean spatiotemporal outcome measures and its variability, for that matter, may provide a much easier way to track rehabilitation progress in clinical and non-clinical settings as they can be assessed with body-worn accelerometers.

The next two chapters will focus on deriving temporal and spatial gait features from a single IMU on the lower back.

Chapter 5

Assessment of Walking Features from Lower Trunk Accelerometry[13]

5.1 Summary of Contents

In ambulatory monitoring scenarios, activities such as walking can be inferred from data provided by body-worn acceleration sensors. In such context, feature extraction plays an important role as this drives the recognition rates in, e.g., identifying people at risk of falling. Various estimation methods of spatiotemporal gait features using only the signal from a waist-mounted inertial sensor exist. However, the detection of time-accurate and robust gait features remains a continuous challenge, especially when considering pathological gait. The proposed quantitative approach consists of three parts: the basic interpretation and transcription of accelerometry data, the validation and accuracy of extracted gait features, and the presentation of alternative routes to obtaining time-accurate step features via simple integration.

5.2 Introduction

Gait is a complex movement pattern that involves the synchronized interaction between body segments and joints. In gait analysis, time-distance variables (e.g. walking speed, stance/swing times, step length) can provide essential information regarding a subject's gait function (Wren, Gorton et al. 2011). Determining these variables usually requires the detection of initial and final foot contact times (IFC and FFC), usually referred to as gait events (GEs), during a stepping cycle. These variables can be estimated from the acceleration signals captured by a single inertial measurement unit near the body's center of mass. Upon being post-processed, the acceleration-time curve data is used, then, to detect walking segments and extract specific gait-related features (Mathie, Coster et al. 2004). When used in conjunction with classification techniques (e.g. *k*-nearest neighbor, linear discriminate analysis, support vector machine), these extracted gait features can be used to distinguish and identify certain gait characteristics (Begg and Kamruzzaman 2005; Steins, Dawes et al. 2014).

The automated recognition of gait changes has many advantages, including the early identification of at-risk gait and the ability to monitor the progress of treatment

[13] In a slight adapted version, this Chapter is submitted for first-round review to Journal of Gait & Posture. Steins Dax, Ruben Zijlstra, Johnny Collett, Patrick Esser, and Helen Dawes. "Assessment of Temporal Walking Features from Lower Trunk Inertial Sensing: A Reference Framework."

outcomes (Begg, Palaniswami et al. 2005). However, it is well known that the performance of activity recognition algorithms heavily rely on robust and time-accurate gait features for test and training data (Bao and Intille 2004). At present, temporal gait feature extraction methods can be improved. A recent study by Trojaniello et al. revealed that current trunk gait detection methods demonstrate acceptable accuracy levels when applied to healthy gait (Trojaniello, Cereatti et al. 2014). Yet when pathological populations were analyzed, a global decrease of their performance was observed (Trojaniello, Ravaschio et al. 2015), especially when obtaining stance and swing duration estimates. Errors of up to 32% of actual values were found across populations. This shortcoming is mainly caused by the inability to correctly identify final foot contacts (FFC) due to the irregular nature of acceleration (McCamley, Donati et al. 2012). Hence, this Chapter aims to establish a reference frame for gait feature extraction from the lower trunk, along the vertical (VT) and anterior-posterior (AP) axes. As such, the accuracy of the timing and location of gait events (GEs) will be compared to that of reference data.

The remainder of this Chapter is organized as follows. Section 5.3 describes previous work on GE detection. Section 5.4 illustrates the experimental set-up, while Section 5.5 presents experimental results. Finally, Section 5.6 concludes the chapter. It is important to note that in the present study, improvements to GE detection were only sought in healthy subjects during straight-line and level walking. The rationale for this gesture is that a fundamental understanding of healthy gait acceleration patterns is vital for finding alternative ways to more precisely capture gait features.

5.3 Previous Works

The location at which an accelerometer is placed on the body is an important consideration in movement measurement, with the accelerometer normally attached to the site whose movement is being studied (Mathie, Coster et al. 2004). Multiple sensors increase the complexity of the monitoring system. For that reason, the use of one sensor attached to a single location near the body's center of mass is a more straightforward approach. This not only simplifies the monitor's design and use, but also permits the study of "whole body" movements (Mathie, Coster et al. 2004; Godfrey, Conway et al. 2008), as the measured site operates as the point through which all gravitational forces for bodily orientations pass. Consequently, the trunk's vertical acceleration pattern represents the summation of the left and right vertical component of the ground force (GRF) from both feet (Cross 1998).

Several authors have used the lower trunk acceleration pattern to identify IFC and FFC events (Menz, Lord et al. 2003; Zijlstra and Hof 2003; Gonzalez, Lopez et al. 2010; McCamley, Donati et al. 2012). Figure 5.1 illustrates GEs and their transcription on the AP and VT lower trunk acceleration pattern. The AP acceleration pattern represents gait braking and propulsion that generally goes from a minimum to a maximum value—identified as IFC (Zijlstra and Hof 2003). After IFC, the trunk accelerates again in AP direction until forefoot loading, when rapid backward

acceleration occurs until heel lift and the beginning of the swing phase (Menz, Lord et al. 2003). Before returning to a maximum value, a gradual increase in forward acceleration takes place after mid-stance, when the body falls forward and downward due to the contralateral foot's push-off moment.

Conversely, the VT acceleration pattern encapsulates trunk motion as well as the shock wave propagation (i.e. impact-related accelerations) along the human musculoskeletal system initiated upon foot-ground contact (Whittle 1999; Kavanagh and Menz 2008). A typical gravity subtracted VT acceleration pattern of the trunk displays three to five peaks depending on the smoothness of step-to-step transition and one negative peak during a step cycle (see Figure 5.1). According to Auvinet et al., the first smaller peak (P1) is associated with IFC, while the second (P2) and third (P3) peak are affiliated with foot-flat and mid-stance events (Auvinet, Berrut et al. 2002). Additionally, the second (V2) and third (V3) valley are related to FFC and the initial push-off (Auvinet, Berrut et al. 2002).

Along the vertical axis, after signal integration, the displacement pattern generally traces a relatively smooth sinusoidal curve, with its highest point occurring during mid-stance and its lowest point during double support. Assuming a pure sinus wave is present, the second derivative would be the original function with its sign reversed. Evidently, the appointed GEs in the VT acceleration pattern give rise to certain theoretical ambiguities or internal contradictions. Menz, Lord, and Fitzpatrick previously reported that P2 results from a heel-strike transient derived by an initial shock wave originating in initial foot-ground, not foot-flat, contact (Menz, Lord et al. 2003). Furthermore, IFC was identified at the initial first valley (V1) preceding P2, not P1. Other GEs, such as V3, seemingly cannot be related to mid-stance, since the VT displacement's highest point should relate to peak negative acceleration. It is apparent that the VT acceleration signal was described from a body's reference point as opposed to the sensor's inertial frame of reference.

It becomes clear that some parts of the VT acceleration pattern require further examination. A thorough understanding of the lower trunk's acceleration signal can not only provide more meaningful temporal gait information, but may also render current methods more applicable to pathological gait. Because of the acceleration pattern's sensitivity to high frequency components and consequent irregularity, it is hypothesized that velocity and displacement signals are more robust for the extraction of gait features.

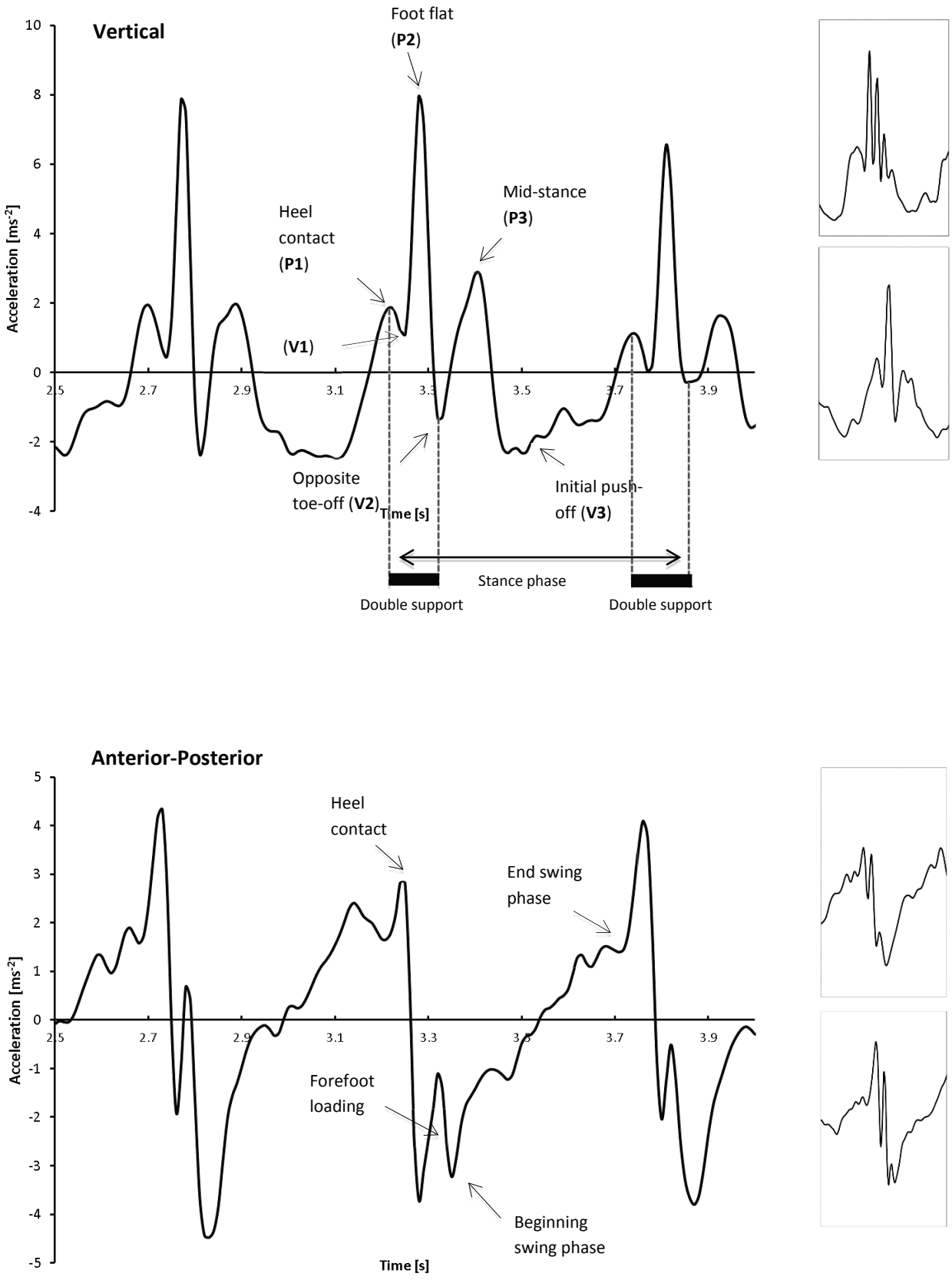

Figure 5.1 Gait events and phases derived from the vertical (top) and anterior-posterior (bottom) trunk acceleration pattern.

5.4 Method

The study was conducted on 4 healthy subjects who had given informed consent (3 males, 1 female; age 25.3 ± 2.5 y.o.; height 1.73 ± 0.15 m; and weight 71.5 ± 17.1 kg). None had a history of balance disorders or lower limb pathology at the time of measurement. The ethics committee of Oxford Brookes University approved all experimental protocol.

A single IMU (MTx, Xsens Technologies, Enschede, Netherlands, ±2*g* range) was attached with double-sided adhesive tape to the dorsal side of the subject's lower trunk at the level of the third lumbar vertebrae. Using an object-centered frame, x- and z-axis were defined as follows: positive Z values denoted posterior AP acceleration, and positive X values denoted downward acceleration. The IMU data collected was processed using a customized script written in LabView™ (LabView 2011; National Instruments, Austin, Texas, USA). The program employed a second-order, zero-phase Butterworth band-pass filter to remove integration drift, with cut-off frequencies at 0.5-25Hz.

Subjects walked twice along a 10m straight walkway at three different walking conditions (slow, preferred, fast), with the walkway featuring a single force platform (Kistler, Type 9260AA6, 60 x 50 cm, 100Hz) located in a calibrated volume with six optoelectronic motion capture systems (Qualisys AB, Oqus 300, Göteborg, Sweden). The frame rate was set to 100 frames/s to preserve signal power. After familiarization, a trial was considered valid if the subject correctly hit the force platform.

Timing of important GEs and phases in the acceleration signal relative to the stance phase were determined by comparing IMU data with the two reference systems. Particular reference GEs and phases were defined in the vertical GRF pattern during the stance phase, as shown in Figure 5.2. The vertical GRF pattern exhibits two distinct peaks (typical for normal gait), where $F \approx Mg$ and a dip in the middle where $F < Mg$. Shortly after IFC, the force rises from zero to a distinct peak, known as the heel-strike transient (HST) (Smeathers 1989). Body mass negatively accelerates here, causing the GRF to rise to a point above body weight (F_{max1}; first peak), a process known as a loading response. During the loading response, the pretibial muscles maintain the body's forward momentum during gait (Ayyappa 1997), while acting as shock-absorbing mechanisms to regulate the body's forward fall. At mid-stance, the body's COM moves upward, taking the GRF below body weight to a local minimum due to the centripetal force associated with the COM's motion along a curved path (Cross 1998). The body's upward motion negatively accelerates during the stance's first half, ultimately accelerating downward by its second. Now, as a result of the push-off phase, the GRF rises once more to a local maximum (F_{max2}; second peak). FFC refers to the instant, finally, when contact with the ground is lost, and force returns to zero. For a detailed explanation of how ground reaction forces relate to walking, see "Standing, Running, and Jumping on a Force Plate" by Rod Cross, 1998.

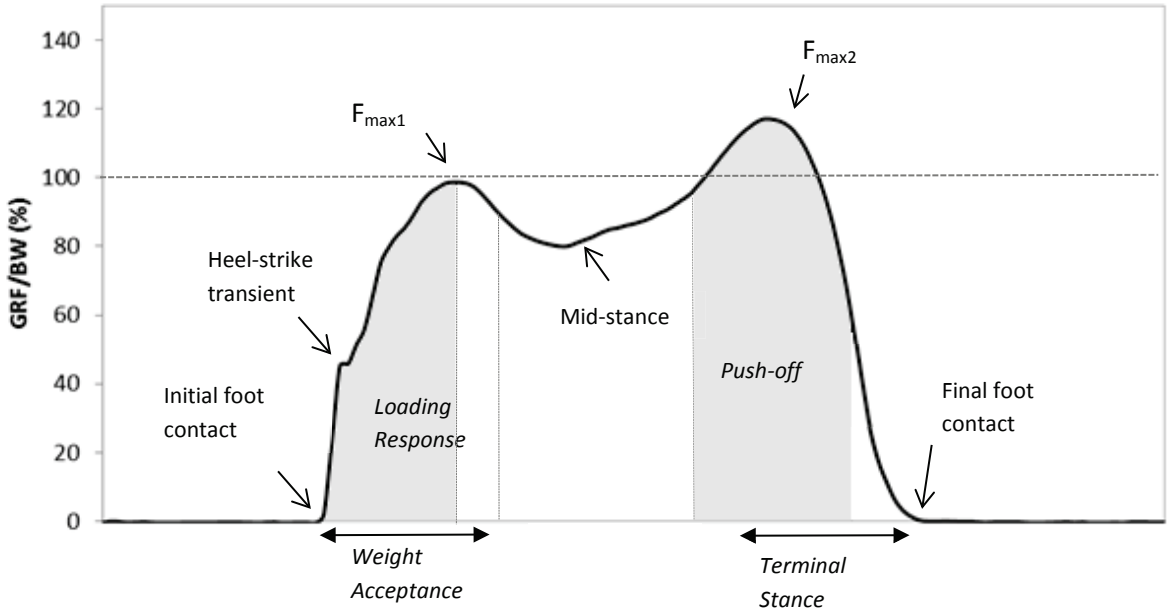

Figure 5.2 Gait events and phases defined from the contact phase of vertical ground reaction force.

For each trial, three retro-reflective markers on each foot (placed on the heel and metatarsal joints I and V) provided a detailed description of foot roll-over movement during stance phase. A typical example of the individual data obtained during overground walking is presented in Figure 5.3. The dashed vertical lines indicate a step cycle's start and end point. Consequently, heel-on-toe contact times were defined as when the marker more or less stopped moving in the vertical direction. By doing so, important time-events relative to foot-ground contact could be determined and cross-referenced.

For each walking speed condition, timing errors between identified GEs and IMU and reference systems were averaged over repeated trials. Timing errors were calculated and expressed in terms of mean relative (RE) and absolute error (AE) between measured and estimated GEs, along with their standard deviations and limits of agreement (95%CI).

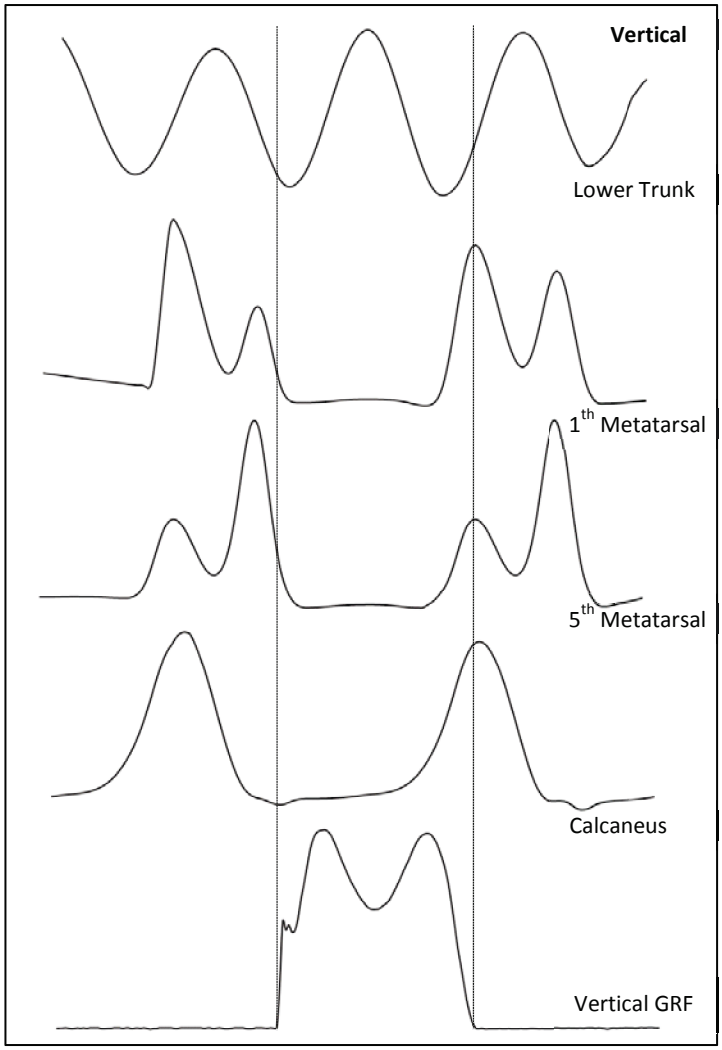

Figure 5.3 Representative example of data obtained from overground walking. The upper four traces indicate displacement of the trunk and foot, the lower trace indicate the vertical ground reaction force component. The dashed vertical lines in the figure indicate the start and end of a step cycle.

5.5 Results

A total of 24 steps (*N*=4) was used for GE detection in the VT and AP acceleration signal. Figure 5.4A and 5.4B illustrate how the trunk's VT and AP acceleration, velocity, and displacement patterns relate to the vertical GRF pattern during walking. Mean absolute errors on each identified GE are reported in Table 5.1. Table 5.2 builds on the findings from Table 5.1, displaying the relative error, standard deviation, and 95% confident interval (CI) from the most appropriate signal.

Vertical

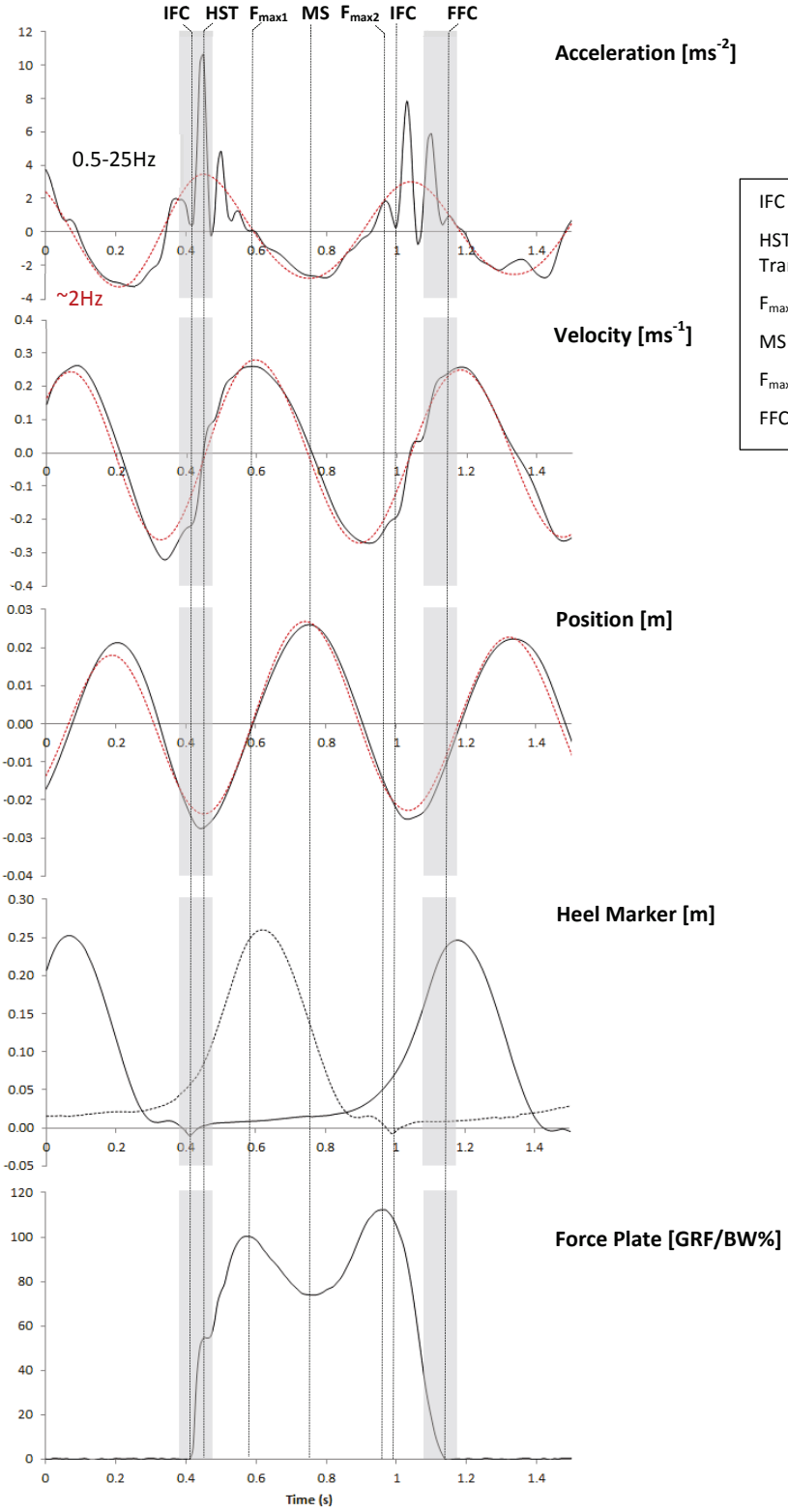

Figure 5.4A Illustrates VT acceleration, velocity, and position pattern during overground walking. The GRF pattern (bottom). The GRF pattern (bottom figure) studied in conjunction with the heel marker trajectory served to verify specific gait events. The solid black line in the position, velocity, and acceleration charts represents the normal curve, while the dotted red line represents the gait curve without shock wave propagation (filtered: ~2Hz).

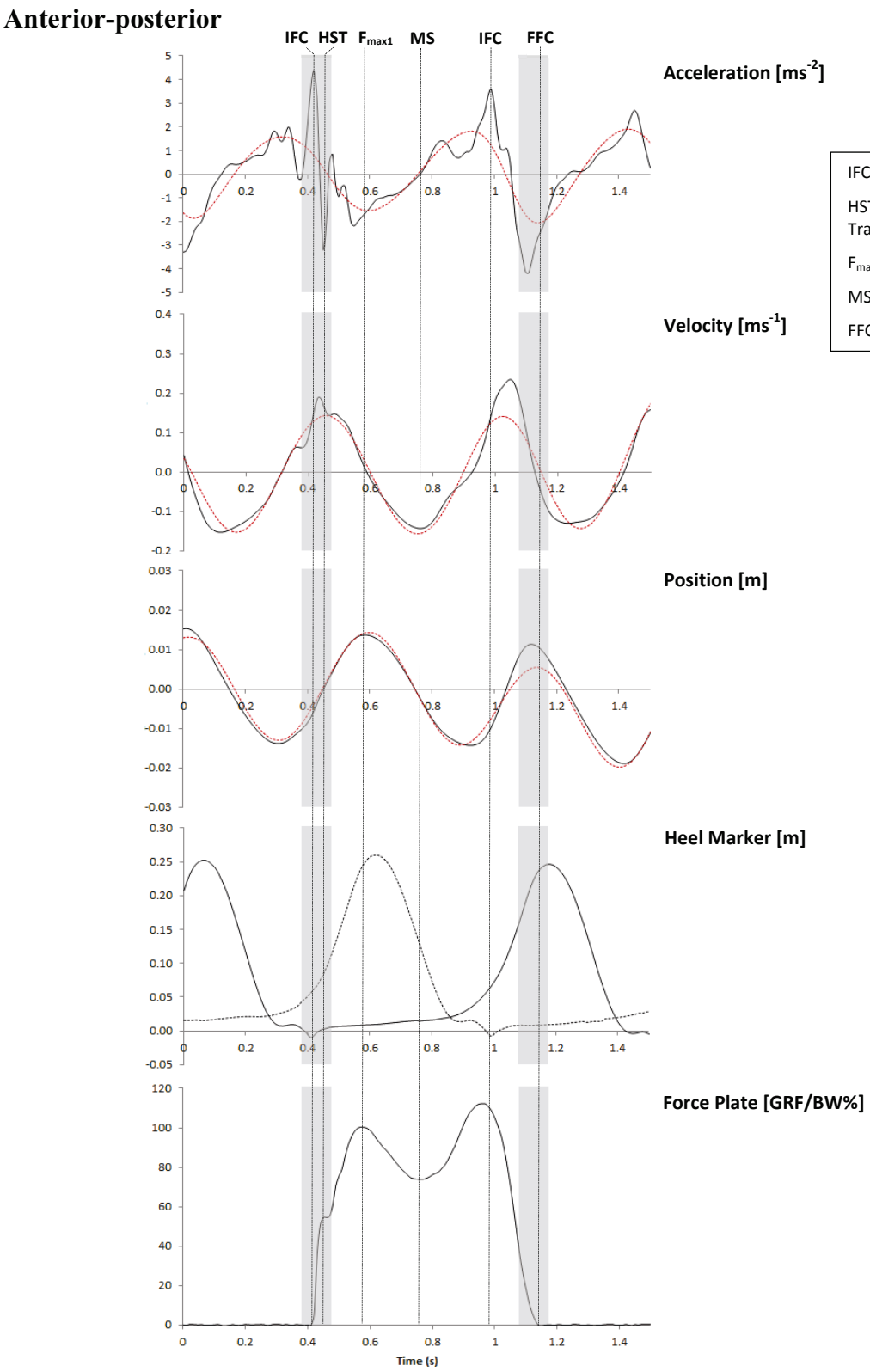

Figure 5.4B Illustrates AP acceleration, velocity, and position pattern during overground walking.

Table 5.1 Mean absolute difference between measured (reference data) and estimated GEs are shown, together with relevant standard deviations.

	VT						AP					
	Acceleration	**Velocity**	**Position**	**Acceleration***	**Velocity***	**Position***	**Acceleration**	**Velocity**	**Position**	**Acceleration***	**Velocity***	**Position***
IFC	0.007(0.007)						0.006(0.005)					
HST	0.013(0.009)	0.008(0.012)	0.048(0.007)				0.010(0.009)		0.022(0.036)			
MS		0.020(0.013)	0.016(0.010)	0.035(0.027)						0.029(0.022)	0.018(0.020)	0.018(0.016)
F_{max1}		0.037(0.026)	0.031(0.028)	0.037(0.020)	0.035(0.018)	0.037(0.022)		0.039(0.024)	0.039(0.023)	0.022(0.019)	0.021(0.021)	0.021(0.019)
F_{max2}	0.013(0.010)											
FFC										0.027(0.010)	0.027(0.013)	0.024(0.014)

The intensity is of the color is proportional to the accuracy of the GE, with mean absolute errors less than <.01s denoted in dark red, errors <.02s light red, and errors >.02s in grey tones.

* ~2Hz filtered signal

Table 5.2 The accuracy of identified GEs during slow, preferred, and fast walking speeds. The mean differences (relative and absolute) between identified GEs from IMU and reference data, along with relevant standard deviations and limits of agreements (95%), are reported.

		Accuracy (Mean ± S.D.)		**Limits of Agreement**	
Events	**Location**	**Mean difference (s)**	**Mean absolute difference (s)**	**Upper (s)**	**Lower (s)**
IFC	Peak positive AP acceleration	0.001(0.006)	0.006(0.005)	0.013	-0.006
HST	*Zero-crossing* VT velocity	0.007(0.012)	0.008(0.012)	0.031	-0.014
MS	Peak positive VT displacement	0.004(0.018)	0.016(0.010)	0.035	-0.003
F_{max1}	Peak positive AP displacement*	-0.002(0.028)	0.021(0.019)	0.053	-0.057
F_{max2}	Peak positive VT displacement	-0.006(0.016)	0.013(0.010)	0.025	-0.036
FFC	Peak negative AP acceleration*	0.027(0.010)	0.027(0.010)	0.048	0.007

* ~2Hz filtered signal

5.6 Discussion

To the author's knowledge, this is the first study that provides a complete referential framework for gait feature extraction from lower trunk accelerometry. While based exclusively on results from young healthy participants (excluding those with pathological gait), this study's analysis of the trunk's VT and AP acceleration pattern (and of their integrands) demonstrates, nevertheless, that a combination of both signals may provide more nuanced information regarding a person's gait, ultimately permitting more clinically relevant gait features to be extracted.

The reference frame work for lower trunk gait features extraction not only allows for accurate estimates of IFC and FFC, but also permits the computation of stance sub-phase durations. Unlike other methods that rely on multiple sensor placements, this single sensor setup can provide information about left-right asymmetry of stance, swing, and sub-stance phases with minimal discomfort for the subjects.

Although slight differences were observed between subjects accelerometry recordings, most signal features were shared. Breaking down the physical interpretation of the gravity subtracted vertical acceleration signal demonstrates that the transient vibrations (i.e. peak accelerations) on top of the acceleration's movement component are primarily related to shock wave propulsions during stance. The rate at which these oscillations decay depends on the amount of the "system's" dampening. Frequencies associated upon foot-ground contact range from 10 to 75Hz (Simon, Paul et al. 1981; Smeathers 1989). Other high frequency accelerations, such as artifact acceleration due to soft tissue movement and the sensor's mass, may also be present in the signal. In-depth analysis of the trunk's VT acceleration shows that this pattern possesses two to three—sometimes even four—distinct peaks shortly after IFC (see Figure 5.4A). The first peak after IFC corresponds to the HST, an acceleration 'shock wave' that passes up the limb after IFC. The location and timing of the particular event can also be found in the signal's filtered form (i.e. step frequency). The others peaks are related to the leading limb's loading response phase and the trailing limb's pre-swing phase, alternately conceived as the contralateral foot's initial push-off phase. The occurrence of several peaks after HST is most likely associated with the step-to-step transition's smoothness. Upon passing, the acceleration pattern reaches a local minimum related to MS. At MS, a transition from braking to propulsion unfolds. The trunk begins to accelerate forward and downward. Depending on the sensor's reference frame, such acceleration may be seen as either positive or negative. The pattern repeats itself after this point.

In contrast to the trunk's VT acceleration pattern, AP acceleration manifests as a basic pattern, one mainly related to the braking and propulsion of gait. In Figure 5.4B, AP acceleration reaches a local maximum at IFC. IFCs were derived with errors less than 0.01s, comparable to those reported by Zijlstra and Hof during treadmill walking (Zijlstra and Hof 2003), and were associated with the AP signal's 'main' peak—preceding its zero-crossing point. However, the use of thresholding or peak detection methods may not always be suitable for the extraction of this particular GE as its peak magnitude may vary across people, hampering the automatic detection of such events in some cases (Boutaayamou, Schwartz et

al. 2015). Trojaniello et al., already reported that the aforementioned method frequently fails if not corrected for inclination changes (Trojaniello, Cereatti et al. 2014). Frequency-derived measures, for that reason, may be a good or even a better alternative, as this technique doesn't require any time-accurate detection of IFCs to approximate step- or stride times (Weiss, Sharifi et al. 2011). Yet, the calculation of, for instance, loading rates—acceleration of the trunk at impact (IFC to HST) and double support times (IFC to FFC) require the exact time location of IFCs. After IFC, the AP acceleration pattern sharply declines to a local minimum, which is when the forefoot loading phase commences. It should be noted that deriving the beginning of the forefoot loading phase requires care here, as the minimum sometimes corresponds to the HST occurrence.

Moving ahead in the gait cycle, FFC can only be found in the 2Hz filtered AP signal. This particular event is hard to detect in the original AP signal since it occurs in the terminal phase of the step-to-step transition, where transient vibrations emanating from the leading limb's foot-flat moment coincides with the trailing limb's FFC. Consequently, FFC identification is a relatively less accurate process (0.027±0.010s). At the first half of the MS, the motion of the lower trunk is being negatively accelerated in order to counterbalance the lower extremity's opposite movement. Upon heel lift, during the second half of MS the forward acceleration gradually builds throughout the swing phase till IFC occurs. The pattern repeats itself after this point.

Other alternative methods for GE detection worth considering are wavelet techniques to analyze acceleration signals. McCamley et al., for instance, most recently proposed using continuous wavelet transforms to derive IFCs and FFCs, and ultimately achieved comparable levels of accuracy (McCamley, Donati et al. 2012). Although this method does not rely on particular signal features to determine single step timing, rendering it potentially more suitable for the detection of changes in gait variability (Godfrey, Del Din et al. 2015), the presence or, better yet, the absence of certain features in the signal may well be linked to other equally important aspects of pathological gait. This framework offers the opportunity to extract additional information, and therefore merits further study.

Chapter 6

A Modified Step-length Estimation Model[14]

6.1 Summary of Contents

Estimating step length with IMUs is important for physical activity monitoring and clinical gait analysis. Several methods based on the use of a single IMU mounted on the lower back have been proposed, showing satisfactory results when applied with a correction factor. This study, however, presents a modified step length estimation model, based on the lower trunk's vertical and anterior-posterior excursion, which eliminates the need for such a correction factor. Theoretical work was supported by treadmill data acquired from young healthy adults who walked across a range of speeds and step frequencies. This model's performance in relation to direct step length measurement was compared to that of two established step length estimation models. The same subjects were assessed four times along a 10m walkway at their preferred walking speed. Experimental results indicate that the proposed model allows for more accurate mean step length estimations than the two alternative models do, with errors less than 3% for all subjects (mean error of 0.80 ± 2.01cm).

6.2 Introduction

In biomechanics, the body's COM frequently functions as a key reference point to estimate mechanical energy changes and gait quality (Cavagna, Willems et al. 2000). The COM trajectory can also be used to estimate spatiotemporal gait features such as step length. Step length estimations are often based on a simple stiff-legged inverted pendulum model pivoting about the ankle. This well-known approach captures a mathematical relationship between the vertical COM excursion and step length, where vertical amplitude changes (h) depend on step length (Zijlstra and Hof 1997). Reversing this relationship allows for step length to be estimated when leg length (l) goes as follows: step length = $2\sqrt{2hl - h^2}$.

This model, however, underestimates mean step length by roughly 20%. Although Zijlstra suggested such underestimation could be corrected by adjusting the pendulum length to a point closer to the actual COM, this gesture did not, in practice, yield more accurate outcomes (Zijlstra 2004). A generic correction factor of 1.25 on the model was consequently proposed, but proved ineffectual, as its new estimates were somewhat inconsistent, especially among those with gait disorders (Esser, Dawes et al. 2011). On the other hand, while individual multiplication factors noticeably improved step length estimations under straight overground walking conditions (Zijlstra and Zijlstra 2013), they required knowledge of a

[14] In a slight adapted version, this Chapter is submitted for first-round review to Journal of Biomechanics. D. Steins, J. Collett, P. Esser, and H. Dawes. "A Modified Step-length Estimation Model for Gait Analysis."

predetermined distance to be derived, rendering them incompatible for any unconstrained and immediate assessment.

In light of these limitations, González et al. adjusted the model by adding a value proportional to the foot length to account for the missing double support phase (Gonzalez, Alvarez et al. 2007). The addition of such value originates from Cavagna, Thys, and Zamboni, whose results demonstrated that during the support phases, forward displacement of the COM remains relatively constant (Cavagna, Thys et al. 1976). Nonetheless, this modification did not yield better results. Step length was still underestimated, with errors up to 15% at fast walking speeds (Gonzalez, Alvarez et al. 2007). This model, moreover, requires the detection of specific gait events (i.e., initial and final foot contacts) to distinguish between single and double stance phases, which in itself can be a cumbersome process (Gonzalez, Alvarez et al. 2009). That being said, both models were, despite this, deemed highly reliable, with good-to-excellent agreement levels (Zijlstra and Zijlstra 2013).

Human walking should, instead, be approached as a motion of two-coupled pendula, in which the stance leg behaves like an inverted pendulum and the swing leg like a regular one. The inverted pendulum model can effectively explain that an increase in walking speed increases vertical COM excursions, in turn, as a subject makes longer steps. However, it fails to explain why the actual vertical excursion is far less than predicted (Stern, Demes et al. 2004). Potential reasons for this shortfall include the negligence of the trailing ankle's plantar flexion near the end of stance phase (Kerrigan, Della Croce et al. 2000), which would lengthen both the pendulum, and the pelvic rotation about the vertical axis (Kerrigan, Riley et al. 2001; Liang, Wu et al. 2014). Consequently, this one-dimensional representation might be somewhat misleading, as it disregards any horizontal displacement in time (Stern, Demes et al. 2004). By including the trunk's concomitant motion in the sagittal plane (flexion and extension), one that occurs during the gait cycle in response to limb movement (Chung, Park et al. 2010), the COM's vertical pathway elongates in the plane of progression, thereby effectively lengthening steps.

Replacing the inverted pendulum model with a conventional pendulum model of the swing leg to allow for horizontal trunk movement may play a crucial role in obtaining more accurate step length estimations. Thus, it is hypothesised that: 1) modelling by lower trunk motion, the anterior-posterior (AP) COM displacement pattern contributes to step length estimations, AP displacements being related to walking speed and step frequency; and 2) incorporating AP displacements allows for more reliably accurate step length estimations than those derived from previous models (Zijlstra and Hof 1997; Gonzalez, Alvarez et al. 2007). The objective of the present study, hence, to evaluate this new step length estimation model's reliability and agreement based on vertical (VT) and AP COM displacements against those belonging to other trunk-based estimation models. Normative COM data is presented to support this model this new model over the course of the discussion.

6.3 Methods

The experimental protocol was formed from data gathered by two independent experiments. The first examined the trajectory of the 'COM' pattern, in terms of amplitude changes, drawing upon both VT and AP excursions on a treadmill at a broad range of predefined walking speeds and step frequencies. This permitted each independent variable to be controlled and its effect isolated. Results of the first experiment provided strong evidence for the inclusion of AP trunk motion in a new step length estimation model. The second overground walking experiment then compared the performance (i.e. reliability and validity) of this new model against that of two established step length estimation models (Zijlstra and Hof 1997; Gonzalez, Alvarez et al. 2007).

6.3.1 Subjects

Ten young adult subjects (5M/5F, 25.6 ± 3.5 years, mean age ± S.D.) participated in this study. Potential subjects were excluded if they had a condition that affected gait. The study was performed in accordance with the declaration of Helsinki and approved Oxford Brookes University ethics committee (#120622). All subjects were informed of the study and provided written consent. Their average height, weight, foot size, and leg length[a,b,c] were 1.73 ± 0.12m, 73.0 ± 17.1kg, 0.26 ± 0.02m, and 0.91 ± 0.07m[a], 0.81 ± 0.07m[b], 1.05 ± 0.08m[c]. In both experiments, subjects walked barefoot and wore their usual attire. Measurements of leg length were made according to the standards set by three predefined models; the distance between a) the ground and the top of right trochanter major femoris; b) the lateralus malleolus and the greater trochanter major femoris; and c) the ground to the lower trunk marker).

6.3.2 Model

The model represents a pendulum-like swing leg with a moving pivot to allow for horizontal trunk fluctuations during walking (Winter, Patla et al. 1990). The mathematical details of the step length estimation model are as follows. To account for the plantar flexion of the trailing ankle near the stance phase's end, the magnitude of the lower limb's angular excursion was initially considered to predict the virtual leg length of the swing leg at the beginning and end of the step. The calculated estimates of the angular excursion based on leg length and the VT COM excursion, however, did not seem to match those reported by others (Lee and Farley 1998; Stern, Demes et al. 2004). To correct for this, the trunk's horizontal displacement was assumed to correspond with the ankle plantar flexion or "push-off" in late stance accompanied with pelvic rotation to assist the forward progression of the contralateral leg into swing (McGibbon 2003). Using the total AP and VT displacement of the trunk, a prediction of the virtual leg length was made at the beginning and end of the step cycle using simple trigonometry shown in Figure 6.1:

$$h' = \sqrt{\Delta x^2 + \Delta y^2} \tag{6.1}$$

h' denotes the missing leg length, and *Δx* and *Δy* represent the net amplitude changes in the AP and VT direction during the single and double support phase. By conceiving the swing leg as a stance leg, the distance without trunk motion in the sagittal plane can subsequently be calculated as:

$$d = 2\sqrt{2h'l + h'^2} \tag{6.2}$$

where *l* refers to the leg length, measured as the distance from the ground to the lower trunk, and *d* the estimated stepping distance.

During walking, the trunk's posterior tilting occurs at the initiation of the single support phase to counterbalance the lower extremity's opposite movement (see Figure 6.2). On the other hand, the trunk begins to bend anteriorly right before initial foot contact through the double support phase, which appears to enhance forward progression when the body is stabilized by double support. (Chung, Park et al. 2010). The pattern of trunk tilt motion is biphasic similar to that of pelvic rotation (Crosbie, Vachalathiti et al. 1997). Thus, it can be assumed, that the local minimum of AP trunk displacements corresponds to the local maximum of internal pelvic rotations. Considering that pelvic rotation, during normal walking, contributes to step length (Liang, Wu et al. 2014), adding AP trunk displacements (*x*) to the equation results in:

$$d = 2\sqrt{2h'l + h'^2} + 2\Delta x \tag{6.3}$$

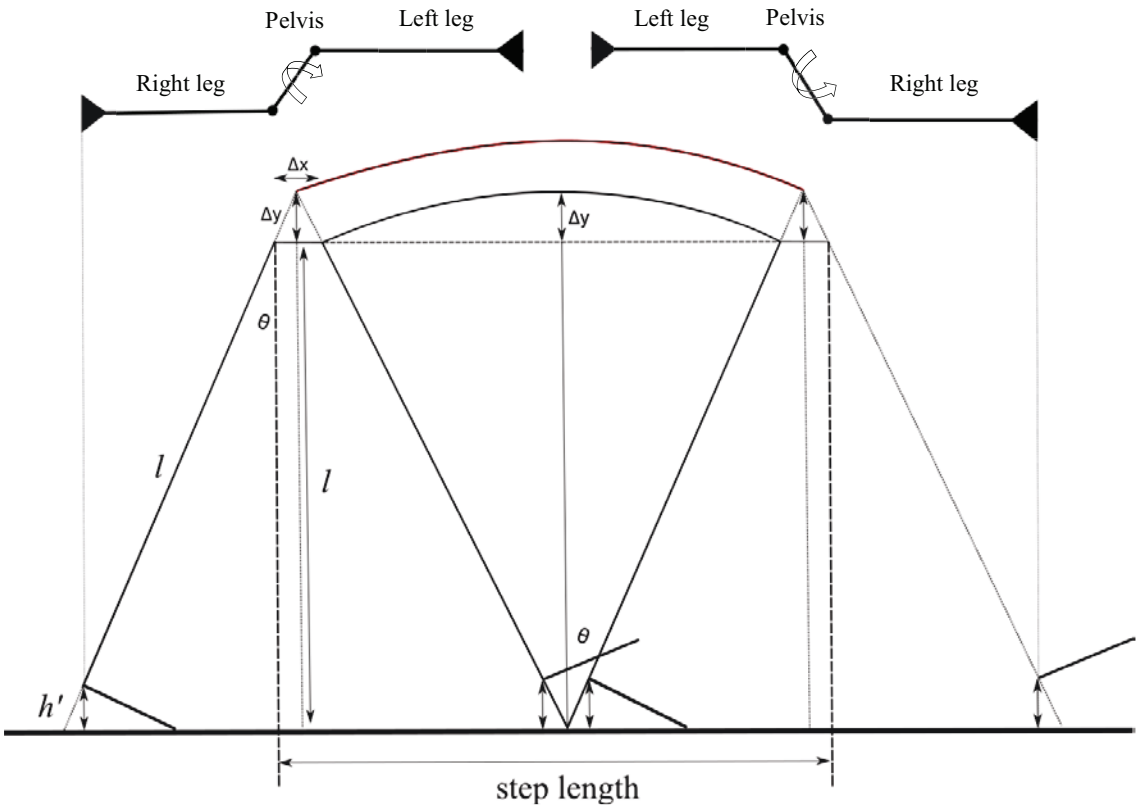

Figure 6.1 Adjustment of the inverted pendulum model to allow for horizontal trunk motion. Step length can be determined from the amplitude fluctuations in the anterior-posterior (*Δx*) and vertical (*Δy*) direction.

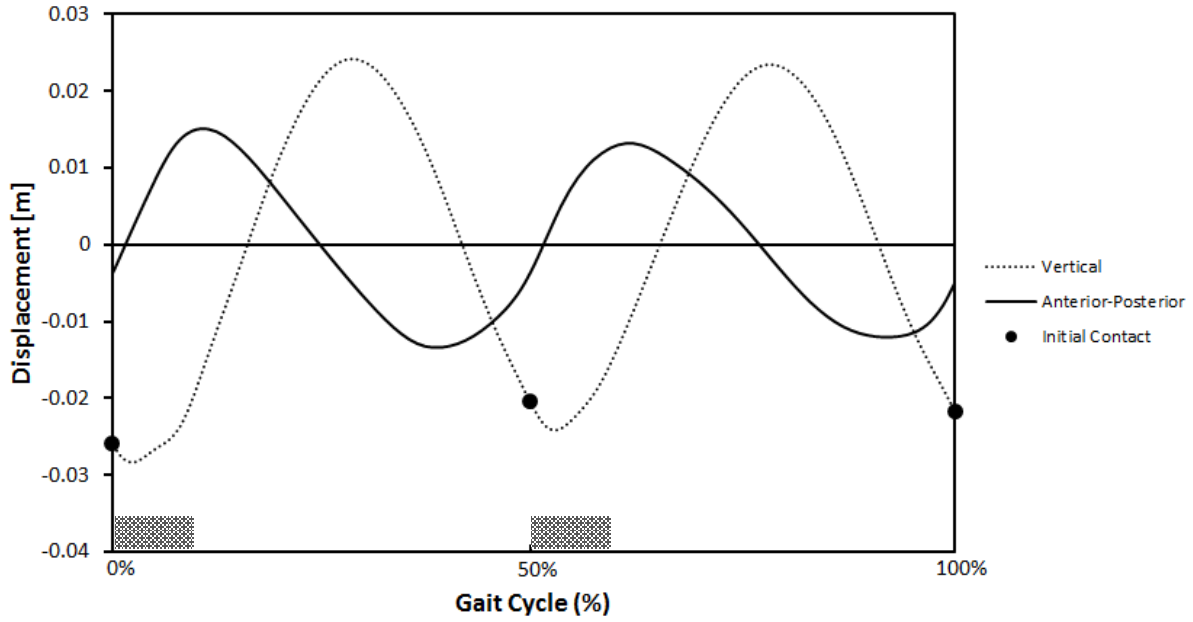

Figure 6.2 Trunk motion in two planes. The graphs depict trunk displacement in the vertical and horizontal plane using the object reference frame. Note two repetitive motions in both axes during one stride. The grey bars represent the double support phases.

6.3.3 Experimental Manipulation

Experiment 1

Subjects walked on a treadmill for five blocks (30s duration) at walking speeds of 0.7, 1.0, 1.2, 1.4, and 1.6ms^{-1} and step frequencies of 1.7, 1.8, 1.9, 2.0, and 2.1Hz. Subjects were instructed to walk in accordance with an auditory cue presented by a metronome (MetroTimer 3.0 for iOS, by ONYX Apps). Prior to testing and data collection, subjects familiarized themselves with the given speed and step frequency. Walking trials were accepted for inclusion if the subject's step frequency was within ±5% of the given cues. Trials not meeting this benchmark were re-performed. In order to analyse steady-state walking, only the middle 10s of each block were used for analysis, resulting in approximately 18-21 recorded step cycles during each walking conditions.

Experiment 2

The experiment had two aims: 1) to establish a valid method for the detecting sequential foot contacts to obtain reference step length estimations, and 2) to determine the validity of the proposed step length estimator. For the former, two retro-reflective markers on each heel proved to be a valid method for estimating sequential foot contacts. The validity of the proposed step length estimator was assessed with the same ten subjects. For this experiment, subjects were asked to walk four times along a 10m walkway at their preferred walking speed.

6.3.4 Data Acquisition

For both walking experiments, linear accelerations of the lower trunk were measured by one 6-DOF inertial sensor (MTx, Xsens Technologies, range of ±2*g*). The inertial sensor was attached with double-sided adhesive tape over the L3-L4 spinous process, a region suggested to have low transverse plane rotation in relation to axial rotation of the pelvis and thorax (Moe-Nilssen 1998). Prior to all testing sessions, each accelerometer axis was calibrated through a horizontal reference surface to ensure that vertical axis output was ±1*g* and horizontal axes outputs were 0*g*. Accelerometer data was sampled at 100Hz using a portable data logger, which was attached to a belt worn by the subject.

6.3.5 Data Analysis

Following the experiments, analog data were downloaded from the data logger onto a PC and analysed via a customized LabView™ program (LabView 2011; National Instruments, Texas, USA). The program employed an infinite-impulse response Butterworth band-pass filter to remove integration drift, with cut-off frequencies at 0.5-25Hz. Subsequently, AP and VT displacement data were obtained by Simpson's rule of numerical integration. Using an object-centered frame, x- and z-axis were defined as follows: positive Z values denoted posterior AP acceleration, and positive X values downward acceleration. For the treadmill walking experiment, amplitude changes of the VT and AP displacement were averaged over a continuous 10s period for each walking condition and normalized to leg length.

6.3.5.1 Initial Foot Contact

The overground walking experiment required a valid method for detecting sequential foot contacts to obtain reference step lengths for comparisons. A single force plate (FP; Kistler 9260AA3, Kistler Group, Switzerland, 100Hz) located in a calibrated volume with six optoelectronic motion capture systems (Qualists Oqus 300, Qualisys AB, Göteborg, Sweden) was used to acquire reference data. The frame rate was set to 100 frames/s to preserve signal power. Retro-reflective markers were attached on each foot (on the heel), and over the center of the IMU using double-sided adhesive tape. Instances of initial foot contact were determined from marker positions and the force platform (see Figure 6.3). Only trials containing clean FP hits were included.

6.3.5.2 Step Length

Mean reference step length estimates were derived by dividing the distance travelled by the number of steps. Steps were identified using the instants of heel-strike from the AP trunk accelerations (Zijlstra and Hof 2003). Individual reference step length calculations were determined from the middle three to six steps of a walk by using the method described in 6.2.5.1. Mean and individual step length estimates were determined using two variations of the inverted pendulum (IP) model that will be referred to as the Z-Method (Zijlstra and Hof 1997) and G-Method (Gonzalez, Alvarez et al. 2007). The first, prescribed by Zijlstra and

Hof, uses a simple IP walking model: step length $=1.25 * 2\sqrt{2hl - h^2}$, where h is the vertical amplitude change, and l is the leg length[a]. Step length was subsequently obtained by applying a multiplication factor of 1.25 to correct for underestimation. The second estimator is based on a two-stage IP model, where step length was calculated by adding the forward displacements during double and single stance phases: step length $= C * 2\sqrt{2h_b l - h^2}$, where h_b is the vertical amplitude change during the single support phase (computed as the difference between the maximum and minimum determined from the initial foot contact event), l is the leg length[b], and C is a predetermined constant of 75% of the foot length to account for the double stance phase. Foot length was calculated as follows: foot length [cm] $= \frac{EU}{1.5} - 1.5$.

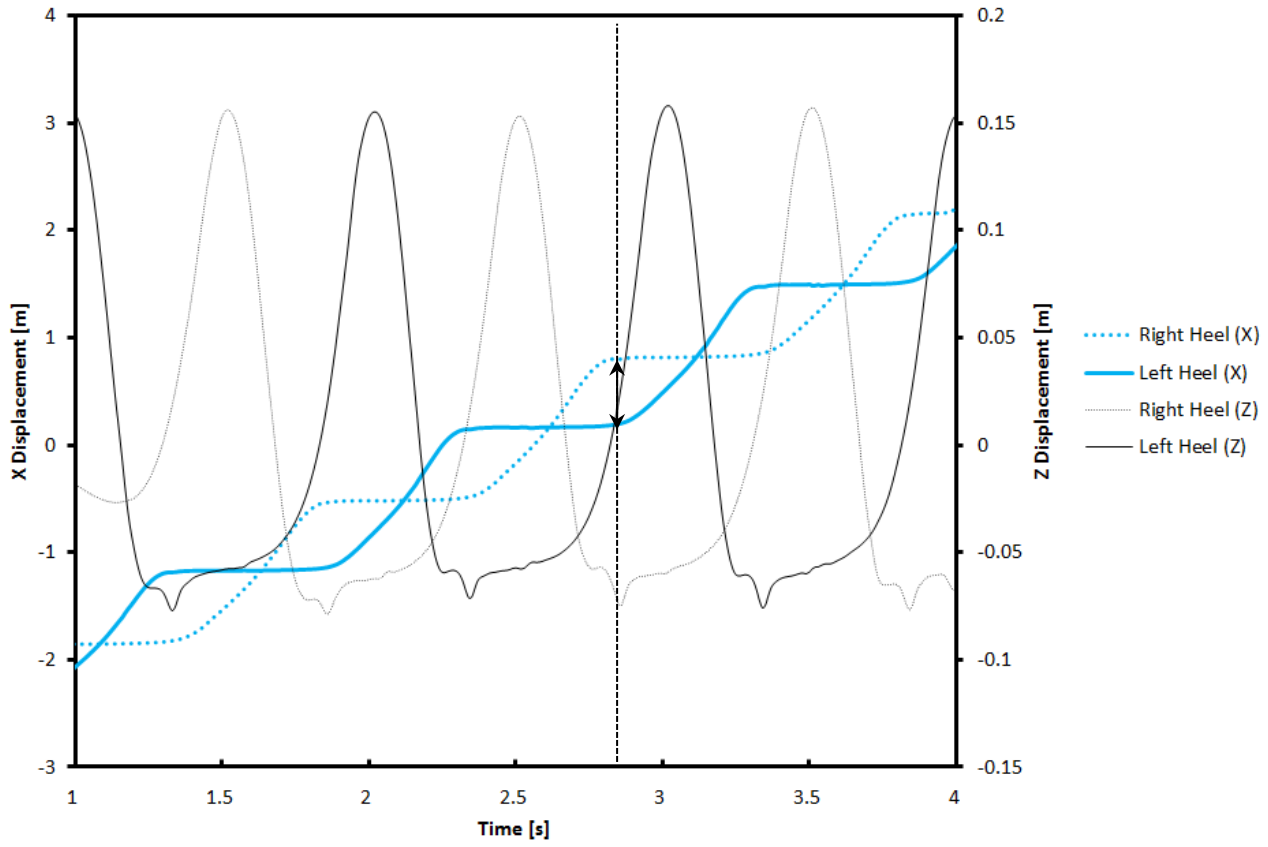

Figure 6.3 Calculation of reference step lengths. As the leg and foot are swung forward, the heel just clears the ground and then rises to a second peak. The incline following the second peak has been determined as the initial foot contact event (dotted line). The difference between heel markers at that point is taken as step length. Reference step lengths were afterward determined as the distance in the X displacement between each heel marker.

6.3.6 Statistical Analysis

For the treadmill experiment, all COM displacements were normalized to leg length and checked for normality with the Shapiro-Wilk test. Two-way repeated-measures ANOVA examined the main interaction effects of walking speed and step frequency on normalized COM displacements. Additional polynomial contrasts were performed to examine any

measurement trends. Five one-way repeated-measures ANOVAs were also used to test the interaction effect of step frequency on each walking speed, and vice-versa. A Fisher's least significant difference (LSD) was performed if significant differences were observed.

Following the overground walking experiments, mean and standard deviations of the estimated step lengths (i.e. average and step-to-step estimates) were calculated for all trials. Intra-session reliability was using a two-way repeated-measures ANOVA and analyzed through intraclass correlation coefficients (ICCs) of the type 3,1 and 3,*k*. Agreement between each method and the relevant gold standard values were tested by a repeated-measures ANOVA and analyzed with ICCs of the type (3,1 and 3,*k*) with associated confidence intervals (95% CI) and limits of agreement (LOA). The presence of heteroscedasticity was tested using regression analysis on absolute residuals. ICCs were interpreted as ≥0.90 excellent, ≥0.75 good, and ≥0.70 moderate. Statistical significance was set at $p<.05$.

6.4 Results

The results of the treadmill experiment are reported in Table 6.1. The table presents the mean and standard deviation of the normalized VT and AP displacements for each walking condition, and the subject's cadence (steps/min). Figure 6.4 shows the mean normalized peak-to-peak amplitudes of the estimated COM in their dependency of walking speed and step frequency (A-D) as well as their interaction effect (E-F). The test-retests results of the overground walking experiment are reported in Table 6.2. Measures of absolute and relative agreement between estimated and reference step lengths are reported in Table 6.3. In more detail, participant demographic, anthropometric and performance characteristics are reported as supplementary data (See Appendix A and B).

6.4.1 Center-of-Mass Displacements during Treadmill Walking

All ten subjects successfully completed the treadmill walking experiment and a total of 250 walking trials (10 x 25 walking conditions) were included for analysis. The compliance to the predetermined step frequency was satisfactory (see Table 6.1.). The overall VT displacement ranged from 1.2cm at $0.7ms^{-1}$ to 5.4cm at $1.6ms^{-1}$, and AP displacement ranged from 1.1cm at $0.7ms^{-1}$ to 2.7cm at $1.6ms^{-1}$. A two-way repeated-measures ANOVA demonstrated a significant overall effect of speed and step frequency for both VT, $F(1.65,14.442)=666.965$, $p<.0001$ and AP COM displacements, $F(2.197,19.769)=399.451$, $p<.00001$. A significant interaction effect was also found between walking speed and frequency on both VT, $F(2.020,18.179)=27.498$, $p<.0001$, $r=.87$ as well as AP displacements, $F(3.297,29.677)=18.107$, $p<.0001$, $r=.82$. Both VT and AP excursions changed substantially across walking conditions, exhibiting a strong linear relationship, $r=.99$, $p<.01$. In-depth analysis revealed two distinct linear trends (Figure 6.4E), in which VT COM displacement primarily depend on step length at speeds below $1.2ms^{-1}$ ($r=.99$, $p<.01$) and on both step length and frequency at higher speeds ($r=.99$, $p<.01$). These results indicate that the amplitudes changes in both VT and AP direction strongly rely on the subject's speed and step frequency.

6.4.2 Reliability of the Estimated Step Length

A total of 40 walking trials (10 x 4 sessions) were obtained and used for the comparative analysis. Test-retest results for averaged and individual step length estimates are shown in Table 6.2. Repeated-measures ANOVA revealed a significant difference between test session 1 and 2 for individual step length estimates. Relative reliability assessed with an ICC (3,*k*) and ICC (3,1) demonstrated excellent test-retest reliability for averaged estimates (ICCs ranging from .901 to .938) and good test-retest reliability for individual estimates (ICCs ranging from .781 to .874).

6.4.3 Agreement of SL Models with Reference Step Length

Table 6.3 presents the results of overall agreement and Figure 6.5 shows the comparison using box plots. There was a significant systematic difference on both averaged and individual step length estimates, as determined by a repeated-measures ANOVA (Averaged: $F[1.716,66.936]=27.1$, $p<.001$; Individual: $F[2.212,314.157]=27.6$, $p<.001$). A Fisher's LSD test revealed that Z-method significantly underestimates ($p<.001$) average step length by -2.4cm. No differences were found for both G-method (-0.4cm, $p=.35$) and the new proposed method (0.1cm, $p=.80$). For individual estimates based on three to six steps all step length models acquired significant differences, Z-method (-2.9cm, $p<.001$), G-method (-1.1cm, $p<.001$) and S-method (-0.8cm, $p=.02$).

Relative agreement, expressed by ICC (3,*k*) on averaged estimates, was excellent for S-method (ICCs ranging from 0.90 to 0.97) and good for both Z-method and G-method (ICCs ranging from 0.79 to 0.89). On individual step length estimates, the ICC (3,1) showed poor-to-good agreement for all three methods (ICCs ranging from 0.59 to 0.85). A visual check by Box plots for averaged step length estimates displayed a good distribution of agreement, with no heteroscedasticity for S-method ($r=.12$, $p=.15$). On the contrary, the agreement between Z-method and reference data was poor, with strong evidence for a non-linear form of heteroscedasticity for both Z- ($r=.81$, $p<.001$) and G-method ($r=.66$, $p<.001$).

Table 6.1 Anterior-posterior (AP) and vertical (VT) COM displacement values during treadmill walking (mean ± SD)

Speed (ms^{-1})	**AP COM Range (cm) Step frequency (Hz)**					**VT COM Range (cm) Step frequency (Hz)**					**Cadence (steps/min)**
	1.7	1.8	1.9	2.0	2.1	1.7	1.8	1.9	2.0	2.1	
0.7	1.6 ± 0.3#	1.3 ± 0.3#	1.1 ± 0.3#	1.0 ± 0.2#	0.9 ± 0.1#	1.5 ± 0.4	1.5 ± 0.4	1.4 ± 0.5	1.4 ± 0.4	1.5 ± 0.5	101.4 ± 0.7
1.0	2.4 ± 0.5#	2.0 ± 0.4#	1.7 ± 0.3#	1.4 ± 0.3#	1.2 ± 0.2#	2.6 ± 0.4	2.5 ± 0.5	2.4 ± 0.6	2.3 ± 0.6	2.3 ± 0.6	107.6 ± 0.8
1.2	2.9 ± 0.5#	2.4 ± 0.5#	1.8 ± 0.4#	1.6 ± 0.3#	1.4 ± 0.4#	3.4 ± 0.5	3.3 ± 0.5	2.8 ± 0.5	2.9 ± 0.6	2.6 ± 0.5	114.4 ± 1.1
1.4	3.5 ± 0.5#	3.0 ± 0.5#	2.4 ± 0.5#	2.1 ± 0.4#	1.8 ± 0.4#	5.6 ± 1.2#	4.9 ± 0.6#	4.4 ± 0.5#	4.2 ± 0.6#	3.9 ± 0.7#	119.5 ± 0.5#
1.6	3.9 ± 0.4	3.3 ± 0.5	2.7 ± 0.5	2.5 ± 0.4	2.0 ± 0.4	7.6 ± 1.6#	6.5 ± 1.3#	5.7 ± 0.8#	5.2 ± 0.5#	4.8 ± 0.7#	124.7 ± 1.8#

Group mean ± standard deviation
Note: Overall significance was $p<.00001$.
P-value represents the one-way ANOVA for repeated-measures.
Individual comparisons with significance from the direct adjacent step frequency ($p<.01$).

Table 6.2 Intra-session reliability of the step length methods for averaged and individual step data (n=10)

	Averaged						Individual					
	t1	**t2**	**t3**	**t4**	$ICC_{3,k}$ *r*[Lb-Ub]	*p*-Value	**t1**	**t2**	**t3**	**t4**	$ICC_{3,1}$ *r*[Lb-Ub]	*p*-Value
***Ref.* step length [m]**	0.69 ± 0.05 0.61 – 0.79	0.71 ± 0.05 0.66 – 0.82	0.70 ± 0.05 0.63 – 0.79	0.70 ± 0.06 0.61 – 0.82	.90 [.76-.97]	.027	0.69 ± 0.06 0.59 – 0.81	0.71 ± 0.05 0.65 – 0.83	0.70 ± 0.05 0.63 – 0.80	0.70 ± 0.06 0.60 – 0.83	.84 [.74-.92]	.004
Z-method	0.66 ± 0.08 0.52 – 0.78	0.69 ± 0.08 0.55 – 0.85	0.67 ± 0.07 0.56 – 0.80	0.68 ± 0.09 0.51 – 0.84	.93 [.82-.98]	.018	0.66 ± 0.08 0.49 – 0.79	0.69 ± 0.09 0.53 – 0.86	0.67 ± 0.07 0.51 – 0.81	0.68 ± 0.09 0.48 – 0.86	.87 [.77-.93]	.016
S-method	0.69 ± 0.06 0.59 – 0.78	0.70 ± 0.07 0.63 – 0.84	0.69 ± 0.06 0.61 – 0.79	0.69 ± 0.07 0.58 – 0.82	.90 [.76-.97]	.042	0.68 ± 0.06 0.55 – 0.79	0.70 ± 0.07 0.61 – 0.85	0.69 ± 0.07 0.56 – 0.79	0.69 ± 0.07 0.55 – 0.83	.78 [65-.88]	.414
G-method	0.66 ± 0.07 0.54 – 0.77	0.69 ± 0.07 0.55 – 0.81	0.68 ± 0.06 0.56 – 0.76	0.69 ± 0.07 0.54 – 0.81	.94 [.82-.98]	.001	0.68 ± 0.07 0.54 – 0.80	0.70 ± 0.07 0.57 – 0.85	0.69 ± 0.06 0.55 – 0.79	0.69 ± 0.08 0.53 – 0.84	.89 [.81-.94]	.075

Group mean ± standard deviation, minimum and maximum are indicated for all four test sessions (t1 – t4).
P-value represents the one-way ANOVA for repeated-measures.

Table 6.3 Concurrent validity of the step length methods with reference step length for averaged across four walking trials and individual step data (n=10)

		ICC$_{3,k}$ and ICC$_{3,1}$ (95% CI)									
Step Length	Method	**t1** *r*[Lb-Ub]	**MD ± LOA** [cm]	**t2** *r*[Lb-Ub]	**MD ± LOA** [cm]	**t3** *r*[Lb-Ub]	**MD ± LOA** [cm]	**t4** *r*[Lb-Ub]	**MD ± LOA** [cm]	**Overall** *r*[Lb-Ub]	**MD ± LOA** [cm]
Averaged	**Z-method**	.82[.17-.96]	-2.9 ± 5.5	.85[.40-.96]	-2.5 ± 6.4	.79[.24-.95]	-2.7 ± 6.4	.89[.60-.97]	-1.9 ± 6.8	.84[.47-.93]	-2.5 ± 6.1**
	S-method	.95[.81-.99]	0.2 ± 3.6	.97[.87-.99]	0.1 ± 3.3	.90[.66-.97]	-0.4 ± 5.0	.96[.85-.99]	0.4 ± 4.0	.95[.90-.97]	0.1 ± 2.0
	G-method	.89[.63-.97]	-0.7 ± 5.7	.87[.58-.97]	-0.6 ± 6.6	.86[.53-.96]	-0.5 ± 5.5	.89[.62-.97]	0.1 ± 6.7	.87[.77-.93]	-0.4 ± 6.0
Individual	**Z-method**	.68[.25-.85]	-3.4 ± 8.7**	.59[.31-.77]	-2.7 ± 10.7**	.66[.31-.83]	-2.8 ± 8.4**	.77[.47-.90]	-2.7 ± 8.3**	.68[.41-.81]	-2.9 ± 9.1**
	S-method	.77[.59-.87]	-0.7 ± 7.4	.63[.40-.79]	-0.9 ± 9.1	.64[.40-.80]	-0.6 ± 9.6	.85[.70-.92]	-1.1 ± 6.6	.73[.64-.80]	-0.8 ± 8.2#
	G-method	.77[.58-.87]	-1.3 ± 7.8	.68[.47-.82]	-1.0 ± 8.8	.74[.54-.86]	-1.2 ± 7.0	.84[.70-.92]	-1.0 ± 6.8	.76[.67-.83]	-1.1 ± 7.6**

Group mean ± standard deviation of the error are indicated for all four test sessions (t1 – t4).

Abbreviations: ICC, intraclass correlation coefficient; MD: mean difference; 95% CI, 95% confidence interval; Lb-Ub: lower and upper bound of associated 95% confidence interval; LOA: limits of agreement.

Significant difference between reference and step length estimates at p<.05.

** Significant difference between reference and step length estimates at p<.01

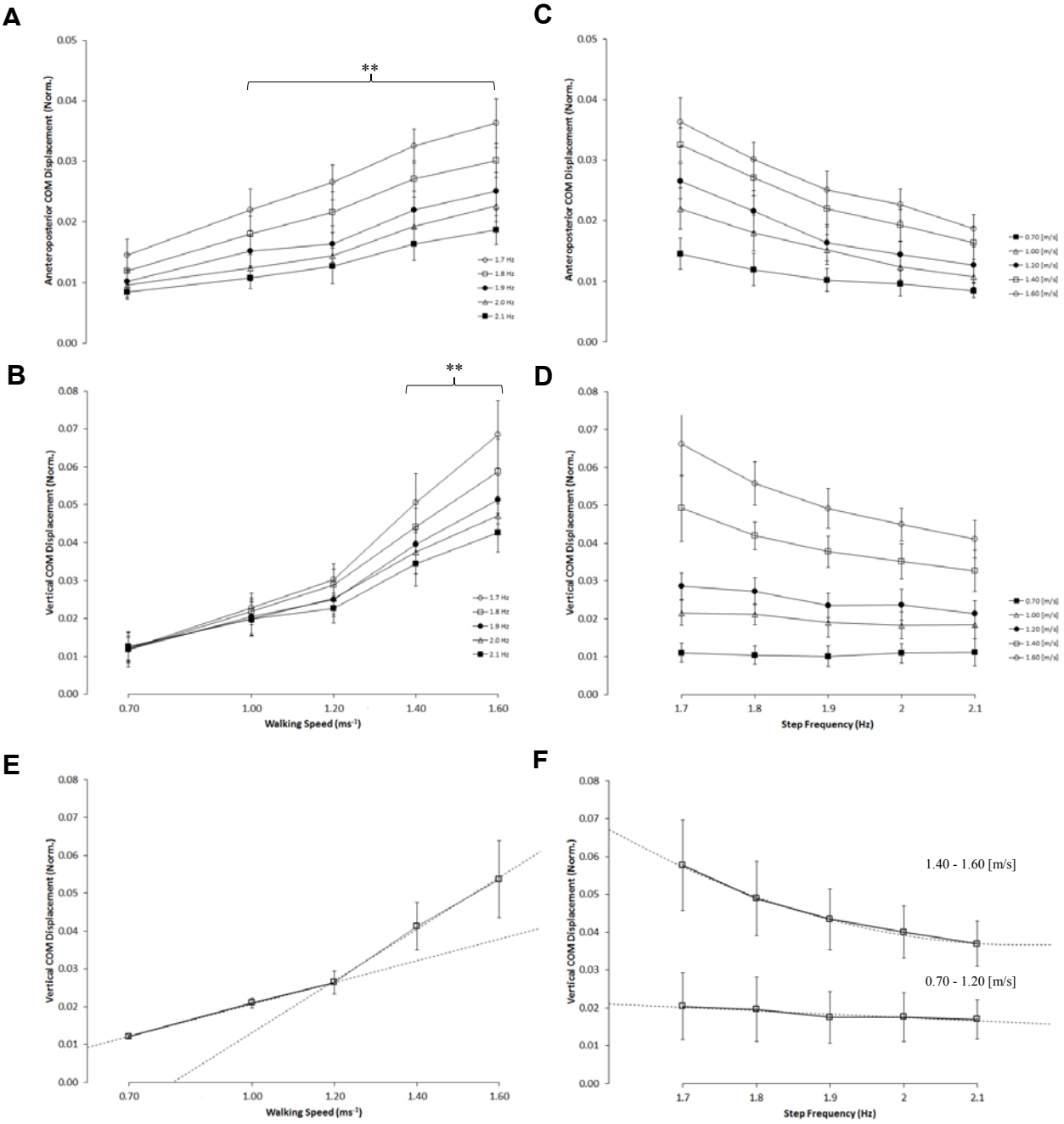

Figure 6.4 Estimated COM displacement across five different walking speeds and step frequencies. A&B, reduction in VT and AP COM displacement with increasing step frequencies; C, increase in AP COM displacement with increasing walking speeds; D, invariable VT COM displacement with walking speeds up to 1.2ms^{-1}, but increasing at a higher walking speed; E&F, demonstrates the interaction effect of walking speed and step frequency on the averaged VT COM displacement. All data are represented as a relative mean amplitude change of COM displacements for each condition. Data are mean ± S.D. $^{**}p<.01$ vs. different step frequencies for VT and AP COM displacement.

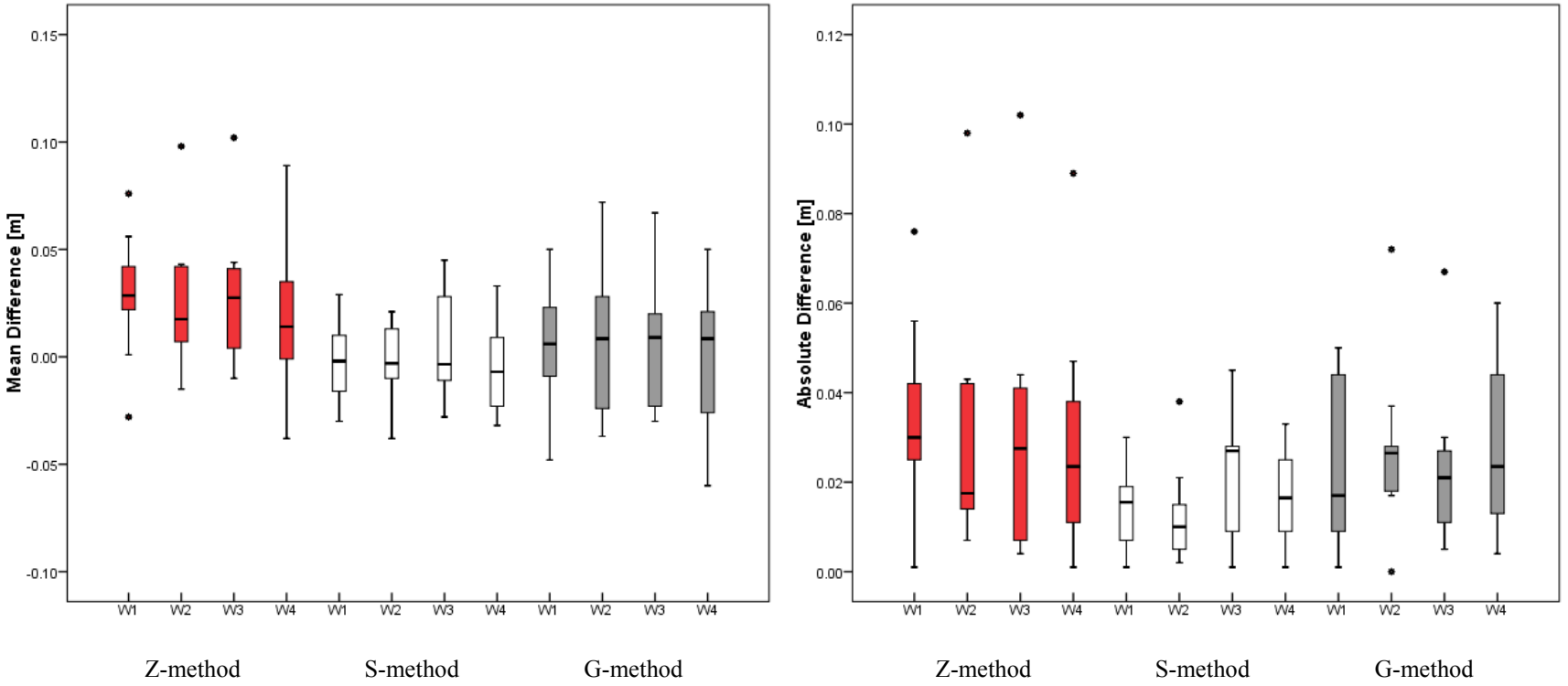

Figure 6.5 Minimum, first quartile (q_1), median, third quartile (q_3) and maximum values of: (a) estimation errors as obtained for each of the tested methods for mean step length estimates; (b) absolute estimation errors as obtained for each of the tested methods for mean step length estimates. Errors larger than $q_1 = 1.5(q_3 + q_1)$ or smaller than $q_1 = 1.5(q_3 - q_1)$ are considered outliers and represented with stars. Methods with their four walks are listed in the x-axis (Z-method: red box; S-method: white box; G-method: grey box).

6.5 Discussion

This Chapter presents a modified step length estimation model based on the pendulum-like swing leg. In the following, basic characteristics of the estimated COM trajectory and its underlying relationship will be discussed. The validity of this mathematical relationship will be evaluated as well.

Biomechanical COM analysis can be expressed and measured in many ways. At present, this study's measured COM values may differ to some extent from those reported in literature. Several factors contribute to these deviations, such as the types of movement (overground vs. treadmill), estimation methods, and walking conditions prescribed, not to mention the sex, and age of participants. The purpose of this study, however, was not to examine such differences, but to more accurately examine the COM trajectory in dependency of walking speed and cadence.

This data complements and refines the behaviour of the estimated COM trajectory in gait. Under freely-selected gait (i.e. speed and cadence), a number of studies characterized the relationship between VT displacements and walking speed as linear (Miff, Gard et al. 2000; Orendurff, Segal et al. 2004), which is only dependent on the step length (Zijlstra and Hof 1997; Miff, Gard et al. 2000). This study demonstrates that under controlled walking conditions (i.e. fixed speed and step frequency), this relationship becomes exponential, where VT displacements primarily depend on step length at speeds below $1.2ms^{-1}$ and on both step length and frequency at higher speeds. The effect of speed and cadence on VT and medio-lateral COM displacement has already been reported elsewhere (Staszkiewicz, Ruchlewicz et al. 2010), where VT COM excursions decrease in dependency of both under controlled conditions. Examining this effect of COM displacements in the AP direction demonstrates that AP excursions increase linearly with speed (r=.71, p<.0001) and depend on both step length and step frequency at all speeds (from 0.7 to $1.6ms^{-1}$). Furthermore, we postulated that AP displacements may correspond to the pelvic contribution to step length. In accordance with Liang et al., our results not only show that AP excursions increase with bigger steps and faster speeds (Liang, Wu et al. 2014). The results provide evidence that, estimations of step length should consider both VT and AP displacement of the trunk.

The results of the overground walking experiment provided evidence that our proposed model estimates mean step length as good if not better than other models in use. The model proved to be highly reliable across test sessions and demonstrated good-to-excellent levels of agreement against reference data. Although good-to-excellent levels of agreement were obtained for both Z- and G-method, both permit a small systematic bias with significant heteroscedastic error. Estimation errors above 5cm were mainly found in subjects making smaller steps, suggesting that walking speed might be the limiting factor. Although we did not test these models under such stringent conditions, absolute estimations errors were, interestingly, not associated with walking speed (Z-method: r=.01, p=.98; G-method: r=.13, p=.49) but strongly related with the subject's leg-to-foot ratio (curvilinear regression: Z-method: r=75, p<.001; G-method: r=.51, p=.004). Current IP models rest on the magnitude of the VT COM displacement, which depend on the pendulum's angular excursion.

Consequently, a shorter pendulum would require a larger angular excursion for the same displacement. By adding a foot-ankle complex, in similar fashion to that of a foot-rocker, would prolong the COM trajectory in forward direction. If a person has relatively big feet in relation to its legs, than that person would still be able to make equal steps to someone with longer legs, but relatively smaller feet. In retrospect, this might be one reason why current IP models in use suffer from such singularities. The addition of AP displacements, however, demonstrates promising results under self-selected walking speeds during straight-line walking. In its current form, the proposed method accurately estimates mean step length without the need for any correction factor. When examining the potential to calculate individual step-to-step based estimates, all models, including the newly proposed model, significantly underestimates step length with errors up to ~14cm. Monitoring step-to-step variability by an IMU on the lower trunk, for that matter, becomes unfeasible (i.e. insufficient sensitivity). The main factors behind such errors are: 1) AP trunk excursions are limited to displacements in the transverse plane, and 2) rotational motion (i.e. transverse and axial rotation) has a contaminating effect on the accelerometer output. Improvements to the proposed method can, therefore, be sought in applying a tilt correction procedure to compensate for such body orientations.

6.6 Conclusion

This study presents a modified step length algorithm that is highly reliable and has good-to-excellent agreement to reference mean step length data for preferred, straight-line walking in healthy adults. Unlike other models, this IP model does not require a correction factor. Future work will look at the performance of this model under various walking conditions and in pathological gait.

Chapter 7

A Smart Device Inertial-sensing Method for Gait Analysis[15]

7.1 Summary of Contents

This chapter both proposes a method reliant on an iPod's inertial sensors to measure lower trunk vertical displacements in the global frame as well as assesses its validity and reliability against that of a 3D motion capture system and conventional IMU for averaged and individual step data. This method utilizes a Kalman filter and a quaternion rotation matrix approach to transform translatory accelerations from the object in the global frame. The results demonstrate that the proposed mathematical transformation of acceleration data achieves reliable COM measurements in the global *Z*-axis during a 10m walk test, thus offering a solution for clinical and non-clinical gait analysis outside the constraints of laboratory settings.

7.2 Introduction

For years, gait analyses have been confined to clinical settings and conventional lab-based equipment (Horvath, Tihanyi et al. 2001; Sutherland 2002). Although the brunt of current evidence suggests that clinical gait analysis noticeably enhances the diagnostic and treatment process, whether it equally impacts patient outcomes and social well-being remains equivocal (Wren, Gorton et al. 2011) (as discussed in Chapter Four). More specifically, it is cumbersome in that its data acquisition procedures are often time-consuming, its lab equipment is costly and requires trained personnel (Henriksen, Lund et al. 2004), and it cannot consistently account for a subject's daily functioning (Kiani, Snijders et al. 1997; Baker 2006).

Wearable motion-sensing systems emerge as a preferable research option in many cases, as they are portable, more affordable than their laboratory counterparts, widespread, and relatively easy to operate (Steins, Dawes et al. 2014). Contemporary gait analysis studies, in fact, draw upon wearable system applications founded on inertial measurement units (IMUs), because they can assess gait patterns and mobility levels with a reliability that cannot be gleaned solely through accelerometers (Giansanti, Macellari et al. 2003; Kavanagh and Menz 2008).

[15] In slightly adapted form, this chapter originally appeared in the Journal of Biomechanics. See D.Steins, H. Dawes, J. Collett, and P. Esser, "A Smart Device Inertial-sensing Method for Gait Analysis," J. Biomechanics 2014 Nov 28;47(15):3780-5

Advances in wearable systems render smart devices, such as the iPod Touch, available for remote computing purposes. Already containing an IMU attuned to the device's orientation, such smart technology possesses the potential to measure those physical parameters (e.g. linear acceleration, angular velocity) necessary for non-clinical measurements. Until now, studies have exclusively examined a smart device's tri-axial accelerometer's capacity (Lemoyne, Mastroianni et al. 2010; LeMoyne, Mastroianni et al. 2011) and feasibility (Chan, Huiru et al. 2011; Nishiguchi, Yamada et al. 2012; Yang, Zheng et al. 2012) for gait analysis, indoor localization (Rui, Bannoura et al. 2013), and evaluation of motion data quality (Nymoen, Voldsund et al. 2012). A smart device's inertial sensing capabilities, however, have not been explored, despite their potential to track gait characteristics with the reliability and accuracy defining the gold standard 3D motion capture system (Wong, Wong et al. 2007) or conventional inertial sensor (Esser, Dawes et al. 2009).

Addressing such critical gaps, this study aims to: 1) propose a method relying on a smart device's inertial sensors that reliably measures the body's COM trajectories in the global frame, and 2) assess this method's validity against that of a 3D motion capture system and conventional IMU for averaged and individual step data.

7.3 Materials and Methods

Overground walking was studied in ten subjects: age 25.6 ± 3.5years, height 1.73 ± 0.17m, and mass 73.0 ± 17.1kg. Linear accelerations of the lower trunk were measured by two inertial measurement units: one Xsens 6-DOF inertial sensor (MTx, Xsens Technologies, Netherlands) with a measurement range of ±2*g*, and one inertial sensor-embedded smart device (iPod Touch 4th generation, iOS operating system version 6.0.1, Apple, UK) with a measurement range of ±2*g* and 16 bit data output. Like the iPhone 4 and 5, the iPod Touch contains an LIS331DLH tri-axial accelerometer and L3G4200D tri-axial gyroscope manufactured by STMicroelectronics. The Xsens inertial sensor was attached to the iPod with double-sided adhesive tape and secured on the dorsal side of the subject's lower trunk at the level of the third lumbar vertebrae, a positioning considered reliable for gait analysis (Henriksen, Lund et al. 2004) because closely reflecting actual COM accelerations during walking (Moe-Nilssen 1998). Global axes were defined as thus: positive *Z* values, upward acceleration. Note: to be uniform with the literature on the signal description, the acceleration signal was inverted.

A retro-reflective marker was additionally positioned over the middle of the Xsens sensor to measure trunk displacement with an optical motion capture system (Oqus 300, Qualisys, Sweden). A total of six cameras were employed to obtain a high resolution of the calibrated volume. Xsens and Qualisys data were both measured at 100Hz, whereas the iPod was consistently sampled at around 100Hz (±2Hz).

7.3.1 Test Procedure

All subjects were instructed to walk a 10m distance over a straight walkway arranged in a gait laboratory. The distance was accurately determined by a digital distance measuring

wheel. Start and finish lines were clearly demarcated. The intra-rater reliability of the iPod Touch was measured within four walks of the subject's self-selected walking speed (SSWS), ensuring that all factors, such as the attachment of devices, were kept constant. All subjects were familiarized with the testing procedure prior to testing.

A smart application developed by Wildknowledge (UK)[16], which incorporates the Kalman filter and quaternion rotation matrix, provided an easily accessible tool for COM measurements. All functionalities were directly available using the user interface, as illustrated in Figure 7.1. The smart application instructed subjects with five built-in voice commands throughout the walk, 1) stand still, 2) start walking, 3) stop walking, 4) stand still, and 5) measurement complete.

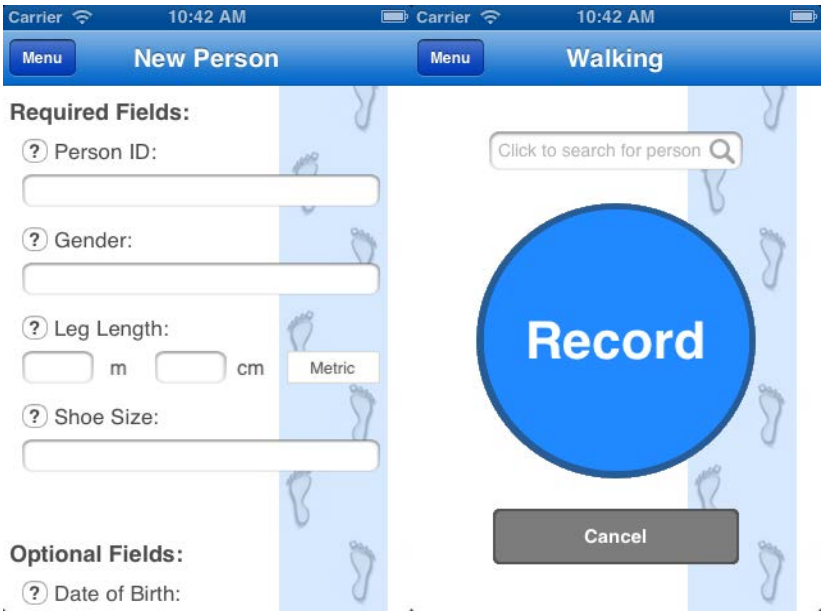

Figure 7.1 User interface of the iPod's smart application.

7.3.2 Signal Generation, Transfer, and Storage Procedure

After each walking trial, the data is send over to a server for offline analysis. On this server owned and hosted by Wildknowledge, the data is subjected to an initial post-processing step to obtain an estimate of the device's orientation for each sample, see Figure 7.2. This step is fully automatized and involved to use of an extended Kalman filter—designed by Dr. Ian Sheret (explained in the next section). An integrated quaternion-rotation matrix approach provided transposed vertical acceleration about the origin using an estimate of the true attitude quaternion. Combined with a data filtering approach prior to each numerical integration step (as described in section Chapter Three), acceleration, velocity, and

[16] Wildknowledge is a spin-out company from Oxford Brookes University that specializes in use of mobile devices to record data in the field. In this project they were entrusted with the the front –and back-end development of the smart application.

displacement data was obtained. The back-end programming langue used to run this code is done on Python. The back-end coding remains, however, a black box to the author.

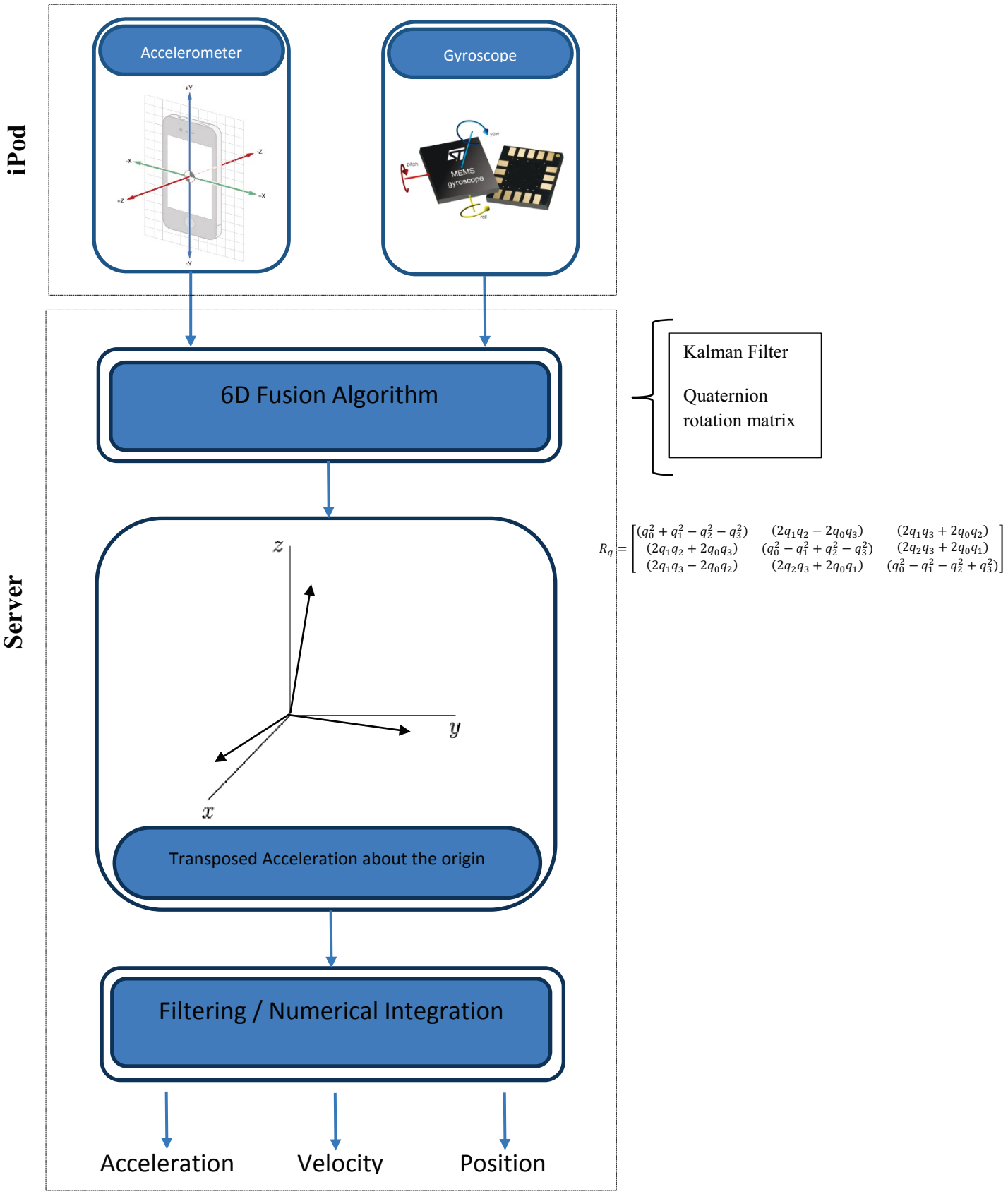

Figure 7.2 Data flow chart

7.3.3 Data Processing

DC-coupled accelerometers generally measure some degree of the gravitational acceleration, depending on the degree of deviation from the global horizontal. This misalignment contaminates true linear acceleration data (Kavanagh and Menz 2008) and was therefore preemptively corrected.

In order to align acceleration measurements with the global frame, an accurate estimate of IMU orientation was required. For the iPod, this orientation was estimated using an extended Kalman filter, which recruited the observed acceleration and angular rate to estimate the device orientation for each sample. The filter design uses an indirect filter with attitude parameterized using quaternion algebra (Trawny and Roumeliotis 2005). The state vector is

$$\mathbf{x}(t) = \begin{bmatrix} \bar{q}(t) \\ \mathbf{b}_a(t) \\ \mathbf{b}_\omega(t) \\ \mathbf{v}(t) \\ \mathbf{r}(t) \\ \mathbf{r}_f(t) \end{bmatrix} \tag{7.1}$$

where $\bar{q}(t)$ is the attitude quaternion (consistent with the definition in [16]), b_a is the accelerometer bias, b_ω is the gyro bias, $v(t)$ is the velocity, $r(t)$ is the position, and $r_f(t)$ is the estimate at time t of the final position (used to support bounded position constraints described below). The Kalman filter does not track the state directly, but rather the difference between the true state and the estimated state. The attitude error is parameterized as an error quaternion:

$$\overset{L}{G}\bar{q} = \overset{L}{\hat{G}}\hat{\bar{q}} \otimes \overset{\hat{G}}{G}\delta\bar{q} \tag{7.2}$$

where $\overset{L}{G}\bar{q}$ is the true attitude quaternion (L and G indicating the local and global coordinate frames), $\overset{L}{\hat{G}}\hat{\bar{q}}$ is the estimated attitude quaternion, $\overset{\hat{G}}{G}\delta\bar{q}$ is the error quaternion, and $\otimes$ indicates quaternion multiplication. Note this definition of the error quaternion is different from that used in [16], but has the advantage of simplifying the calculation of discrete-time update equations. The error quaternion is generally very small, and hence a small angle approximation can be used:

$$\delta\bar{q} \approx \begin{bmatrix} \frac{1}{2}\delta\theta \\ 1 \end{bmatrix} \tag{7.3}$$

Errors on the rest of the error states are simply the difference between the true and estimated states, e.g.

$$\Delta \mathbf{b}_a = \mathbf{b} - \hat{\mathbf{b}}_a \tag{7.4}$$

The full error state used by the Kalman filter is then

$$\tilde{\mathbf{x}} = \begin{bmatrix} \delta\boldsymbol{\theta} \\ \Delta \mathbf{b}_a \\ \Delta \mathbf{b}_\omega \\ \Delta \mathbf{v} \\ \Delta \mathbf{r} \\ \Delta \mathbf{r}_f \end{bmatrix} \tag{7.5}$$

During processing, the direct state, error state, and covariance are propagated forward in time using the observed local frame angular rates and specific accelerations measured by gyros and accelerometers. The direct state is propagated using the Runge-Kutta algorithm. The error state and covariance are propagated using the discrete time version of the state transition matrix. At the end of each integration step, the estimated error state is fed back into the direct state, and the direct state quaternion is normalized.

Bounded position constraints are provided to the Kalman filter at the start and end of each dataset, allowing an accurate estimate of attitude to be obtained throughout. In the initial period, the bounded position constraint is supplied by providing a pseudo-measurement $\mathrm{r} = 0$, with a small uncertainty to account for sensor movement of the sensor. In the final period, the pseudo-measurement is of $\mathrm{r} - \mathrm{r_f} = 0$ again with a small uncertainty. To improve the accuracy of the final estimate, the data is analyzed in both forward and reverse directions, and the two estimates are optimally combined based on their covariance matrices. The final result is an accurate estimate of the orientation of the device as a function of time.

Analysis of the iPod data necessitated careful treatment of sample frequencies and times because, unlike the MTx inertial sensor, samples from the gyro and accelerometer were not intrinsically synchronized and recorded at exactly 100Hz, see Figure 7.3 and 7.4. An initial processing step was therefore required to resample the gyro and accelerometer data onto a common time grid, using the accurate timestamps provided.

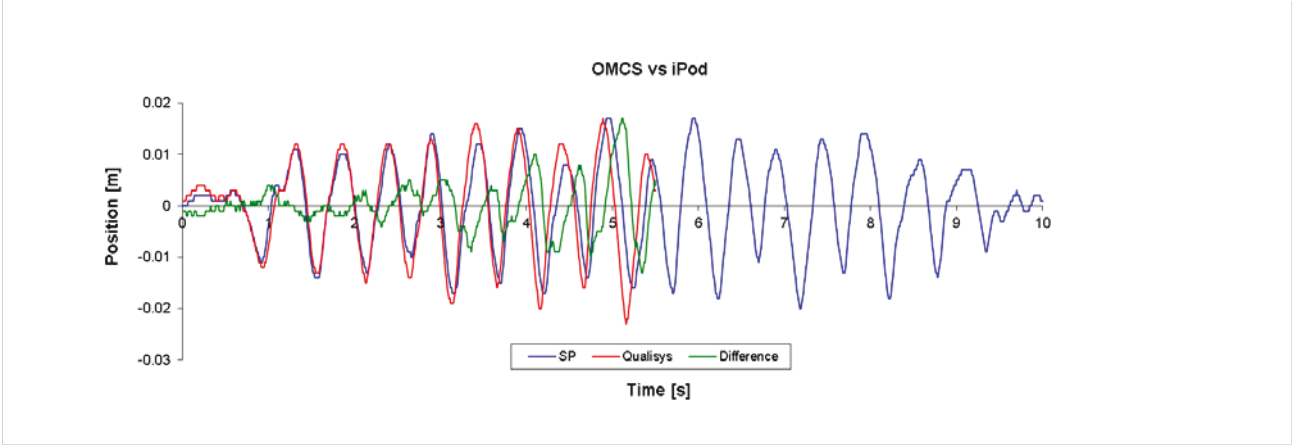

Figure 7.3 The original iPod's acceleration output integrated to relative position and compared to the OMCS. Time delay and amplitude errors increase with time.

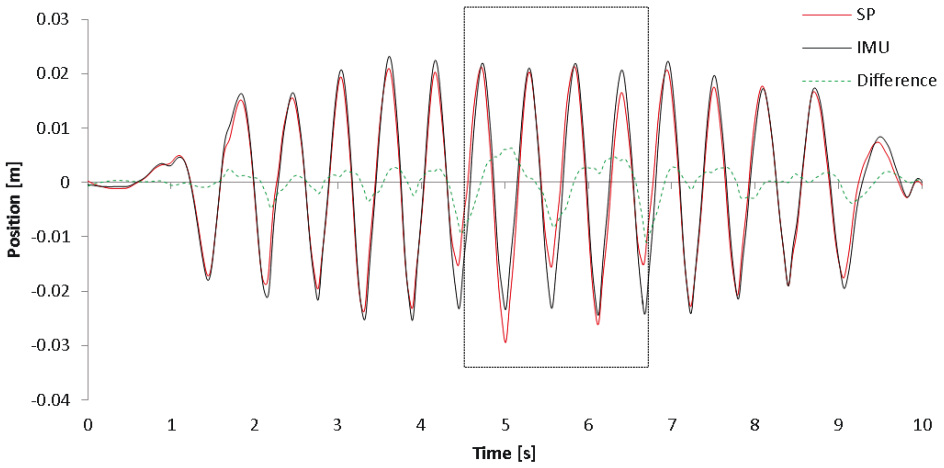

Figure 7.4. The initial results using the above described inertial-sensing method. Amplitude errors clearly arise during the mid-section of the walking test, due to gyro sample droppings. Consequently, gaps were filled with a linear interpolation.

Both the iPod and MTx acceleration data were transposed using the following quaternion-based matrix multiplication approach

$$R_q = \begin{bmatrix} 1-2(q_2^2+q_3^2) & 2(q_1q_2-q_0q_3) & 2(q_1q_3+q_0q_2) \\ 2(q_1q_2+q_0q_3) & 1-2(q_1^2+q_3^2) & 2(q_2q_3-q_0q_1) \\ 2(q_1q_3-q_0q_2) & 2(q_2q_3+q_0q_1) & 1-2(q_1^2+q_2^2) \end{bmatrix}$$

A second order IIR filter, supplied with forward and backward Butterworth coefficients (cut-off frequency, 0.5-25Hz), was applied to reduce drift and integration error. Amplitude changes in vertical displacement (m) were doubly integrated according to the Simpson rule. Typical vertical COM trajectories formed by corrected acceleration signals are illustrated in Figure 7.5.

7.3.4 Statistical Analysis

The Shapiro-Wilk test was used to check data normality (Razali, Wah et al. 2011). Bland-Altman plots were generated to examine agreement, heteroscedasticity, and systematic error between systems (Atkinson and Nevill 1998; Bland and Altman 1999). Any systematic error detected between systems was tested by one-way analysis of variance (ANOVA) between-subjects design.

Inter-rater reliability was analyzed through intraclass correlation coefficients (ICCs) of the type 3,1 (two-way mixed), expressed with associated 95% confidence intervals (CI) and interpreted as >0.75 excellent, 0.40-0.75 fair-to-good, and <0.40 poor in reliability (Shrout and Fleiss 1979). Absolute reliability was formulated as a standard error of measurement (SEM) (Weir 2005). Precision levels were evaluated through Bland and Altman's 95% limits of agreement (Bland and Altman 1999). All statistics were performed using SPSS version 21 with statistical significance being set at $p<.05$.

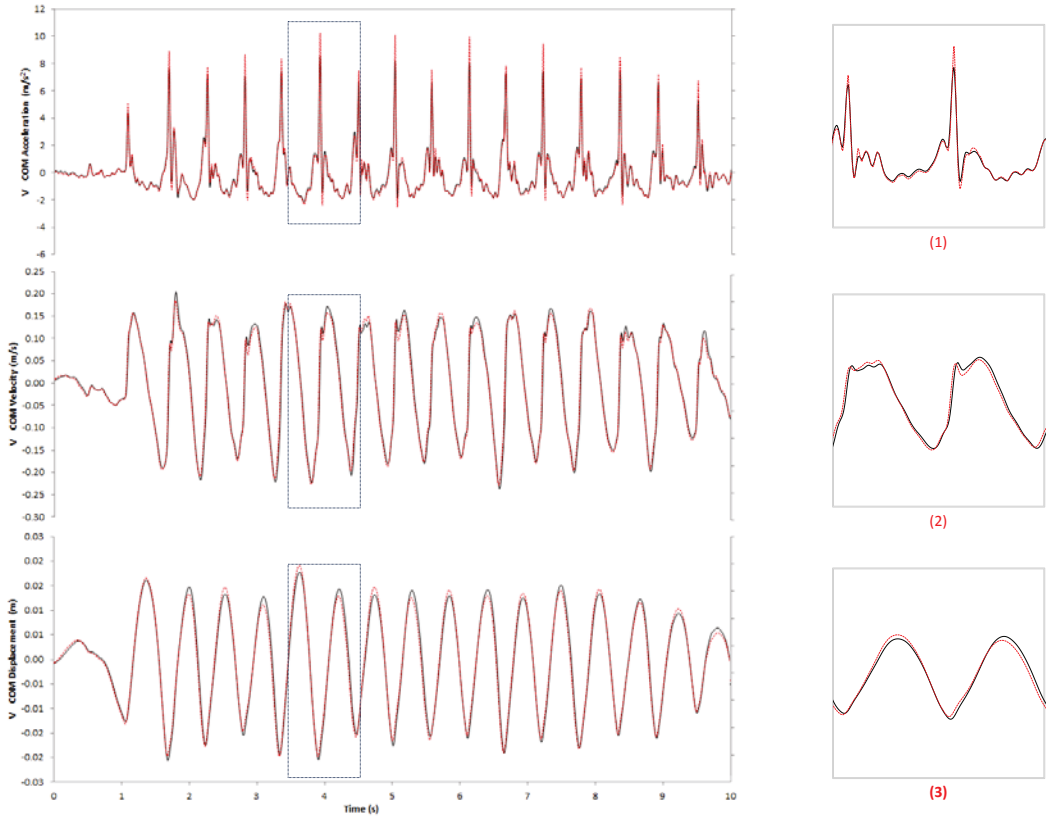

Figure 2 A standard COM plot of the vertical acceleration, velocity, and displacement pattern during a 10m walking trial. The gait pattern slightly changes when transposed from the object onto the global frame; black line represents the object frame. The red dotted line denotes the transposed data.

7.4 Results

All data were normally distributed. Measures of absolute and relative reliability on each parameter are reported in Table 7.1; the table also illustrates the Pearson *r* to discern whether error size correlates with individual mean values. Individual and averaged step data on peak-to-trough differences in position and acceleration were evaluated between systems and illustrated in Figure 7.7 by Bland-Altman plots. The signal error between the iPod and Xsens sensor compiled over a 10m walk is plotted in Figure 7.6.

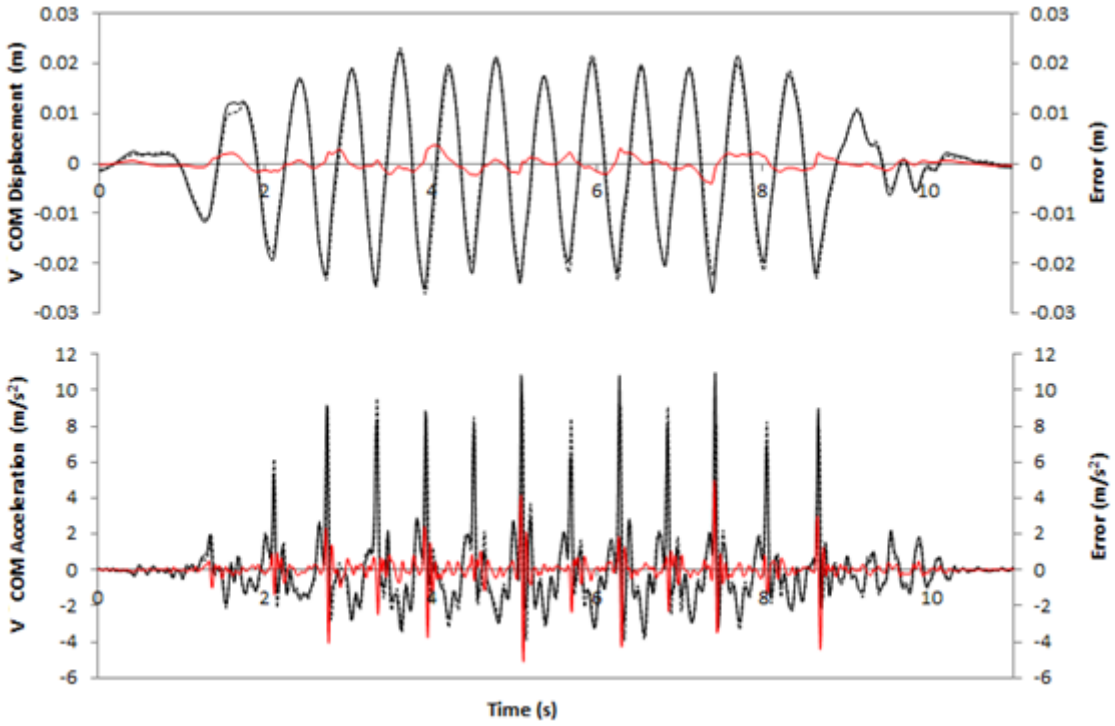

Figure 7.6 Randomly chosen vertical COM acceleration and displacement trajectory. The black dotted line represents the iPod Touch. The solid black line represents indicates the Xsens inertial sensor. The red line signifies the overall error calculated as the difference between the Xsens and iPod at t_n.

A one-way ANOVA demonstrated no significant differences between systems in position for averaged step data (n=120, F[2,117]=1.231, *p*=.296), whereas a one-way ANOVA on individual step data indicated a significant difference between the relative vertical COM displacement of the iPod and the 3D motion capture system (n=894, F[2,891] = 5.523, *p*=.004). A Bonferroni post-hoc test (*p*<.05) revealed that the iPod measures significantly lower displacement values than its gold standard counterpart does (*p*=.003). Conversely, no significant difference was discovered between the iPod and Xsens (*p*=.215). In both cases, the iPod underestimated vertical COM displacements as a result of a systematic error (M= -.0022m, CI= -.0038 to -.0006m). An additional one-way ANOVA on acceleration data exhibited no significant difference between systems on averaged and individual step data (*p*≥.05).

ICCs were generally high for both individual and averaged step data in position, especially

for peak and amplitude values ranging from .80 to .96 (see Table 7.1). As for acceleration, the iPod achieved fair-to-excellent levels of reliability (ICCs ranging from .54 to .95). SEMs were calculated to distinguish low reliability coefficients secured through small within-group variability. SEMs for both individual and averaged step data in position and acceleration showed high measurement precision. In position, measurement errors up to 0.003m were ascertained, while for acceleration, up to 1.69ms^{-2}.

Bland-Altman plots on averaged and individual step data demonstrated moderate levels of agreement for position data, displaying no heteroscedasticity. The 95% limits of agreement on averaged step data (0.0072m [18.5%], -0.0026m [6.7%]) contained 38 out of 40 difference scores, whereas limits on individual step data were somewhat higher (0.0118m [30.3%], -0.0075m [-19.2%]), covering 878 out of 894 difference scores. For both averaged and individual step data, a systematic error was found (0.0012-0.0022m) (see Figure 7.7).

Bland-Altman plots for acceleration data were, conversely, poor and displayed heteroscedasticity (r=.46, p<.01). The iPod's mean difference was 0.565ms^{-2}, with 95% limits of agreement on averaged step data (2.63ms^{-2} [24.5%], -1.46ms^{-2} [13.6%]) containing 38 out of 40 difference scores. On individual step-to-step data, the limits were slightly higher (3.84ms^{-2} [37.8%], -2.71ms^{-2} [25.3%]), enclosing 878 out of 894 difference scores.

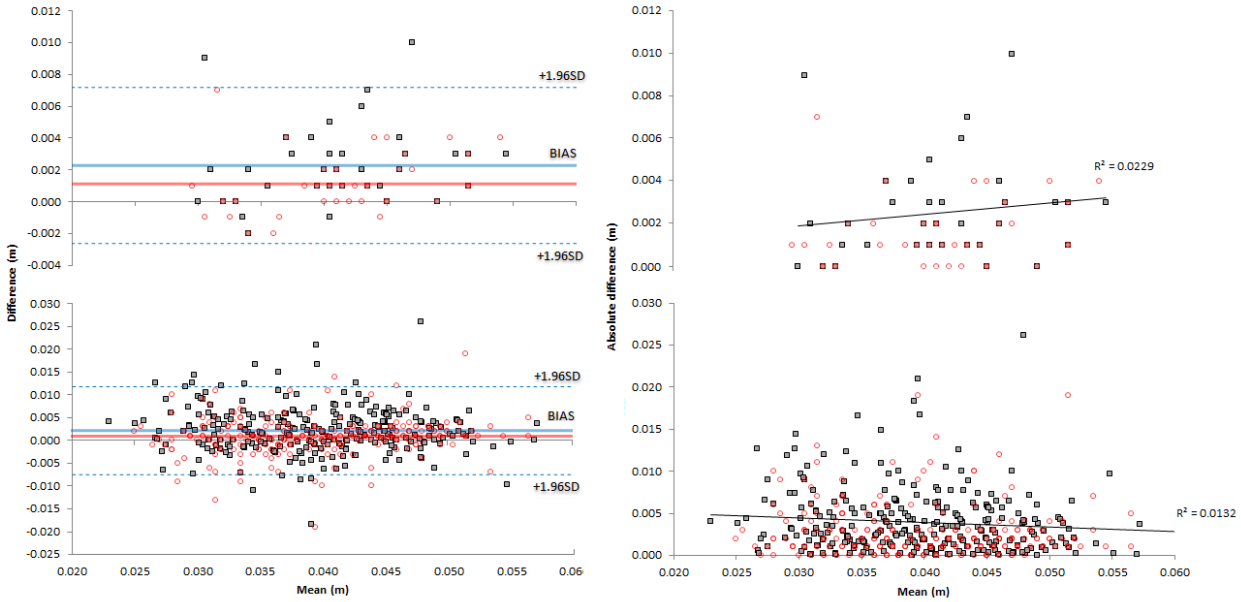

A

Position

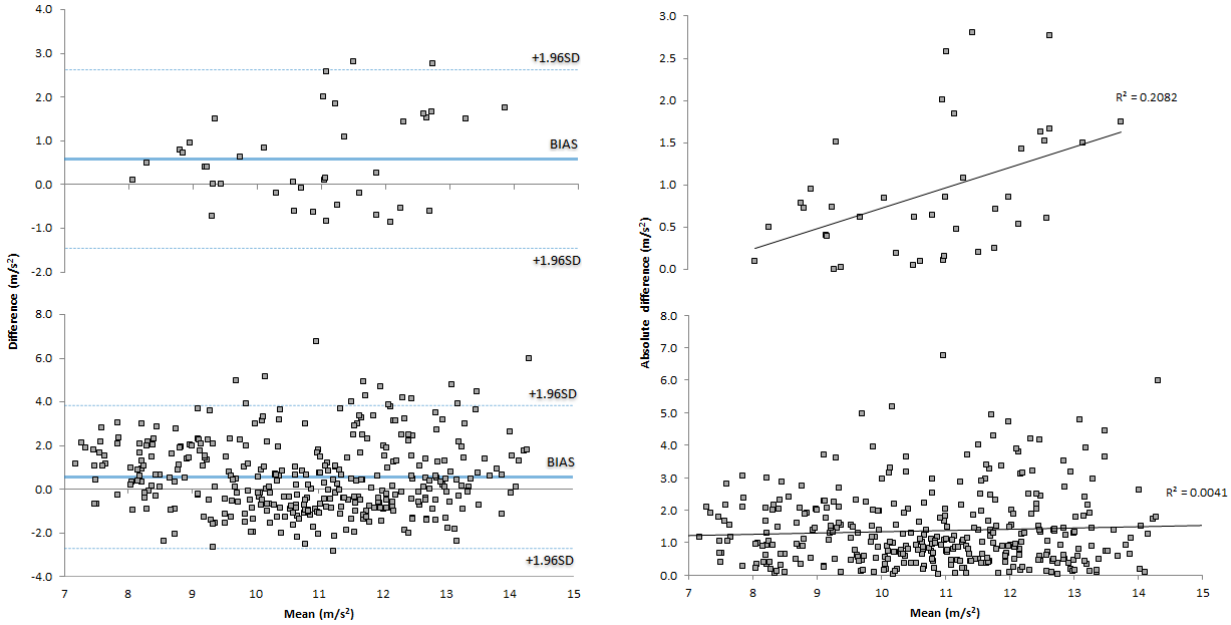

B

Acceleration

Figure 7.7 Bland-Altman plots of individual and averaged step data at preferred walking speeds. In the upper graph (A), iPod (black dots) and Xsens (red dots) agreement is compared to the optical motion capture system. In the lower graph (B) iPod acceleration is compared to that of the Xsens. The solid blue line represents systematic error, while dashed lines indicate 95% limits of agreement. On averaged step data, the iPod displayed heteroscedasticity (r=.46, p<.01).

Table 7.1 Measures of absolute and relative reliability

	Parameter	iPod (Mean ± S.D.)	Xsens (Mean ± S.D.)	OMCS (Mean ± S.D.)	Averaged across each walking trial ICC (3,1)				Individual footsteps ICC(3,1)			
					iPod vs. Xsens *r*[Lb-Ub]	iPod vs. OMCS *r*[Lb-Ub]	SEM	Pearson *r*	iPod vs. Xsens *r*[Lb-Ub]	iPod vs. OMCS *r*[Lb-Ub]	SEM	Pearson *r*
Peak	Position (m)	0.019 (0.004)	0.019 (0.004)	0.020 (0.004)	.959[.866-.983]	.910[.447-.971]	0.001/0.001	.23	.880[.847-.906]	.859[.773-.906]	0.001/ 0.002	.06
	Acceleration (ms^{-2})	7.63 (1.69)	7.79 (1.90)		.781[.624-.878]		1.12	.53**	.540[.471-.603]		1.44	.17**
Trough	Position (m)	-0.020 (0.006)	-0.021 (0.004)	-0.021 (0.005)	.910[.700-.964]	.187[-.136-.471]	0.002/0.003	.72**	.707[.641-.762]	.570[.474-.651]	0.002/ 0.004	.15**
	Acceleration (ms^{-2})	-3.11 (0.84)	-3.02 (0.78)		.950[.891-.976]		0.48	-.06	.756[.711-.795]		0.63	-.14**
Amplitude	Position (m)	0.039 (0.008)	0.040 (0.007)	0.041 (0.008)	.952[.831-.981]	.878[.475-.956]	0.001/0.002	.21	.863[.818-.896]	.797[.687-.862]	0.003/ 0.003	.05
	Acceleration (ms^{-2})	10.73 (2.02)	10.81 (2.14)		.808[.667-.894]		1.18	.46**	.599[.536-.656]		1.69	.03

OMCS: Optical Motion Camera System; SD: standard deviation; ICC: intra-class correlation coefficient; Lb-Ub: lower and upper 95% confidence interval for ICC (3,1);

SEM: standard error of the measurement (iPod - Xsens/ iPod – OMCS).

*. Significant at the .01 level (2-tailed)

7.5 Discussion

Optical motion capture systems are widely agreed to be the gold standard for gait analysis. Such systems, though, are strictly constrained to laboratory settings. An inexpensive portable monitor, epitomized by the iPod Touch, can overcome this limitation to assess gait at remote sites, summoning new research possibilities for physical activity monitoring. More specifically, remote monitoring allows research teams to better understand the impact of clinical interventions on patient mobility, independence, and quality of life.

Unlike previous studies (Nishiguchi, Yamada et al. 2012; Yang, Zheng et al. 2012) that only examine the measuring potential of a smart device's tri-axial accelerometer, this study develops and compares a new inertial-sensing method based on the iPod Touch against the gold standard in terms of position (Qualisys) and acceleration (Xsens). To the authors' knowledge, this method is the first to explore the accuracy of a smart device's inertial-sensing capabilities for obtaining COM displacement data during walking.

Results indicate that the proposed mathematical transformation of acceleration data via an extended Kalman filter applied in conjunction with a quaternion rotation matrix achieves reliable COM measurements in the global *Z*-axis during a 10m walk test. The levels of agreement, however, were only moderate (errors rising to 25% of the measurement range), with a small systematic error of 2.2mm and a typical error of ≤3mm.

Measurement errors can potentially be attributed to the Kalman filter's inaccuracy and the sensor administration process. For each walking trial, sensors were placed on top of one another, subjecting the top sensor to a greater force of linear acceleration at the time of foot contact. A Pearson *r* correlation confirmed that step length harbors a negative relationship with the magnitude of the linear acceleration (r=.46, p<.05).

To optimize this smart device method, the orientation estimates posited by the Kalman filter should be further examined through a segmental analysis technique as opposed to a single marker method. In addition, sensor estimates should be separately reexamined. Although of course, this has not been verified, the smart device method in its present state should be capable of deriving accurate temporal gait components (cadence, step time, walking speed, etc.), as they remain unaffected by amplitude change errors. The specific smart device application used in this study, moreover, can perform a single gait test—including the setup, measurement, and analysis phase—in just 5-10 minutes (depending on the user's experience), achieving measurement levels similar to those gathered by a conventional inertial sensor.

Chapter 8

Conclusion

8.1 Summary

The general conclusions that can be derived from this body of work are discussed in this Chapter. The feasibility of using an iPod Touch as a tool for gait assessments in clinical and non-clinical environments are described followed by the improvements to identify and estimate spatiotemporal gait features are discussed as a novel means to derive more clinically relevant outcomes measures.

8.2 Utilizing a Smart Device as a Novel Ambulatory Monitoring System

MEMS technology has revolutionized many aspects of telerehabilitation by taking healthcare access beyond the walls of traditional clinical facilities. Being able to monitor movement accurately and sensitively at home and other unsupervised environments through the commercial development of wearable and ambient “smart health devices"—in this case, the iPod Touch—may allow researchers to, as emphasized throughout this work, gather additional data with which to evaluate treatment outcomes for subjects with neurological or musculoskeletal conditions.

On top of their internet-based communicative properties, iPods do not have an upper limit on their quality of service and can thereby allow the telecare industry to address mobility, usability, interoperability, intelligence, and adaptability in a systematic, cost-effective way. They epitomize a type of patient-oriented technology that enables individuals to gain a more active managerial role in their own healthcare. The use of smart health devices (in conjunction with wearables) to help individuals to initiate and sustain a healthy life style is not new. In the fitness domain, these devices, known as fitness trackers, are commonly used to track your sleep, blood pressure, heartrate, and physical activity and. In the past, Nike was one of the first to introduce such system, called the Nike+ system, a foot pod wirelessly connected to an iPod that let the runner monitor the duration and distance of a workout. For that matter, the arrival of smart health devices offer the possibility to obtain data over long time periods, taken under real-life circumstances.

To test the iPod’s feasibility to function as a potential ambulatory monitoring system for quick gait assessments, this thesis developed and assessed the accuracy of an integrated inertial-sensing method on the lower back during short distance walks in healthy participants. A quaternion-based fusion of accelerometer and gyroscope data, reliant on a Kalman filter, was used to derive COM (i.e. lower trunk) accelerations in the local origin about the *Z*-axis. Thereon, post-processing of data was found to be necessary for coping with the noisy nature of inertial sensors in the iPod, as shown in Chapter Three. After gravity subtraction, a 2nd

order Butterworth band-pass filter with cut-off frequencies from 0.5 to 25Hz was found to be effective for removing drift and noise problems before each integration step. The process described above provided a possible means to determine 'true' vertical acceleration, velocity, and relative displacement of the COM during walking.

The main reason to *why* this work only focused on deriving accurate displacement in the vertical plane, stems from Dr. Patrick Esser's thesis who used a specific quaternion rotation matrix approach for the sole purpose of obtaining more accurate linear displacements in the vertical plane—as it drives several gait models, including the original step length model by Zijlstra & Hof (Zijlstra and Hof 1997). This approach is firmly embedded within Oxford Brookes' "*DataGait"*, which a customized gait analyzing program written in LabView and currently in-use for many gait-related research within the Movement Science Group. Needless to say, this thesis demonstrates that the extraction of possibly more accurate spatiotemporal gait features are not necessarily bound by this particular method. Nonetheless, this thesis demonstrates that the sensors of a simple iPod Touch can be used to estimate vertical displacement of the projected COM with millimeter accuracy over short-time periods (Steins, Sheret et al. 2014). Consequently, this supports the feasibility of using such device as a potential ambulatory monitoring system in the near future.

The author is aware that there is still a long way to go before decision makers can rely on telecare services to produce valid and reliable cost-effective data. The work presented before you has shown that an iPod Touch can potentially be used as valid, cost-effective, user-friendly ambulatory monitoring system for gait assessments in clinical and non-clinical settings. A proof of concept, however, is still required.

8.3 Spatiotemporal Gait Feature Extraction

The analysis of human gait is an extensive area of study involving a wide range of parameters. Kinematic and kinetic measures of the body and limbs during gait are thought of as the gold standard for any comprehensive assessment, but measuring these types of parameters can be expensive and time-consuming. On the other hand, examining time-distance variables (i.e. spatiotemporal parameters) by a single inertial measurement unit attached to the lower trunk can be a much easier way to obtain essential information regarding a subject's gait, as discussed in Chapter Five.

This reference point offers the opportunity to assess of stride-to-stride fluctuations, which have been linked to disease severity, risk of falling, and freezing of gait (Hausdorff 2005). Variability of gait has been examined with many different spatiotemporal parameters. Researchers have used everything from single and double-support time to step width and step length (Callisaya, Blizzard et al. 2010; Moe-Nilssen, Aaslund et al. 2010), but perhaps the single most important parameter when it comes to gait variability is stride time. Not only does stride time encompass all phases and events occurring in a single gait cycle, but it is a relatively simple parameter to measure. Even more importantly, this temporal measure is regarded as an overall rhythmic output of the gait system (Beauchet, Herrmann et al. 2008) and its variability may hold the key to better understanding the control of human gait

(Guimaraes and Isaacs 1980; Gabell and Nayak 1984). Both cases rely on the detection of accurate spatiotemporal parameters.

While average spatiotemporal parameters are relatively well understood and commonly used in gait analysis, the individual stride-to-stride fluctuations that occur can provide more info. The alternative methods featured in Chapter Five and Six offer new prospects for clinical and non-clinical gait analysis. Combining both methods into a comprehensive algorithm can lead to an ambulatory activity monitor able to track a subject's rehabilitation progress by evaluating the quality of his or her gait. The feasibility of these methods still requires more rigorous research. For future research, the most urgent questions revolve around the attainment of accurate spatiotemporal parameters for healthy subjects as well as those possessing gait disabilities. Thus far, only healthy subjects participated in this study, covering a predefined distance in a laboratory setting. The issue remains whether similar results can be obtained under real-life circumstances.

8.4 Limitations of the Proposed Studies

First of all, it is important to underline that all of our findings are from our lab-based experiments. This is partially in contrast to our initial aim of this thesis. To solve this problem, in the near future, it will be fundamental:

a) to examine the accuracy of the Kalman filter. Instead of directly exploring linear displacement about the *z*-axis by a single marker method, orientation and position data gleaned from the Kalman filter's improved estimates should be compared against a segmental analysis technique
b) to use another appropriate device (i.e. Apple and Android phones) to record gait
c) to test the performance of the modified step length algorithm under different walking conditions (speed and distance)
d) to explore the attainment of accurate spatiotemporal parameters in clinical and non-clinical environments for healthy subjects as well as those possessing gait disabilities
e) to design and implementing the actual smart application itself for clinician and patient use

In addition, improvements to spatiotemporal gait detection methods have been done in the absence of those possessing gait disabilities. Consequently, positive results gleaned from this work need to be reviewed in presence of pathological gait. Only then will these methods gain clinical relevance.

As far as the iPod's accuracy, only time-accurate results were obtained. This would allow the system to only measure temporal parameters. Measurement errors can potentially be attributed to the Kalman filter's inaccuracy and the sensor administration process. Additional improvements may also be gained by exploring the sensor's error and noise characteristics.

8.5 Final Remarks

Inertial measurement units and other MEMS sensors have become extremely popular for use in movement science. These sensors can be found in many consumer-friendly devices, such as in mobile telephones, which are readily accepted by the general community. Such devices can be used anywhere and by anyone. More importantly, they are not restricted to laboratories and as such allow the field of gait analysis to move outside the boundaries of a laboratory or clinic. This allows the assessment of gait in ways that were not previously available. These assessments, however, require proper validation to ensure the parameters of interest are evaluated properly. The results of the studies performed and reported in this thesis demonstrate that an iPod Touch can potentially be used as an ambulatory monitoring system for quick gait assessments in clinical and non-clinical settings. This, in combination with improvements made to estimate temporal and spatial measurements, may provide physicians and other researcher's alike, more conceivable information regarding a person's gait.

References

Alexander, N. B. and A. Goldberg (2005). "Gait disorders: search for multiple causes." Cleve Clin J Med **72**(7): 586, 589-590, 592-584 passim.

Allet, L., R. H. Knols, et al. (2010). "Wearable systems for monitoring mobility-related activities in chronic disease: a systematic review." Sensors **10**(10): 9026-9052.

Aminian, K., B. Najafi, et al. (2002). "Spatio-temporal parameters of gait measured by an ambulatory system using miniature gyroscopes." J Biomech **35**(5): 689-699.

Arnold, A. S., F. C. Anderson, et al. (2005). "Muscular contributions to hip and knee extension during the single limb stance phase of normal gait: a framework for investigating the causes of crouch gait." J Biomech **38**(11): 2181-2189.

Atkinson, G. and A. M. Nevill (1998). "Statistical methods for assessing measurement error (reliability) in variables relevant to sports medicine." Sports Med **26**(4): 217-238.

Auvinet, B., G. Berrut, et al. (2002). "Reference data for normal subjects obtained with an accelerometric device." Gait Posture **16**(2): 124-134.

Ayyappa, E. (1997). "Normal Human Locomotion, Part 2: Motion, Ground-Reaction Force and Muscle Activity." JPO: Journal of Prosthetics and Orthotics **9**(2): 49-57.

Baker, R. (2006). "Gait analysis methods in rehabilitation." J Neuroeng Rehabil **3**: 4.

Bao, L. and S. Intille (2004). Activity Recognition from User-Annotated Acceleration Data. Pervasive Computing. A. Ferscha and F. Mattern, Springer Berlin Heidelberg. **3001:** 1-17.

Barbeau, H. and J. Fung (2001). "The role of rehabilitation in the recovery of walking in the neurological population." Curr Opin Neurol **14**(6): 735-740.

Barth, J., J. Klucken, et al. (2011). "Biometric and mobile gait analysis for early diagnosis and therapy monitoring in Parkinson's disease." Conf Proc IEEE Eng Med Biol Soc: 868-871.

Beauchet, O., F. R. Herrmann, et al. (2008). "Concurrent validity of SMTEC footswitches system for the measurement of temporal gait parameters." Gait Posture **27**(1): 156-159.

Begg, R. and J. Kamruzzaman (2005). "A machine learning approach for automated recognition of movement patterns using basic, kinetic and kinematic gait data." Journal of Biomechanics **38**(3): 401-408.

Begg, R. K., M. Palaniswami, et al. (2005). "Support vector machines for automated gait classification." IEEE Trans Biomed Eng **52**(5): 828-838.

Benedetti, M. G., R. Piperno, et al. (1999). "Gait abnormalities in minimally impaired multiple sclerosis patients." Multiple Sclerosis **5**(5): 363-368.

Berg, K., S. Wood-Dauphinee, et al. (1995). "The Balance Scale: reliability assessment with elderly residents and patients with an acute stroke." Scandinavian journal of rehabilitation medicine **27**(1): 27-36.

Berlin, J. E., K. L. Storti, et al. (2006). "Using activity monitors to measure physical activity in free-living conditions." Physical Therapy **86**(8): 1137-1145.

Bland, J. M. and D. G. Altman (1999). "Measuring agreement in method comparison studies." Stat Methods Med Res **8**(2): 135-160.

Blumrosen, G. and A. Luttwak (2013). "Human body parts tracking and kinematic features assessment based on RSSI and inertial sensor measurements." Sensors (Basel) **13**(9): 11289-11313.

Boenig, D. D. (1977). "Evaluation of a clinical method of gait analysis." Phys Ther **57**(7): 795-798.

Bonato, P. (2003). "Wearable sensors/systems and their impact on biomedical engineering." IEEE Engineering in Medicine and Biology Magazine **22**(3): 18-20.
Bonato, P. (2005). "Advances in wearable technology and applications in physical medicine and rehabilitation." J Neuroeng Rehabil **2**(1): 2.
Boutaayamou, M., C. Schwartz, et al. (2015). "Development and validation of an accelerometer-based method for quantifying gait events." Med Eng Phys **37**(2): 226-232.
Brandes, M., W. Zijlstra, et al. (2006). "Accelerometry based assessment of gait parameters in children." Gait Posture **24**(4): 482-486.
Brennan, D. M., S. Mawson, et al. (2009). "Telerehabilitation: enabling the remote delivery of healthcare, rehabilitation, and self management." Stud Health Technol Inform **145**: 231-248.
Brooke, J. and W. H. (1973). Human movement--field of study, Henry Kimpton.
Bussmann, J. B. and H. J. Stam (1998). "Techniques for measurement and assessment of mobility in rehabilitation: a theoretical approach." Clinical Rehabilitation **12**(6): 455-464.
Callisaya, M. L., L. Blizzard, et al. (2010). "Ageing and gait variability--a population-based study of older people." Age Ageing **39**(2): 191-197.
Cancela, J., M. Pansera, et al. (2010). "A comprehensive motor symptom monitoring and management system: the bradykinesia case." Conf Proc IEEE Eng Med Biol Soc: 1008-1011.
Catani, F., M. G. Benedetti, et al. (1999). "Analysis of function after intra-articular fracture of the os calcis." Foot Ankle Int **20**(7): 417-421.
Cavagna, G. A. (1975). "Force platforms as ergometers." Journal of Applied Physiology **39**(1): 174-179.
Cavagna, G. A., N. C. Heglund, et al. (1977). "Mechanical work in terrestrial locomotion: two basic mechanisms for minimizing energy expenditure." Am J Physiol **233**(5): R243-261.
Cavagna, G. A., F. P. Saibene, et al. (1963). "External work in walking." Journal of Applied Physiology **18**: 1-9.
Cavagna, G. A., H. Thys, et al. (1976). "The sources of external work in level walking and running." J Physiol **262**(3): 639-657.
Cavagna, G. A., P. A. Willems, et al. (2000). "The role of gravity in human walking: pendular energy exchange, external work and optimal speed." The Journal of Physiology **528**(Pt 3): 657-668.
Chan, H. K. Y., Z. Huiru, et al. (2011). Feasibility study on iPhone accelerometer for gait detection. Pervasive Computing Technologies for Healthcare (PervasiveHealth), 2011 5th International Conference on**:** 184-187.
Chau, T., S. Young, et al. (2005). "Managing variability in the summary and comparison of gait data." J Neuroeng Rehabil **2**: 22-22.
Cheung, V. H., L. Gray, et al. (2011). "Review of accelerometry for determining daily activity among elderly patients." Arch Phys Med Rehabil **92**(6): 998-1014.
Chung, C. Y., M. S. Park, et al. (2010). "Kinematic aspects of trunk motion and gender effect in normal adults." Journal of NeuroEngineering and Rehabilitation **7**: 9-9.
Collen, F. M., D. T. Wade, et al. (1990). "Mobility after stroke: reliability of measures of impairment and disability." Disability & Rehabilitation **12**(1): 6-9.
Crosbie, J., R. Vachalathiti, et al. (1997). "Patterns of spinal motion during walking." Gait & Posture **5**(1): 6-12.
Cross, R. (1998). "Standing, walking, running, and jumping on a force plate." American Journal of Physics **67**(4): 304-309.

Cuesta-Vargas, A. I., A. Galán-Mercant, et al. (2010). "The use of inertial sensors system for human motion analysis." Physical Therapy Reviews **15**(6): 462-473.
Culhane, K. M., M. O'Connor, et al. (2005). "Accelerometers in rehabilitation medicine for older adults." Age Ageing **34**(6): 556-560.
de Bruin, E. D., A. Hartmann, et al. (2008). "Wearable systems for monitoring mobility-related activities in older people: a systematic review." Clinical Rehabilitation **22**(10-11): 878-895.
De Groot, M. H., S. J. Phillips, et al. (2003). "Fatigue associated with stroke and other neurologic conditions: Implications for stroke rehabilitation." Arch Phys Med Rehabil **84**(11): 1714-1720.
DeLuca, P. A., R. B. Davis, et al. (1997). "Alterations in surgical decision making in patients with cerebral palsy based on three-dimensional gait analysis." Journal of Pediatric Orthopaedics **17**(5): 608-614.
Dempster, W. T. (1955). "Space requirements of the seated operator: geometrical, kinematic, and mechanical aspects of the body, with special reference to the limbs."
Department of Health (2004). The NHS Improvement Plan - Putting People at the Heart of Public Services. D. o. Health, TSO (The Stationery Office).
Des Jarlais, D. C., C. Lyles, et al. (2004). "The Trend Statement." from http://www.cdc.gov/trendstatement/docs/TREND_Checklist.pdf.
Dobkin, B. H. and A. Dorsch (2011). "The promise of mHealth: daily activity monitoring and outcome assessments by wearable sensors." Neurorehabilitation and Neural Repair **25**(9): 788-798.
Dobkin, B. H., X. Xu, et al. (2011). "Reliability and validity of bilateral ankle accelerometer algorithms for activity recognition and walking speed after stroke." Stroke **42**(8): 2246-2250.
Domingos, P. (2012). A few useful things to know about machine learning. Communications of the ACM, Association for Computing Machinery. **55** 78-87.
Donelan, J. M., R. Kram, et al. (2002). "Mechanical work for step-to-step transitions is a major determinant of the metabolic cost of human walking." J Exp Biol **205**(Pt 23): 3717-3727.
Elble, R. J. (2005). "Gravitational artifact in accelerometric measurements of tremor." Clin Neurophysiol **116**(7): 1638-1643.
Eng, J. and D. Winter (1993). "Estimations of the horizontal displacement of the total body centre of mass: considerations during standing activities." Gait & Posture **1**(3): 141-144.
Esser, P., H. Dawes, et al. (2011). "Assessment of spatio-temporal gait parameters using inertial measurement units in neurological populations." Gait Posture **34**(4): 558-560.
Esser, P., H. Dawes, et al. (2009). "IMU: inertial sensing of vertical CoM movement." J Biomech **42**(10): 1578-1581.
Evans, A. L., G. Duncan, et al. (1991). "Recording accelerations in body movements." Med Biol Eng Comput **29**(1): 102-104.
Fish, D. J. and J.-P. Nielsen (1993). "Clinical Assessment of Human Gait." JPO: Journal of Prosthetics and Orthotics **5**(2): 39/27-36/48.
Gabell, A. and U. S. Nayak (1984). "The effect of age on variability in gait." J Gerontol **39**(6): 662-666.
Gage, J. R. (1994). "The role of gait analysis in the treatment of cerebral palsy." J Pediatr Orthop **14**(6): 701-702.
Gard, S. A. and D. S. Childress (1997). "The effect of pelvic list on the vertical displacement of the trunk during normal walking." Gait & Posture **5**(3): 233-238.

Gard, S. A. and D. S. Childress (1999). "The influence of stance-phase knee flexion on the vertical displacement of the trunk during normal walking." Arch Phys Med Rehabil **80**(1): 26-32.
Gard, S. A. and D. S. Childress (2001). "What determines the vertical displacement of the body during normal walking?" JPO: Journal of Prosthetics and Orthotics **13**(3): 64-67.
Gard, S. A., S. C. Miff, et al. (2004). "Comparison of kinematic and kinetic methods for computing the vertical motion of the body center of mass during walking." Hum Mov Sci **22**(6): 597-610.
Gebruers, N., C. Vanroy, et al. (2010). "Monitoring of physical activity after stroke: a systematic review of accelerometry-based measures." Arch Phys Med Rehabil **91**(2): 288-297.
Giampaoli, S., H. v. Oyen, et al. (2008). "Major and chronic diseases, report 2007."
Giansanti, D., V. Macellari, et al. (2008). "Telemonitoring and telerehabilitation of patients with Parkinson's disease: health technology assessment of a novel wearable step counter." Telemedicine and e-Health **14**(1): 76-83.
Giansanti, D., V. Macellari, et al. (2003). "Is it feasible to reconstruct body segment 3-D position and orientation using accelerometric data?" IEEE Trans Biomed Eng **50**(4): 476-483.
Godfrey, A., R. Conway, et al. (2008). "Direct measurement of human movement by accelerometry." Med Eng Phys **30**(10): 1364-1386.
Godfrey, A., S. Del Din, et al. (2015). "Instrumenting gait with an accelerometer: a system and algorithm examination." Med Eng Phys **37**(4): 400-407.
Goldberger, A. L., L. A. Amaral, et al. (2002). "Fractal dynamics in physiology: alterations with disease and aging." Proc Natl Acad Sci U S A **99 Suppl 1**: 2466-2472.
Gonzalez, R. C., D. Alvarez, et al. (2007). "Modified pendulum model for mean step length estimation." Conf Proc IEEE Eng Med Biol Soc **2007**: 1371-1374.
Gonzalez, R. C., D. Alvarez, et al. (2009). "Ambulatory estimation of mean step length during unconstrained walking by means of COG accelerometry." Comput Methods Biomech Biomed Engin **12**(6): 721-726.
Gonzalez, R. C., A. M. Lopez, et al. (2010). "Real-time gait event detection for normal subjects from lower trunk accelerations." Gait Posture **31**(3): 322-325.
Gordon, K. E., D. P. Ferris, et al. (2009). "Metabolic and mechanical energy costs of reducing vertical center of mass movement during gait." Arch Phys Med Rehabil **90**(1): 136-144.
Gregory, P., J. Alexander, et al. (2011). "Clinical Telerehabilitation: Applications for Physiatrists." Pm&R **3**(7): 647-656.
Grieve, D. W. and R. J. Gear (1966). "The relationships between length of stride, step frequency, time of swing and speed of walking for children and adults." Ergonomics **9**(5): 379-399.
Group, C. (2010). "CONSORT Statement." from http://www.consort-statement.org/resources/downloads/.
Guimaraes, R. M. and B. Isaacs (1980). "Characteristics of the gait in old people who fall." Int Rehabil Med **2**(4): 177-180.
Hansson, G., P. Asterland, et al. (2001). "Validity and reliability of triaxial accelerometers for inclinometry in posture analysis." Medical and Biological Engineering and computing **39**(4): 405-413.
Hartmann, A., S. Luzi, et al. (2009). "Concurrent validity of a trunk tri-axial accelerometer system for gait analysis in older adults." Gait & Posture **29**(3): 444-448.

Hartmann, A., K. Murer, et al. (2009). "Reproducibility of spatio-temporal gait parameters under different conditions in older adults using a trunk tri-axial accelerometer system." Gait & Posture **30**(3): 351-355.
Hausdorff, J. M. (2005). "Gait variability: methods, modeling and meaning." J Neuroeng Rehabil **2**: 19.
Hausdorff, J. M. (2007). "Gait Dynamics, Fractals and Falls: Finding Meaning in the Stride-to-Stride Fluctuations of Human Walking." Hum Mov Sci **26**(4): 555-589.
Hausdorff, J. M. (2009). "Gait dynamics in Parkinson's disease: Common and distinct behavior among stride length, gait variability, and fractal-like scaling." Chaos **19**(2): 026113.
Hausdorff, J. M., C. K. Peng, et al. (1995). "Is walking a random walk? Evidence for long-range correlations in stride interval of human gait." J Appl Physiol (1985) **78**(1): 349-358.
Health, T. G. I. f. G. (2012). "PEDro Scale." from http://www.pedro.org.au/english/downloads/pedro-scale/.
Henriksen, M., R. Christensen, et al. (2008). "Influence of pain and gender on impact loading during walking: a randomised trial." Clin Biomech (Bristol, Avon) **23**(2): 221-230.
Henriksen, M., H. Lund, et al. (2004). "Test-retest reliability of trunk accelerometric gait analysis." Gait Posture **19**(3): 288-297.
Higashi, Y., M. Sekimoto, et al. (2001). Monitoring rehabilitation training for hemiplegic patients by using a tri-axial accelerometer. Proceedings of the 23rd Annual International Conf IEEE Eng Med Biol Soc **2:** 1472 - 1474.
Hoff, J. I., A. A. van den Plas, et al. (2001). "Accelerometric assessment of levodopa-induced dyskinesias in Parkinson's disease." Mov Disord **16**(1): 58-61.
Horvath, M., T. Tihanyi, et al. (2001). "Kinematic and kinetic analysis of gait patterns in hemiplegic patients." Physical Education and Sport **1**(25-35).
Hsiao, H. and W. M. Keyserling (1990). "A three-dimensional ultrasonic system for posture measurement." Ergonomics **33**(9): 1089-1114.
Inman, V. T. (1966). "Human locomotion." Can Med Assoc J **94**(20): 1047-1054.
Johansson, T. and C. Wild (2011). "Telerehabilitation in stroke care - a systematic review." Journal of Telemedicine and Telecare **17**(1): 1-6.
Kairy, D., P. Lehoux, et al. (2009). "A systematic review of clinical outcomes, clinical process, healthcare utilization and costs associated with telerehabilitation." Disabil Rehabil **31**(6): 427-447.
Kalman, R. E. (1960). "A new approach to linear filtering and prediction problems." Journal of basic Engineering **82**(1): 35-45.
Kalman, R. E. and R. S. Bucy (1961). "New results in linear filtering and prediction theory." Journal of basic Engineering **83**(1): 95-108.
Kavanagh, J. J. and H. B. Menz (2008). "Accelerometry: A technique for quantifying movement patterns during walking." Gait & Posture **28**(1): 1-15.
Kelly-Hayes, M., A. Beiser, et al. (2003). "The influence of gender and age on disability following ischemic stroke: the Framingham study." Journal of Stroke and Cerebrovascular Diseases **12**(3): 119-126.
Kerrigan, D. C. (1998). Gait Analysis. Rehabilitation Medicine: Principles and Practise. J. A. DeLisa and B. M. Gans. Philadelphia, Lippincott-Raven.
Kerrigan, D. C., U. Della Croce, et al. (2000). "A refined view of the determinants of gait: significance of heel rise." Arch Phys Med Rehabil **81**(8): 1077-1080.
Kerrigan, D. C., P. O. Riley, et al. (2001). "Quantification of pelvic rotation as a determinant of gait." Arch Phys Med Rehabil **82**(2): 217-220.

Kiani, K., C. J. Snijders, et al. (1997). "Computerized analysis of daily life motor activity for ambulatory monitoring." Technol Health Care **5**(4): 307-318.
Kirtley, C. (2006). Clinical Gait Analysis: Theory and Practice, Elsevier.
Kuo, A. D. (2007). "The six determinants of gait and the inverted pendulum analogy: A dynamic walking perspective." Hum Mov Sci **26**(4): 617-656.
Kuo, A. D. and J. M. Donelan (2010). "Dynamic principles of gait and their clinical implications." Phys Ther **90**(2): 157-174.
Kuo, A. D., J. M. Donelan, et al. (2005). "Energetic consequences of walking like an inverted pendulum: step-to-step transitions." Exerc Sport Sci Rev **33**(2): 88-97.
Lacey, T. "Tutorial: The kalman filter." Georgia Institute of Technology.
Lau, H.-y., K.-y. Tong, et al. (2009). "Support vector machine for classification of walking conditions of persons after stroke with dropped foot." Human Movement Science **28**(4): 504-514.
Lee, C. R. and C. T. Farley (1998). "Determinants of the center of mass trajectory in human walking and running." J Exp Biol **201**(Pt 21): 2935-2944.
Lemoyne, R., T. Mastroianni, et al. (2010). Implementation of an iPhone as a wireless accelerometer for quantifying gait characteristics. In Proceedings of the 32nd Annual International Conference of the IEEE EMBS, Buenos Aires, Argentina.
LeMoyne, R., T. Mastroianni, et al. (2011). "Wireless accelerometer iPod application for quantifying gait characteristics." Conf Proc IEEE Eng Med Biol Soc **2011**: 7904-7907.
Liang, B. W., W. H. Wu, et al. (2014). "Pelvic step: the contribution of horizontal pelvis rotation to step length in young healthy adults walking on a treadmill." Gait Posture **39**(1): 105-110.
Lord, S. E., K. McPherson, et al. (2004). "Community ambulation after stroke: how important and obtainable is it and what measures appear predictive?" Arch Phys Med Rehabil **85**(2): 234-239.
Luinge, H. J. and P. H. Veltink (2005). "Measuring orientation of human body segments using miniature gyroscopes and accelerometers." Medical and Biological Engineering and computing **43**(2): 273-282.
Luinge, H. J., P. H. Veltink, et al. (1999). "Estimating of orientation with gyroscopes and accelerometers (student paper finalist)."
Lyons, G., K. Culhane, et al. (2005). "A description of an accelerometer-based mobility monitoring technique." Med Eng Phys **27**(6): 497-504.
Macko, R. F., E. Haeuber, et al. (2002). "Microprocessor-based ambulatory activity monitoring in stroke patients." Medicine and Science in Sports and Exercise **34**(3): 394-399.
Maki, B. E. (1997). "Gait changes in older adults: predictors of falls or indicators of fear." J Am Geriatr Soc **45**(3): 313-320.
Margaria, R. and R. Margaria (1976). Biomechanics and energetics of muscular exercise, Clarendon Press Oxford.
Mathie, M., A. Coster, et al. (2003). "Detection of daily physical activities using a triaxial accelerometer." Medical and Biological Engineering and computing **41**(3): 296-301.
Mathie, M. J., A. C. Coster, et al. (2004). "Accelerometry: providing an integrated, practical method for long-term, ambulatory monitoring of human movement." Physiol Meas **25**(2): R1-20.
Mau, S. (2005). What is the Kalman Filter and How can it be used for Data Fusion? .
Mayagoitia, R. E., A. V. Nene, et al. (2002). "Accelerometer and rate gyroscope measurement of kinematics: an inexpensive alternative to optical motion analysis systems." J Biomech **35**(4): 537-542.

McCamley, J., M. Donati, et al. (2012). "An enhanced estimate of initial contact and final contact instants of time using lower trunk inertial sensor data." Gait & Posture **36**(2): 316-318.
McCarney, R., J. Warner, et al. (2007). "The Hawthorne Effect: a randomised, controlled trial." BMC medical research methodology **7**(1): 30.
McGibbon, C. A. (2003). "Toward a better understanding of gait changes with age and disablement: neuromuscular adaptation." Exerc Sport Sci Rev **31**(2): 102-108.
Menz, H. B., S. R. Lord, et al. (2003). "Acceleration patterns of the head and pelvis when walking on level and irregular surfaces." Gait Posture **18**(1): 35-46.
Mera, T. O., D. A. Heldman, et al. (2012). "Feasibility of home-based automated Parkinson's disease motor assessment." Journal of Neuroscience Methods **203**(1): 152-156.
Mercer, J. A., P. Devita, et al. (2003). "Individual effects of stride length and frequency on shock attenuation during running." Med Sci Sports Exerc **35**(2): 307-313.
Miff, S. C., S. Gard, et al. (2000). The effect of step length, cadence, and walking speed on the trunk's vertical excursion. Engineering in Medicine and Biology Society, 2000. Proceedings of the 22nd Annual International Conference of the IEEE, IEEE.
Millecamps, A., K. A. Lowry, et al. (2015). "Understanding the effects of pre-processing on extracted signal features from gait accelerometry signals." Computers in biology and medicine **62**: 164-174.
Mitchell, A. J., J. Benito-Leon, et al. (2005). "Quality of life and its assessment in multiple sclerosis: integrating physical and psychological components of wellbeing." Lancet Neurol **4**(9): 556-566.
Mitoma, H., M. Yoneyama, et al. (2010). "24-Hour Recording of Parkinsonian Gait Using a Portable Gait Rhythmogram." Internal Medicine **49**(22): 2401-2408.
Miyazaki, S. (1997). "Long-term unrestrained measurement of stride length and walking velocity utilizing a piezoelectric gyroscope." IEEE Trans Biomed Eng **44**(8): 753-759.
Mizuike, C., S. Ohgi, et al. (2009). "Analysis of stroke patient walking dynamics using a tri-axial accelerometer." Gait & Posture **30**(1): 60-64.
Moe-Nilssen, R. (1998). "A new method for evaluating motor control in gait under real-life environmental conditions. Part 1: The instrument." Clin Biomech (Bristol, Avon) **13**(4-5): 320-327.
Moe-Nilssen, R., M. K. Aaslund, et al. (2010). "Gait variability measures may represent different constructs." Gait Posture **32**(1): 98-101.
Moe-Nilssen, R. and J. L. Helbostad (2002). "Trunk accelerometry as a measure of balance control during quiet standing." Gait & Posture **16**(1): 60-68.
Moore, S. T., H. G. MacDougall, et al. (2007). "Long-term monitoring of gait in Parkinson's disease." Gait & Posture **26**(2): 200-207.
Moore, S. T., H. G. MacDougall, et al. (2008). "Ambulatory monitoring of freezing of gait in Parkinson's disease." J Neurosci Methods **167**(2): 340-348.
Motoi, K., Y. Higashi, et al. (2005). Development of a wearable device capable of monitoring human activity for use in rehabilitation and certification of eligibility for long-term care. Proceeding of the 27th Annual Conf IEEE Eng Med Biol Soc. **1:** 1004-1007.
Murakami, D. and M. Makikawa (1997). "Ambulatory behavior map, physical activity and biosignal monitoring system." Methods Inf Med **36**(4-5): 360-363.
Murray, M. P. (1967). "Gait as a total pattern of movement." Am J Phys Med **46**(1): 290-333.
Murray, M. P., A. B. Drought, et al. (1964). "Walking Patterns of Normal Men." The Journal of Bone & Joint Surgery **46**(2): 335-360.

Najafi, B., K. Aminian, et al. (2002). "Measurement of stand-sit and sit-stand transitions using a miniature gyroscope and its application in fall risk evaluation in the elderly." IEEE Trans Biomed Eng **49**(8): 843-851.
Najafi, B., K. Aminian, et al. (2003). "Ambulatory system for human motion analysis using a kinematic sensor: monitoring of daily physical activity in the elderly." IEEE Trans Biomed Eng **50**(6): 711-723.
Narayanan, U. G. (2007). "The role of gait analysis in the orthopaedic management of ambulatory cerebral palsy." Curr Opin Pediatr **19**(1): 38-43.
National Audit Office (2011). Services for people with neurological conditions, Department of Health.
Neptune, R. R., S. A. Kautz, et al. (2001). "Contributions of the individual ankle plantar flexors to support, forward progression and swing initiation during walking." J Biomech **34**(11): 1387-1398.
Nishiguchi, S., M. Yamada, et al. (2012). "Reliability and validity of gait analysis by android-based smartphone." Telemed J E Health **18**(4): 292-296.
Nymoen, K., A. Voldsund, et al. (2012). "Comparing Motion Data from an iPod Touch to an Optical Infrared Marker-Based Motion Capture System." New Interface for Musical Expression.
Olshausen, B. A. (2000). "Aliasing." PSC 129–Sensory Processes: 3-4.
Orendurff, M. S., A. D. Segal, et al. (2004). "The effect of walking speed on center of mass displacement." J Rehabil Res Dev **41**(6A): 829-834.
Ortega, J. D. and C. T. Farley (2005). "Minimizing center of mass vertical movement increases metabolic cost in walking." Journal of Applied Physiology **99**(6): 2099-2107.
Patel, S., H. Park, et al. (2012). "A review of wearable sensors and systems with application in rehabilitation." Journal of Neuroengineering and Rehabilitation **9**.
Patterson, S. L., L. W. Forrester, et al. (2007). "Determinants of walking function after stroke: differences by deficit severity." Arch Phys Med Rehabil **88**(1): 115-119.
Perry, J. (1992). "Gait Analysis: Normal and Pathological Function." Journal of Pediatric Orthopaedics **12**(6): 815.
Prajapati, S. K., W. H. Gage, et al. (2011). "A Novel Approach to Ambulatory Monitoring: Investigation Into the Quantity and Control of Everyday Walking in Patients With Subacute Stroke." Neurorehabilitation and Neural Repair **25**(1): 6-14.
Preece, S. J., J. Y. Goulermas, et al. (2009). "Activity identification using body-mounted sensors—a review of classification techniques." Physiol Meas **30**(4): R1.
Radin, E. L. and I. L. Paul (1971). "Response of joints to impact loading. I. In vitro wear." Arthritis Rheum **14**(3): 356-362.
Rao, A. K., L. Quinn, et al. (2005). "Reliability of spatiotemporal gait outcome measures in Huntington's disease." Movement Disorders **20**(8): 1033-1037.
Razali, N. M., Y. B. Wah, et al. (2011). "Power comparisons of Shapiro-Wilk, Kolmogorov-Smirnov, Lilliefors and Anderson-Darling tests." Journal of Statistical Modeling and Analytics **2**(1): 21-33.
Roetenberg, D., H. Luinge, et al. (2009). "Xsens MVN: full 6DOF human motion tracking using miniature inertial sensors." Xsens Motion Technologies BV, Tech. Rep.
Roger, M. (1967). du Plessis. Poor Man's Explanation of Kalman Filtering or how I stopped worrying and learned to love Matrix Inversion, Technical report, Autonetics Division, Rockwell International, 3370 Miraloma Avenue, Anaheim, California 92803.
Rui, Z., A. Bannoura, et al. (2013). Indoor localization using a smart phone. Sensors Applications Symposium (SAS), 2013 IEEE**:** 38-42.

Sabatini, A. M., C. Martelloni, et al. (2005). "Assessment of walking features from foot inertial sensing." Ieee Transactions on Biomedical Engineering **52**(3): 486-494.
Sabelman, E., A. Fiene, et al. (2004). Accelerometric activity identification for remote assessment of quality of movement. Proceedings of the 26th Annual International Conf IEEE Eng Med Biol Soc. **26:** 4781-4784.
Saini, M., D. C. Kerrigan, et al. (1998). "The vertical displacement of the center of mass during walking: a comparison of four measurement methods." J Biomech Eng **120**(1): 133-139.
Sakka, S., C. Hayot, et al. (2010). A generalized 3D inverted pendulum model to represent human normal walking. Humanoid Robots (Humanoids), 2010 10th IEEE-RAS International Conference on, IEEE.
Salarian, A., F. B. Horak, et al. (2010). "iTUG, a Sensitive and Reliable Measure of Mobility." IEEE Trans Neural Syst Rehab Eng **18**(3): 303-310.
Salarian, A., H. Russmann, et al. (2007). "Ambulatory monitoring of physical activities in patients with Parkinson's disease." IEEE Trans Biomed Eng **54**(12): 2296-2299.
Salarian, A., H. Russmann, et al. (2007). "Quantification of tremor and bradykinesia in Parkinson's disease using a novel ambulatory monitoring system." IEEE Trans Biomed Eng **54**(2): 313-322.
Salarian, A., C. Zampieri, et al. (2009). "Analyzing 180 degrees Turns Using an Inertial System Reveals Early Signs of Progression of Parkinson's Disease." Proceedings of the Annual Conf IEEE Eng Med Biol Soc, Vols 1-20: 224-227.
Saunders, J. B., V. T. Inman, et al. (1953). "The major determinants in normal and pathological gait." J Bone Joint Surg Am **35-A**(3): 543-558.
Scanaill, C. N., S. Carew, et al. (2006). "A review of approaches to mobility telemonitoring of the elderly in their living environment." Annals of Biomedical Engineering **34**(4): 547-563.
Schrag, A., M. Jahanshahi, et al. (2000). "How does Parkinson's disease affect quality of life? A comparison with quality of life in the general population." Movement Disorders **15**(6): 1112-1118.
Seel, T., J. Raisch, et al. (2014). "IMU-based joint angle measurement for gait analysis." Sensors **14**(4): 6891-6909.
Shannon, C. E. (1948). The mathematical theory of communication.
Shrout, P. E. and J. L. Fleiss (1979). "Intraclass correlations: uses in assessing rater reliability." Psychol Bull **86**(2): 420-428.
Siderowf, A., M. McDermott, et al. (2002). "Test-retest reliability of the unified Parkinson's disease rating scale in patients with early Parkinson's disease: results from a multicenter clinical trial." Mov Disord **17**(4): 758-763.
Simoes, M. A. (2011). Feasibility of Wearable Sensors to Determine Gait Parameters. Master of Science in Mechanical Engineering, University of South Florida.
Simon, S. R. (2004). "Quantification of human motion: gait analysis-benefits and limitations to its application to clinical problems." J Biomech **37**(12): 1869-1880.
Simon, S. R., I. L. Paul, et al. (1981). "Peak dynamic force in human gait." J Biomech **14**(12): 817-822.
Smeathers, J. (1989). "Transient vibrations caused by heel strike." Proceedings of the Institution of Mechanical Engineers, Part H: Journal of Engineering in Medicine **203**(4): 181-186.
Smith, S. (2013). Digital Signal Processing: A Practical Guide for Engineers and Scientists: A Practical Guide for Engineers and Scientists, Newnes.
Smith, S. W. (1997). "The scientist and engineer's guide to digital signal processing."
Spirduso, W. (1995). Physical dimensions of aging. . Campaign, Human Kinetics.

Staszkiewicz, R., T. Ruchlewicz, et al. (2010). "The impact of changes in gait speed and step frequency on the extent of the center of mass displacements." Acta Bioeng. Biomech **12**(3): 13-20.
Steele, B. G., B. Belza, et al. (2003). "Bodies in motion: monitoring daily activity and exercise with motion sensors in people with chronic pulmonary disease." J Rehabil Res Dev **40**(5 Suppl 2): 45-58.
Steins, D., H. Dawes, et al. (2014). "Wearable accelerometry-based technology capable of assessing functional activities in neurological populations in community settings: a systematic review." J Neuroeng Rehabil **11**: 36.
Steins, D., I. Sheret, et al. (2014). "A smart device inertial-sensing method for gait analysis." J Biomech **47**(15): 3780-3785.
Stephens, J. M. and P. A. Goldie (1999). "Walking speed on parquetry and carpet after stroke: effect of surface and retest reliability." Clin Rehabil **13**(2): 171-181.
Stern, J. T., B. Demes, et al. (2004). Modeling human walking as an inverted pendulum of varying length. Shaping Primate Evolution: Form, Function, and Behavior. F. Anapol, R. Z. German and N. G. Jablonski, Cambridge University Press. **40:** 297 - 333.
Stolze, H., S. Klebe, et al. (2004). "Falls in frequent neurological diseases--prevalence, risk factors and aetiology." J Neurol **251**(1): 79-84.
Sutherland, D. H. (2002). "The evolution of clinical gait analysis. Part II kinematics." Gait Posture **16**(2): 159-179.
Sutherland, D. H., R. Olshen, et al. (1980). "The development of mature gait." J Bone Joint Surg Am **62**(3): 336-353.
Tee, K. S., M. Awad, et al. (2011). "Triaxial accelerometer static calibration."
The Neurological Alliance (2003). Neuro Numbers: A brief review of the numbers of people in the UK with a neurological condition.
Theodoridis, S. and K. Koutroumbas (2008). Pattern Recognition.
Thirunarayan, M. A., D. C. Kerrigan, et al. (1996). "Comparison of three methods for estimating vertical displacement of center of mass during level walking in patients." Gait & Posture **4**(4): 306-314.
Tomie, D. H., Jo-Anne (2000). "An assessment of gait analysis in the rehabilitation of children with walking difficulties." Disability & Rehabilitation **22**(6): 275-280.
Trawny, N. and S. I. Roumeliotis (2005). Indirect Kalman Filter for 3D Attitude Estimation, Dept. of Computer Science & Engineering, University of Minnesota**:** 24.
Trew, M. and E. T.H. (2001). Human movement: an introductory text, Hartcourt Publishers Limited.
Troiano, R. P., D. Berrigan, et al. (2008). "Physical activity in the United States measured by accelerometer." Med Sci Sports Exerc **40**(1): 181.
Trojaniello, D., A. Cereatti, et al. (2014). "Accuracy, sensitivity and robustness of five different methods for the estimation of gait temporal parameters using a single inertial sensor mounted on the lower trunk." Gait Posture **40**(4): 487-492.
Trojaniello, D., A. Ravaschio, et al. (2015). "Comparative assessment of different methods for the estimation of gait temporal parameters using a single inertial sensor: application to elderly, post-stroke, Parkinson's disease and Huntington's disease subjects." Gait Posture **42**(3): 310-316.
Turcot, K., R. Aissaoui, et al. (2008). "New accelerometric method to discriminate between asymptomatic subjects and patients with medial knee osteoarthritis during 3-d gait." IEEE Trans Biomed Eng **55**(4): 1415-1422.
Tzafestas, S. G. (2012). Advances in intelligent autonomous systems, Springer Science & Business Media.

Veltink, P. H., H. J. Bussmann, et al. (1996). "Detection of static and dynamic activities using uniaxial accelerometers." Rehabilitation Engineering, IEEE Transactions on **4**(4): 375-385.
Wandersman, A., J. Duffy, et al. (2008). "Bridging the gap between prevention research and practice: the interactive systems framework for dissemination and implementation." Am J Community Psychol **41**(3-4): 171-181.
Weir, J. P. (2005). "Quantifying test-retest reliability using the intraclass correlation coefficient and the SEM." J Strength Cond Res **19**(1): 231-240.
Weiss, A., M. Brozgol, et al. (2013). "Does the evaluation of gait quality during daily life provide insight into fall risk? A novel approach using 3-day accelerometer recordings." Neurorehabilitation and neural repair **27**(8): 742-752.
Weiss, A., T. Herman, et al. (2014). "Objective assessment of fall risk in Parkinson's disease using a body-fixed sensor worn for 3 days."
Weiss, A., S. Sharifi, et al. (2011). "Toward automated, at-home assessment of mobility among patients with Parkinson disease, using a body-worn accelerometer." Neurorehabil Neural Repair **25**(9): 810-818.
Welch, G. and G. Bishop (1995). An Introduction to the Kalman Filter, University of North Carolina at Chapel Hill.
Whittle, M. W. (1997). "Three-dimensional motion of the center of gravity of the body during walking." Hum Mov Sci **16**(2): 347-355.
Whittle, M. W. (1999). "Generation and attenuation of transient impulsive forces beneath the foot: a review." Gait Posture **10**(3): 264-275.
Whittle, M. W. (2007). Gait Analysis: An Introduction, Butterworth Heinemann Elsevier.
WHO (2001). International classification of functioning, disability and health. W.H.O. WHO press, World Health Organization**:** 303.
WHO (2006). Neurological disorders: a public health approach. Neurological disorders: public health challenges. W.H.O. Geneva, Switzerland, W.H.O. press.
Williamson, R. and B. Andrews (2001). "Detecting absolute human knee angle and angular velocity using accelerometers and rate gyroscopes." Medical and Biological Engineering and computing **39**(3): 294-302.
Winiarski, S. and A. Rutkowska-Kucharska (2009). "Estimated ground reaction force in normal and pathological gait." Acta Bioeng Biomech **11**(1): 53-60.
Winter, D. A. (1984). "Kinematic and kinetic patterns in human gait: variability and compensating effects." Hum Mov Sci **3**(1): 51-76.
Winter, D. A. (1991). Biomechanics and motor control of human gait: normal, elderly and pathological.
Winter, D. A., A. E. Patla, et al. (1990). "Assessment of balance control in humans." Med Prog Technol **16**(1-2): 31-51.
Wong, W. Y., M. S. Wong, et al. (2007). "Clinical applications of sensors for human posture and movement analysis: a review." Prosthet Orthot Int **31**(1): 62-75.
Woo, J., S. Ho, et al. (1995). "Age-associated gait changes in the elderly: pathological or physiological?" Neuroepidemiology **14**(2): 65-71.
Woodman, O. J. (2007). "An introduction to inertial navigation." University of Cambridge, Computer Laboratory, Tech. Rep. UCAMCL-TR-696 **14**: 15.
Wren, T. A., G. E. Gorton, 3rd, et al. (2011). "Efficacy of clinical gait analysis: A systematic review." Gait Posture **34**(2): 149-153.
Xu, X., M. A. Batalin, et al. (2011). Robust hierarchical system for classification of complex human mobility characteristics in the presence of neurological disorders. 2011 International Conference on Body Sensor Networks**:** 65-70.

Yang, C.-C., Y.-L. Hsu, et al. (2011). "Real-time gait cycle parameter recognition using a wearable accelerometry system." Sensors **11**(8): 7314-7326.
Yang, C. C. and Y. L. Hsu (2010). "A review of accelerometry-based wearable motion detectors for physical activity monitoring." Sensors **10**(8): 7772-7788.
Yang, M., H. Zheng, et al. (2012). "Assessing the utility of smart mobile phones in gait pattern analysis." Health and Technology **2**(1): 81-88.
Yogev‐Seligmann, G., J. M. Hausdorff, et al. (2008). "The role of executive function and attention in gait." Movement Disorders **23**(3): 329-342.
Zampieri, C., A. Salarian, et al. (2010). "The instrumented timed up and go test: potential outcome measure for disease modifying therapies in Parkinson's disease." Journal of Neurology Neurosurgery and Psychiatry **81**(2): 171-176.
Zampieri, C., A. Salarian, et al. (2011). "Assessing mobility at home in people with early Parkinson's disease using an instrumented Timed Up and Go test." Parkinsonism & Related Disorders **17**(4): 277-280.
Zheng, H., N. D. Black, et al. (2005). "Position-sensing technologies for movement analysis in stroke rehabilitation." Med Biol Eng Comput **43**(4): 413-420.
Zhou, H. and H. Hu (2008). "Human motion tracking for rehabilitation—A survey." Biomedical Signal Processing and Control **3**: 1-18.
Zhou, H., H. Hu, et al. (2010). "Reducing Drifts in the Inertial Measurements of Wrist and Elbow Positions." Instrumentation and Measurement, IEEE Transactions on **59**: 575–585.
Ziaei, M., S. Nabavi, et al. (2012). "The Effect of Shoe Sole Tread Groove Depth on the Gait Parameters during Walking on Dry and Slippery Surface." Int J Occup Environ Med **4**(1 January).
Zijlstra, A. and W. Zijlstra (2013). "Trunk-acceleration based assessment of gait parameters in older persons: A comparison of reliability and validity of four inverted pendulum based estimations." Gait & Posture **38**(4): 940-944.
Zijlstra, W. (2004). "Assessment of spatio-temporal parameters during unconstrained walking." Eur J Appl Physiol **92**(1-2): 39-44.
Zijlstra, W. and K. Aminian (2007). "Mobility assessment in older people: new possibilities and challenges." European Journal of Ageing **4**(1): 3-12.
Zijlstra, W. and A. L. Hof (1997). "Displacement of the pelvis during human walking: experimental data and model predictions." Gait & Posture **6**(3): 249-262.
Zijlstra, W. and A. L. Hof (2003). "Assessment of spatio-temporal gait parameters from trunk accelerations during human walking." Gait & Posture **18**(2): 1-10.
Zwartjes, D. G. M., T. Heida, et al. (2010). "Ambulatory Monitoring of Activities and Motor Symptoms in Parkinson's Disease." IEEE Trans Biomed Eng **57**(11): 2778-2786.

Appendices

Appendix A

Databases*
1. Cochrane Database for Systematic Reviews (CDSR), all of the Cochrane library content, via www.thecochranelibrary.com, (1940 - January 1, week 1, 2013)
2. EMBASE via OvidSP, (1974 - January 1, week 1, 2013)
3. Web of Knowledge ISI (WoK), via http://apps.webofknowledge.com, (1980 - January 1, week 1, 2013)
4. Web of Science via WoK, (January 1, week 1, 2013)
5. Biosis via WoK, (January 1, week 1, 2013)
6. PubMed via NCBI (National Center for Biotechnology Information), (1950 - January 1, week 1, 2013)
7. MEDLINE via WoK and PubMed (1950 – January 1, week 1, 2013)
8. IEEE Xplore, including Individual Online Journals, IEEE/IET Electronic Library (IEL), VDE VERLAG Conference Proceedings (1946 – January 1, week 1, 2013)
*All database searches were originally search on January 1st 2012, with update searches carried out in January 1st 2013

PubMed search strategy

The following search strategy for PubMed and adapted it for the other databases.

1. exp physical examination/ or exp motion/ or exp locomotion/ or exp mobility limitation/
2. (motion) adj5 (sens$ or track$ or captur$ or detect$).tw.
3. mocap/
4. ((activity or inertial or mobility or position) adj5 (sens$ or monitor$)).tw.
5. accelerometer$/ or accelerometry/ or pedometer$/ or inertial sensor$/
6. human locomotion/ or human movement/
7. 1 or 2 or 3 or 4 or 5 or 6
8. exp telemetry/ or telemetries/ or exp rehabilitation/ or telerehabilitation/ or teletherapy/ or telehealth/ or telemedicine/
9. ((community-based or long-term or home or ambulatory) adj5 (rehab$ or recovery or monitor$)).tw.
10. 8 or 9
11. exp wireless technology/
12. ((wearable or remote or portable or mobile) adj5 (system$ or device$ or monitor$)).tw.
13. 11 or 12
14. 7 and 10 and 13

Web of Knowledge (including BIOSIS, MEDLINE since 1950, and Web of Science) search strategy

1. motion or locomotion or mobility NEAR/1 limitation.tw.
2. (motion) NEAR/1 (sens* or track* or captur* or detect*).tw.
3. mocap/
4. ((activity or inertial or mobility or position) NEAR/1 (sens* or monitor*)).tw.
5. accelerometer* or accelerometry or pedometer* or inertial NEAR/1 sensor*
6. human locomotion/ or human movement/
7. 1 or 2 or 3 or 4 or 5 or 6
8. telemetr* or rehabilitation or telerehabilitation or teletherapy or telehealth or telemedicine or mobile NEAR/1 health.tw.
9. ((community-based or long-term or home or ambulatory) NEAR/1 (rehab* or recovery or monitor*)).tw.
10. 8 or 9
11. wireless NEAR/1 technology.tw.
12. ((wearable or remote or portable or mobile) NEAR/1 (system* or device* or monitor*)).tw.
13. 11 or 12
14. 7 and 10 and 13

Cochrane search strategy

1. exp motion/ or exp locomotion/ or exp mobility limitation/
2. (motion) NEXT (sens* or track* or captur* or detect*).tw.
3. mocap/
4. ((activity or inertial or mobility or position) NEXT (sens* or monitor*)).tw.
5. accelerometer*/ or accelerometry/ or pedometer*/ or inertial NEXT sensor*/
6. human locomotion/ or human movement/
7. 1 or 2 or 3 or 4 or 5 or 6
8. exp telemetry/ or telemetries/ or exp rehabilitation/ or telerehabilitation/ or teletherapy/ or telehealth/ or telemedicine/
9. ((community-based or long-term or home or ambulatory) NEAR (rehab* or recovery or monitor*)).tw.
10. 8 or 9
11. exp telecommunications/
12. ((wearable or remote or portable or mobile) NEAR (system* or device* or monitor*)).tw.
13. 11 or 12
14. 7 and 10 and 13

EMBASE search strategy (OvidSP)

1. exp physical examination/ or exp motion/ or exp locomotion/ or exp mobility limitation/ or exp walking difficulty/
2. (motion) adj5 (sens$ or track$ or captur$ or detect$).ti,sh,hw,ab,kw,tw.
3. Mocap. ti,sh,hw,ab,kw,tw.
4. ((activity or inertial or mobility or position) adj5 (sens$ or monitor$)).ti,sh,hw,ab,kw,tw.
5. accelerometer$/ or accelerometry/ or pedometer$/ or inertial sensor$/
6. human locomotion/ or human movement/
7. 1 or 2 or 3 or 4 or 5 or 6
8. exp telehealth/ or exp telemetry/ or exp remote sensing/ or exp telemonitoring/ or rehabiliation/ or telerehabilitation.mp. or telemetries.mp. or exp teletherapy/ or exp telemedicine/ or exp mobile health/
9. ((community-based or long-term or home or ambulatory) adj5 (rehab$ or recovery or monitor$)).ti,sh,hw,ab,kw,tw.
10. 8 or 9
11. exp wireless technology/
12. ((wearable or remote or portable or mobile) adj5 (system$ or device$ or monitor$)).ti,sh,hw,ab,kw,tw.
13. 11 or 12
14. 7 and 10 and 13

IEEE Xplore search strategy

1. exp motion/ or exp locomotion/ or exp mobility limitation/
2. (motion) NEAR (sensing or trackting or capturing or detecting).tw.
3. mocap/
4. ((activity or inertial or mobility or position) NEAR (sensors or monitors)).tw.
5. accelerometers/ or accelerometry/ or pedometers/ or inertial sensors/
6. human locomotion/ or human movement/
7. 1 or 2 or 3 or 4 or 5 or 6
8. exp telemetry/ or telemetries/ or exp rehabilitation/ or telerehabilitation/ or teletherapy/ or telehealth/ or telemedicine/
9. ((community-based or long-term or home or ambulatory) NEAR (rehabilitation or recovery or monitoring)).tw.
10. 8 or 9
11. exp wireless technology/
12. ((wearable or remote or portable or mobile) NEAR (systems or devices or monitors)).tw.
13. 11 or 12
14. 7 and 10 and 13

Appendices

Appendix B

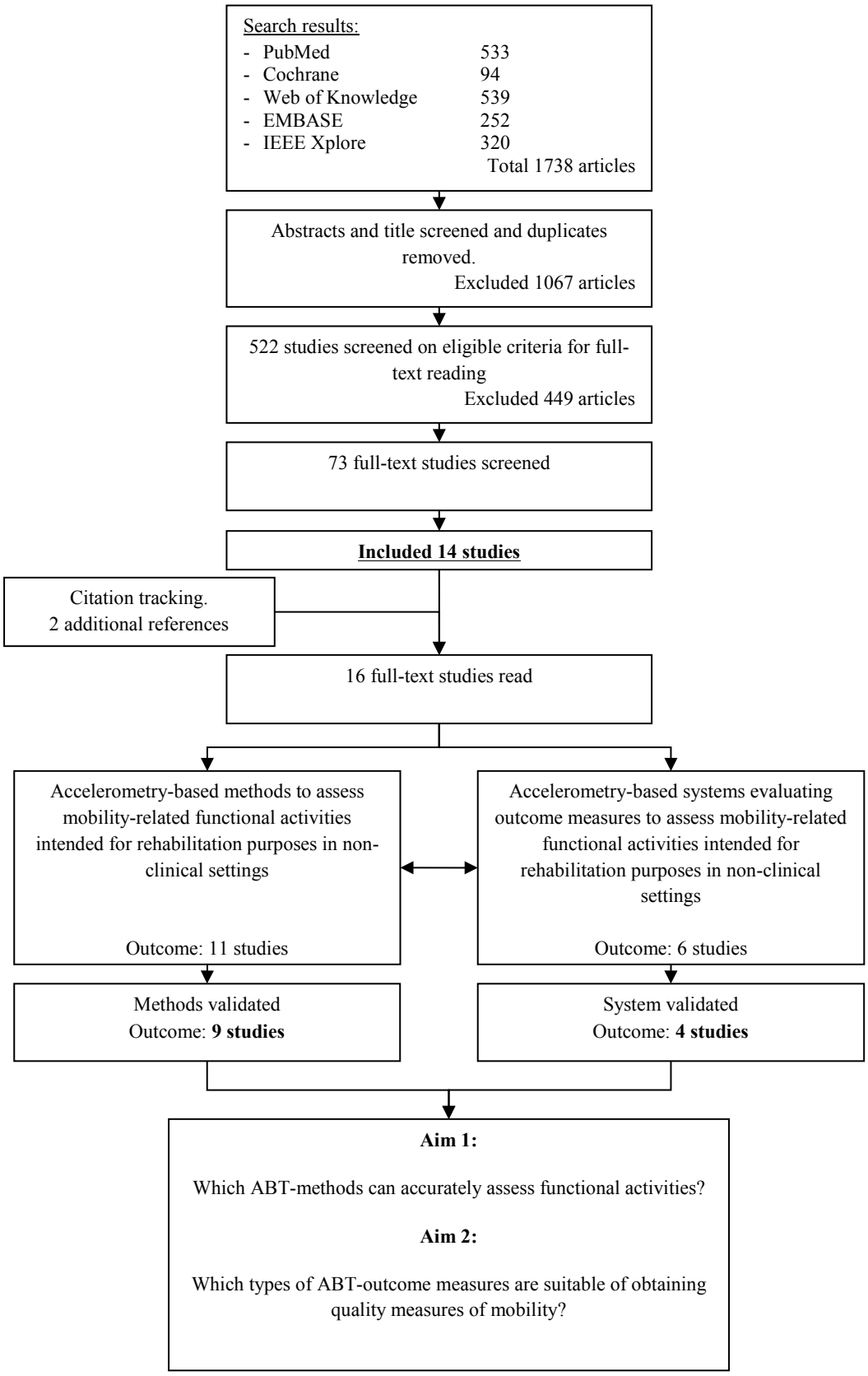

Flowchart of the literature search results.

Appendices

Appendix C

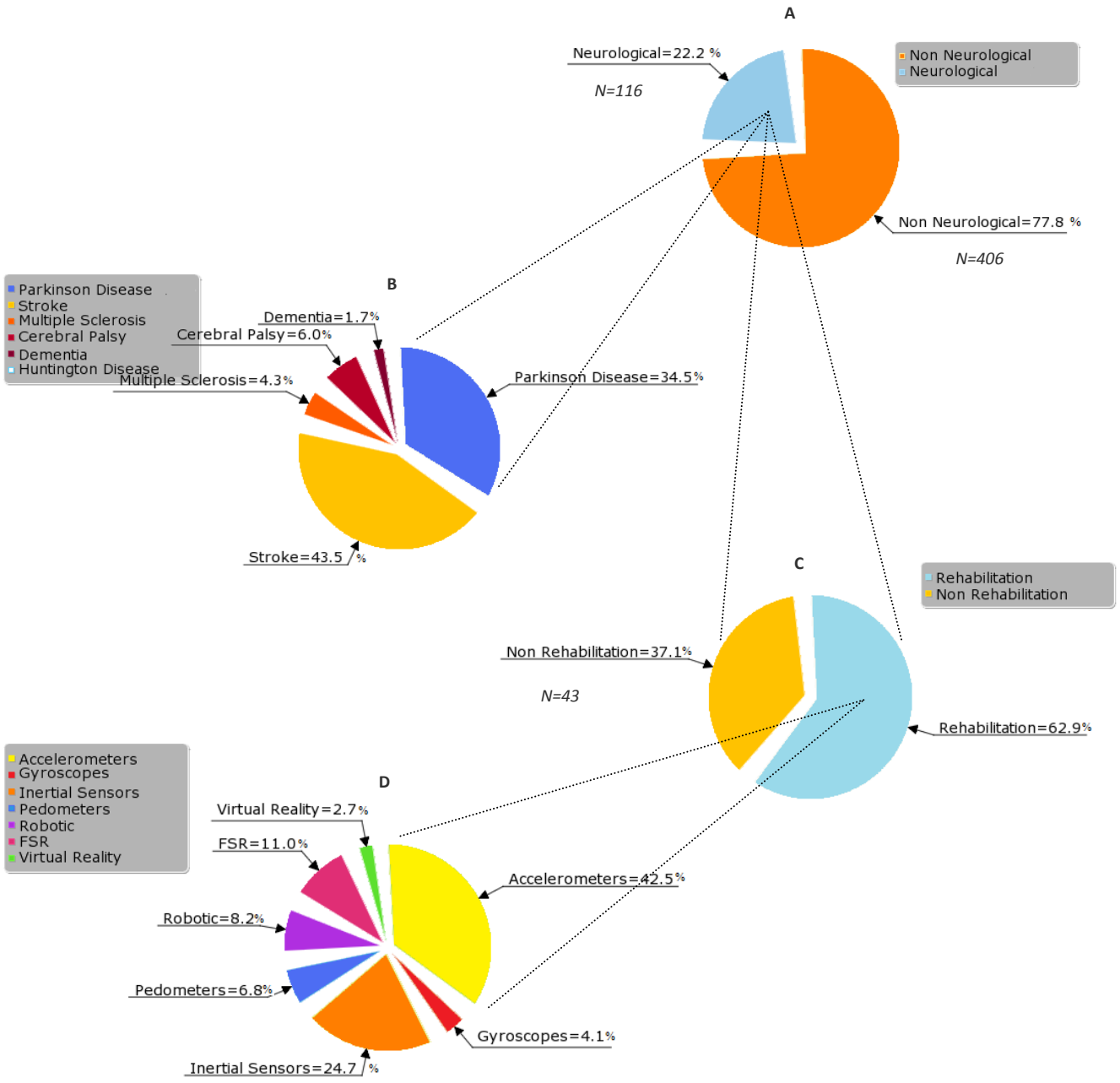

Pie chart of the screening results from the literature search.

Appendix D

Checklist for quality review of studies evaluating AT-outcome measures.

Criteria Customized scale items	Dobkin et al (2011)	Prajapati et al (2011)	Zampieri et al (2011)	Mizuike et al (2009)
External validity				
1. Eligibility criteria specified	1	1	0	1
Internal validity				
2. Baseline characteristics described	1	1	1	1
3. Measurement protocol clearly described	1	1	1	1
4. Measurement procedure is clearly described for each group to allow replication	1	1	1	1
5. Completely defined pre-specified outcome measures	1	1	1	1
6. Outcome measures are reliable and valid	1	1	1	1
7. Statistical methods used to compare groups outcomes	1	1	1	1
8. Between-group statistical comparisons are reported for at least one outcome	1	1	1	1
9. The study provides measures of variability for at least one outcome	1	1	1	1
10. Methods for additional analyses, such as subgroup analyses and adjusted analyses	0	0	1	1
11. Reported trial limitations	0	1	1	1
12. Interpretation of the results	1	1	1	1
Total Score	**10**	**11**	**11**	**12**

Appendices

Appendix E

Checklist for quality review of studies proposing AT-methods.

Criteria Customized scale items	Salarian et al (2007)	Motoi et al (2005)	Zwartjes et al (2010)	Lau et al (2009)	Barth et al (2010)	Yang et al (2011)	Cancela et al (2010)	Moore et al (2007)	Dobkin et al (2011)
Internal validity method									
1. Baseline characteristics described	0	1	0	1	1	0	0	1	1
2. System and devices are clearly described	1	1	0	1	1	1	1	1	1
3. Measurement protocol is clearly described for each group to allow replication	1	0	1	1	1	1	0	1	1
4. Methods of analysis clearly described	1	1	1	1	1	1	1	1	1
5. Classifier(s) are evaluated	1	n/a	0	1	1	n/a	1	n/a	0
6. Statistical methods used to test reproducibility	1	0	1	1	1	0	0	0	1
7. Reported accuracy metrics	1	0	1	1	1	0	0	0	0
8. Reported confidence intervals for classifier performance	0	n/a	0	0	0	n/a	0	n/a	0
9. Study limitations described	0	0	1	0	0	1	0	0	0
10. Interpretation of the results	0	0	1	0	1	1	0	1	1
Construct validity method									
11. Content validity	1	0	1 (Sabatini, Martelloni et al. 2005)	0	0	0	1	0	0
12. Criterion-related validity is obtained	1	1	0	1	0	1	0	1	1
13. Cross-validation (i.e. test and training set)	1	0	1	1	1	0	0	0	0
Total Score	**9**	**4**	**8**	**9**	**8**	**6**	**5**	**6**	**7**

Appendices

Appendix F

Study Characteristics

Reference (Year)	Population	n (E/C)	Mean age, years (range) or SD	Male/Female	Intervention	Setting	Intended for	Medication
Barth et al (2011)	PD	27/16 (healthy controls) Group I: 14 Group II: 13	Group I: 63.4 ± 9.3 / 64.9 ± 6.9 Group II: 66.6 ± 10.5	12/2 – 7/9 9/4 – 7/9	-	Laboratory	Smart home monitoring	Levodopa (mg) Group I: 408 ± 415 Group II: 563 ± 359
Cancela et al (2010)	PD	20/-	- , (18-85)	-	-	Supervised environment (clinic)	Telehealth, Telemedicine, Home monitoring	-
Dobkin et al (2011)	Stroke	12/6 (healthy controls)	58.9 ± 12.6 / 40.0 ± -	6/6 – 3/3	-	Clinic indoor to outdoor, Home setting	Rehabilitation, Community	-
Lau et al (2009)	Stroke	7/-	45.6 ± 5.4	5/2	-	-	Rehabilitation, Home monitoring	-
Mizuike et al (2009)	Stroke	63/21 (healthy controls elderly)	69.4 ± 10.2 / 74.8 ± 6.9	46/17 – 4/17	-	Hospital	Rehabilitation	-
Moore et al (2007)	PD	7/10	72.0 ± 7.4 / 38.0 ± 7.7	3/4 – 5/5	-	Clinic (indoor to outdoor), Home setting	Telerehabilitation and medication	-
Motoi et al (2005)	Stroke	7/-	68.6 ± 10.2	4/3	-	Laboratory	Rehabilitation	
Prajapati et al (2011)	Stroke	16/-	59.74 ± 15.3	12/4	-	Rehabilitation hospital	Home monitoring	-